KINEMATICAL AND DYNAMICAL PROPERTIES OF THE FIELD OF PRESSURE, WITH APPLICATION TO WEATHER FORECASTING

BY

SVERRE PETTERSSEN

(Manuscript received 17th January 1933)

INTRODUCTION

In the succeeding chapters we shall endeavour to develop, partly on kinematical and partly on dynamical principles, the inter-relations between the field of pressure on one hand, and the various changes in the future pressure distribution on the other, and show how these relations may be applied to the problems of weather chart analysis and weather forecasting.

The so-called Norwegian methods of weather chart analysis are well-known from numerous papers of Bjerknes, Bergeron and Solberg. These methods which have been developed to a rather high degree of perfection, chiefly aim at a *physical* analysis of the weather charts. A systematic treatise on this subject has recently been rendered by Bergeron in his: *Die dreidimensional verknüpfende Wetteranalyse*, the second part of which is not yet published. In the present paper the writer has endeavoured not to discuss things which are likely to be treated by Bergeron. There is, therefore, very little said about physical weather chart analysis.

The physical analysis, naturally, forms the basis of rational weather forecasting. The step from the completed physical analysis to the forecast is, however, a difficult one. It is this step that the writer has endeavoured to facilitate in the present memoir. The leading idea is: to develop methods for evaluating the instantaneous velocity and acceleration of the various pressure formations, such as: cyclones, anticyclones, troughs, wedges, fronts etc. Furthermore, to evaluate the displacement and variation in intensity during the forecasting period. These questions are discussed in chapters I to IV and VI. Chapter V deals with the properties of fronts, convergence in the air masses, and vertical velocity. Finally, chapter VII gives numerous examples of the application to the weather charts.

Throughout, it has been a leading idea to express the forecasting equations in terms of pressure only, because atmospheric pressure is the only element for which no question of representativeness arises.

The preliminary investigations, which form the basis of this paper, have been extended to many problems which are not contained in this publication. For several reasons it was necessary to limit the purview to problems which are so closely connected to weather chart work, that their solutions can be applied directly in the daily weather service. For this reason, the paper has no pretentions of being a complete treatise on the subject advertised in the title. It is, however, hoped that clarity and applicability are gained by limiting the scope. In fact, practical applicability is the one thing aimed at in the present memoir. Questions of purely theoretical value have persistently been

left out. Amongst such questions are: (1) the connection between the distribution of pressure and pressure changes on one hand, and the transfer of energy on the other, (2) the connection between the vertical distribution of solenoids and the horizontal distribution of pressure, and (3) vertical velocity and transformation of energy. It is intended to return to these problems in a later communication.

CHAPTER I.
DEFINITIONS AND GENERAL EQUATIONS.

1. Characteristic Curves in the Field of Pressure. The field of atmospheric pressure in a level surface at an instant $t = t_1$ may be represented by means of equiscalar curves for unit values of pressure.

During an interval of time $\triangle t$ the pressure may vary by the amount $\triangle p$. This variation is uniquely determined by the new position of the equiscalar curves, or isobars. When, on the other hand, the instantaneous distribution of pressure and the instantaneous pressure variation are known, it is possible to compute the displacement of the isobars.

Let $p = p(x, y, t)$ represent the distribution of pressure (p) at (say) sea level. For any instant $t = t_1$, the isobars are given by

$$p = p_0,\ p_1,\ p_2,\ \text{etc.}$$

where p_0, p_1, etc. are constant values. The isobars may be called curves for characteristic pressure values.

The field of pressure frequently exhibits characteristic curves of higher order. Let

$$\frac{\partial p}{\partial t} = T(x, y, t)$$

represent the distribution of pressure variation (or barometric tendencies). The equiscalar curves for $\frac{\partial p}{\partial t}$ (or isallobars), are then given by

$$\frac{\partial p}{\partial t} = T_0,\ T_1,\ T_2,\ \text{etc.}$$

where T_0, T_1, etc. are characteristic constant values.

Furthermore, the pressure distribution may exhibit more complicated characteristic curves, such as trough lines, wedge lines, symmetry lines etc., which are characterized by constant values of certain derivatives of the pressure function.

A pressure center (high, low or neutral point) may be defined by the intersection of characteristic curves derived from the pressure function.

It is, therefore, convenient to deduce general equations for the displacement of such curves. In the succeeding chapters we shall specialize these equations, and demonstrate how the instantaneous displacement of the entire pressure field may be diagnosed, and how the future distribution of atmospheric pressure may be forecasted.

2. Definition of Velocity and Acceleration of Characteristic Curves. Let $p = p(x, y, t)$ be the pressure function in a system of co-ordinates (x, y). We introduce the symbol

$$p_{lmn} = \frac{\partial^{l+m+n} p}{\partial x^l \partial y^m \partial t^n}. \tag{1}$$

A characteristic curve in the pressure field may then be defined by[1])

$$p_{lmn} = \text{constant}. \tag{2}$$

[1]) The definition may be extended to any function $f(x, y, t)$, and therefore, also to $f(p(x, y, t))$.

Thus $p_{000} = p =$ constant, represents an isobar, $p_{001} = \frac{\partial p}{\partial t} =$ constant, represents an isallobar, etc.

The characteristic curves themselves may be identified by means of numbers which denote the constant values of p_{lmn}.

In order to be able to define the movement of such characteristic curves, we must 'label' the curve elements in such a way that they become autonomous, and thus may be recognized from one chart to the other.

The curve elements may be individualized in different ways. Let us consider the isochrones (S) (see fig. 1) of an individual characteristic curve, and draw the normal curves (C) to these isochrones. A curve element (e) may then be individualized in such a way, that it is always to be found on the initial characteristic curve and on the initial normal curve. An imaginary particle, which is forced to remain on the curve element, would have an instantaneous velocity which is perpendicular to the isochrone. If the isochrones be curved lines, the acceleration of such a particle would have one component perpendicular to the isochrone and one component tangential to it.

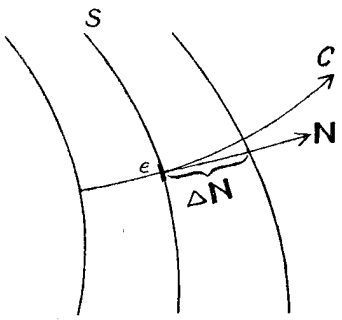

Fig. 1.

The displacement of a curve element tangential to the curve itself is of no consequence for the future distribution of the scalar function. We shall, therefore, choose to work with another notation for individual curve elements.

Let us again consider the isochrones of a characteristic curve and the normals (straight lines) to the isochrones. The curve elements may now be identified as being always on the initial characteristic curve and on the initial normal. With this notation, the velocity and the acceleration of an imaginary particle that remains on the line element, would always be directed along the initial normal.

Let $\triangle \boldsymbol{N}$ be the displacement along the normal during the time interval $\triangle t$. We then define the velocity ($\boldsymbol{C}$) of the element of the characteristic curve as:

$$\boldsymbol{C} = \lim_{\triangle t \to 0} \left(\frac{\triangle \boldsymbol{N}}{\triangle t} \right) \tag{3}$$

The acceleration $\boldsymbol{A}$ of the line element may be defined as the change in velocity per unit time. Or

$$\boldsymbol{A} = \frac{d\boldsymbol{C}}{dt} \tag{4}$$

The velocity, which is equal to the velocity of an imaginary particle that, during its motion, is forced to remain on the curve element, is a function of t and N only. Choosing a system of co-ordinates whose x-axis coincides with N, we may write

$$A = \frac{dC}{dt} = \frac{\partial C}{\partial t} + C \frac{\partial C}{\partial x} \tag{5}$$

The acceleration of a curve element thus has no component perpendicular to the x-axis.

It is sometimes convenient to have a wider definition of the velocity and acceleration of a curve element. Let again S (see fig. 2) be the position of the curve in question. Draw an arbitrary line L through P. The velocity of the curve element at P along the line L, may then be defined as

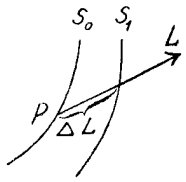

Fig. 2.

(6) $$C_L = \lim_{\Delta t \to 0} \left(\frac{\Delta L}{\Delta t} \right).$$

Analogously we may define the acceleration as

(7) $$A_L = \frac{dC_L}{dt},$$

and in analogy with (5) we may write:

(8) $$A_L = \frac{\partial C_L}{\partial t} + C_L \frac{\partial C_L}{\partial x}$$

when the x-axis coincides with the line L.

3. Choice of Systems of Co-ordinates. In order to obtain analytical expressions for the velocity and the acceleration of moving characteristic curves, it is convenient to consider the phenomenon in question relative to two systems of co-ordinates. In this paragraph we propose to develop general equations for the transformation from one system of co-ordinates to another.

Let

$$p = p\,(x, y, t)$$

be the pressure function in a system of co-ordinates (xy) which is fixed to the earth ($t =$ time).

Let

$$P = P(x', y', t)$$

be the pressure function in a moving system of co-ordinates ($x'\,y'$), and let the vector symbol ∇ denote the ascendant of a scalar function. We then have for the same individual particle:

(1) $$\frac{dp}{dt} = \frac{dP}{dt}$$

and

(2) $$\nabla p = \nabla P$$

The substantial derivatives with regard to t may be written:

(3) $$\frac{dp}{dt} = \frac{\partial p}{\partial t} + \boldsymbol{V} \cdot \nabla p$$

where $\boldsymbol{V}$ is the velocity of the particle in the fixced system of co-ordinates. Likewise we have:

(4) $$\frac{dP}{dt} = \frac{\partial P}{\partial t} + \boldsymbol{V}' \cdot \nabla P$$

where $\boldsymbol{V}'$ is the velocity of the particle relative to the moving system of co-ordinates.

Subtracting (4) from (3), and substituting (1) and (2), we get:

$$0 = \frac{\partial p}{\partial t} - \frac{\partial P}{\partial t} + (\boldsymbol{V} - \boldsymbol{V}') \cdot \nabla p$$

Putting $(\boldsymbol{V} - \boldsymbol{V}') = \boldsymbol{C} =$ the velocity of the moving system of co-ordinates, we may write:

(5) $$\frac{\partial P}{\partial t} = \frac{\partial p}{\partial t} + \boldsymbol{C} \cdot \nabla p$$

which is the equation of transformation. $\frac{\partial P}{\partial t}$ then stands for the local pressure variation in the moving system of co-ordinates, and $\frac{\partial p}{\partial t}$ is the local variation (or the pressure tendency) observed at a fixed station.

A ship furnished with a barograph, and sailing with the velocity C in a pressure field whose ascendant is ∇p, where the barometric tendency is $\frac{\partial p}{\partial t}$, would record a pressure variation equal to $\frac{\partial P}{\partial t}$.

Instead of choosing different notations for the pressure functions in the two systems of co-ordinates, it is admissible to choose different symbols for the differentiations with respect to the two sets of variables. Choosing the symbol ∂ for differentiation in the fixed system, and δ in the moving one, and realizing that the transformation is valid for any function, we may write symbolically:

$$\frac{\delta}{\delta t} = \frac{\partial}{\partial t} + \boldsymbol{C} \cdot \nabla \tag{6}$$

and this equation multiplied symbolically by any scalar function φ, gives the general equation of transformation.

The second derivative with respect to time in the moving system of co-ordinates is found by applying the operator defined by (6) once more, viz:

$$\frac{\delta^2}{\delta t^2} = \frac{\partial\left(\frac{\partial}{\partial t} + \boldsymbol{C} \cdot \nabla\right)}{\partial t} + \boldsymbol{C} \cdot \nabla\left(\frac{\partial}{\partial t} + \boldsymbol{C} \cdot \nabla\right),$$

which developed gives:

$$\frac{\delta^2}{\delta t^2} = \frac{\partial^2}{\partial t^2} + 2\boldsymbol{C} \cdot \nabla \frac{\partial}{\partial t} + \frac{\partial \boldsymbol{C}}{\partial t} \cdot \nabla + \boldsymbol{C} \cdot \nabla (\boldsymbol{C} \cdot \nabla) \tag{7}$$

which is the general formula for the transformation of the second derivative in a moving system of co-ordinates.

Interpreting $\boldsymbol{C}$ as the velocity of an element of a characteristic curve, it follows that $\boldsymbol{C}$ is permanently directed along the x-axis. We, therefore. have:

$$\boldsymbol{C} \cdot \nabla = C \frac{\partial}{\partial x}$$

$$2\boldsymbol{C} \cdot \nabla \frac{\partial}{\partial t} = 2C \frac{\partial^2}{\partial x \partial t}$$

$$\frac{\partial \boldsymbol{C}}{\partial t} \cdot \nabla = \frac{\partial C}{\partial t} \frac{\partial}{\partial x}$$

$$\boldsymbol{C} \cdot \nabla (\boldsymbol{C} \cdot \nabla) = C \frac{\partial}{\partial x}\left(C \frac{\partial}{\partial x}\right) = C \frac{\partial C}{\partial x} \frac{\partial}{\partial x} + C^2 \frac{\partial^2}{\partial x^2}$$

Substituting in (6), we get

$$\frac{\delta}{\delta t} = \frac{\partial}{\partial t} + C \frac{\partial}{\partial x} \tag{8}$$

Equation (7) now becomes

$$\frac{\delta^2}{\delta t^2} = \frac{\partial^2}{\partial t^2} + 2C \frac{\partial^2}{\partial x \partial t} + \left(\frac{\partial C}{\partial t} + C \frac{\partial C}{\partial x}\right) \frac{\partial}{\partial x} + C^2 \frac{\partial^2}{\partial x^2}$$

Substituting again from 2 (5) we get

$$\frac{\delta^2}{\delta t^2} = \frac{\partial^2}{\partial t^2} + 2C \frac{\partial^2}{\partial x \partial t} + C^2 \frac{\partial^2}{\partial x^2} + A \frac{\partial}{\partial x} \tag{9}$$

which is the most convenient equation for the transformation. The particular choice of system of co-ordinates, naturally, does not encroach on the generality of the equations (8) and (9).

The term $\frac{\delta^2}{\delta t^2}$, when applied to pressure, may be interpreted as the 'curvature' of the barogram recorded on a ship that sails with the velocity C and acceleration A along a line where the pressure variations at a fixed station are definedby $\frac{\partial^2 p}{\partial t^2}, \frac{\partial^2 p}{\partial x \partial t}, \frac{\partial^2 p}{\partial x^2}$ and $\frac{\partial p}{\partial x}$.

4. Velocity and Acceleration of a Characteristic Curve. According to the definition of a characteristic curve, we have:

(1) $$p_{lmn} = \text{constant.}$$

In a system of co-ordinates that moves with the curve element in question, we must have:

(2) $$\frac{\delta p_{lmn}}{\delta t} = 0$$

or more generally:

(3) $$\frac{\delta^i p_{lmn}}{\delta t^i} = 0$$

Applying the operator defined by **3** (8), we get from (2):

(4) $$\frac{\partial p_{lmn}}{\partial t} + C \frac{\partial p_{lmn}}{\partial x} = 0$$

Putting

$$\frac{\partial p_{lmn}}{\partial t} = p_{lmn+1}$$

and

$$\frac{\partial p_{lmn}}{\partial x} = p_{l+1mn}$$

we get from (4)

(5) $$C = -\frac{p_{lmn+1}}{p_{l+1mn}}$$

which is the general formula for the instantaneous velocity along the x-axis of an element of a characteristic curve.

The acceleration of the curve element is obtained from (3) by putting $i = 2$ and applying the operator defined by **3** (9), to p_{lmn}, viz:

$$0 = \frac{\partial^2 p_{lmn}}{\partial t^2} + 2C \frac{\partial^2 p_{lmn}}{\partial x \partial t} + C^2 \frac{\partial^2 p_{lmn}}{\partial x^2} + A \frac{\partial p_{lmn}}{\partial x}$$

Writing

$$\frac{\partial^2 p_{lmn}}{\partial t^2} = p_{lmn+2} \text{ etc., we get}$$

(6) $$A = -\frac{p_{lmn+2} + 2C p_{l+1mn+1} + C^2 p_{l+2mn}}{p_{l+1mn}}$$

which is the general formula for the acceleration along the x-axis of an element of a characteristic curve defined by $p_{lmn} = \text{constant.}$

CHAPTER II.

THE DISPLACEMENT OF ISOBARS AND ISALLOBARS.

5. Velocity of the Isobars. The equations developed in Chapter I, may be used for deducing equations for the displacement of the isobars. With the symbols defined by **2** (1), we have for an individual isobar:

$$p_{000} = p = \text{constant.}$$

The velocity of the isobar is obtained by substituting $p_{lmn} = p_{000}$ in the general equation **4** (5), viz:

$$C_i = -\frac{p_{001}}{p_{100}} = -\frac{\frac{\partial p}{\partial t}}{\frac{\partial p}{\partial x}} \tag{1}$$

It is convenient to choose the x-axis normal to the isobar at the point in question, the positive direction of the x-axis pointing towards high pressure. $\frac{\partial p}{\partial x}$ then is the total pressure ascendant. For unit isobars we may then put

$$\frac{\partial p}{\partial x} = |\nabla p| = \frac{1}{h}$$

where h is the distance between two neighbouring unit isobars. Formula (1) then becomes

$$C_i = -\frac{\partial p}{\partial t} h \tag{2}$$

or, when we put $\frac{\partial p}{\partial t} = T =$ barometric tendency:

$$C_i = -Th \tag{3}$$

Thus, *the normal velocity of the isobar is equal to minus the tendency multiplied by the distance between unit isobars.* The velocity is positive when the tendency is negative and *vice versa.*

By means of formula (3) it is possible to evaluate the instantaneous velocity of displacement of the entire field of pressure. The formula may also be used for extrapolating the pressure distribution after a moderate interval of time. As the time unit in barometric tendencies is 3 hours, the extrapolated displacement of the isobar is equal to the instantaneous velocity multiplied by the number of 3-hour intervals. It is most convenient to use the distance between two 5 to 5 isobars and one fifth of the barometric tendency, one fifth being the tendency unit in the international code.

How far the displacement can be extrapolated depends on the acceleration, and in paragraph 7 we shall find a formula for the instantaneous acceleration. By discussing this formula we can estimate the constancy of the isobar velocity. In this connection we may note, that whereas both tendencies and pressure gradients may vary rather rapidly at a fixed station, the variations in a system of co-ordinates that follows the pressure system, generally are very small. This especially applies to the parts of the isobars which intersect the path of the pressure center.

From formula (3) we can also compute the variation in pressure gradient in the moving pressure system. Let p_1 and p_2 be two neighbouring isobars, whose velocities are C_1 and C_2 respectively. The instantaneous variation in h between these two isobars is $(C_2 - C_1)$. After an interval of time t, the distance h is given by

$$h = h_0 + (C_2 - C_1)\, t \tag{4}$$

and the pressure gradient is equal to $\frac{1}{h}$. Assuming the wind velocity to be proportional to the pressure gradient, a quantitative wind forecast can be obtained from equation (4).

The field of isallobars not only causes variations in the wind force, but also alters the wind direction.

The translation of the isobar is given by formula (3). The rotation is expressed by

$$\frac{\partial C_i}{\partial y} = -\left(I_y h + T\frac{\partial h}{\partial y}\right) \tag{5}$$

where I_y is the component of the isallobaric ascendant along the isobar, and T is the barometric tendency.

When the isallobars are parallel to the isobars, we have $I_y = 0$, and therefore

$$\frac{\partial C_i}{\partial y} = -T\frac{\partial h}{\partial y} \tag{6}$$

and the isobars veer for falling pressure when the isobars diverge.

When the isobars are parallel, we have $\frac{\partial h}{\partial y} = 0$, and hence

$$\frac{\partial C_i}{\partial y} = -I_y h \tag{7}$$

and $\frac{\partial C_i}{\partial y}$ has sign opposite to I_y.

For the estimation of the change in pressure distribution, it is important to note the position of the isallobars relative to the isobars.

6. Velocity of Isallobars. An isallobar is given by the equation

$$T = \frac{\partial p}{\partial t} = \text{constant}.$$

The velocity C_T of an isallobar is obtained from **4** (5) by substituting $p_{lmn} = p_{001} = T$, viz:

$$C_T = -\frac{p_{002}}{p_{101}} = -\frac{\frac{\partial T}{\partial t}}{\frac{\partial T}{\partial x}} \tag{1}$$

In a system of co-ordinates whose x-axis is perpendicular to the isallobar we have that $\frac{\partial T}{\partial x}$ is equal to the total isallobaric ascendant, when the positive direction of the x-axis points from low to high values of tendency. For unit isallobars we may write

$$\frac{\partial T}{\partial x} = |\nabla T| = \frac{1}{H},$$

where H is the distance between two neighbouring unit isallobars. Substituting in (1) we get

$$C_T = -\frac{\partial T}{\partial t}H = -\frac{\partial^2 p}{\partial t^2}H. \tag{2}$$

Formula (2) is completely analogous with the formula for the velocity of an isobar. The velocity is positive when the barogram is curved anticyclonically and *vice versa*.

When the tendency is uniform, $\frac{\partial T}{\partial t} = 0$ and, therefore, $C_T = 0$, except in the center of isallobaric systems, where $H = \infty$. C_T is then given by an indeterminate expression of the type $\frac{0}{0}$.

The quantity $\frac{\partial^2 p}{\partial t^2}$ may be computed from two consecutive values of barometric tendency. Conversely, if C_T can be obtained with sufficient accuracy from two consecutive (preferably three-hourly) weather charts, we may substitute for $\frac{\partial^2 p}{\partial t^2}$ by means of (2) (see paragraph 8).

The acceleration of the isallobars is easily obtained in the same way as the acceleration of the isobars (see paragraph 8). The equation for the acceleration would, however, contain the term $\frac{\partial^3 p}{\partial t^3}$, which, at present, is not obtainable from the weather charts.

Formula (2), however, gives the instantaneous displacement of the field of isallobars, and it is frequently important to calculate the movement of the system of isallobars relative to the pressure system. In general, there is little difference between the acceleration of the pressure system and the acceleration of the isallobaric system. We thus can obtain the relative displacement of the two systems with a high degree of approximation.

7. Acceleration of Isobars. With the symbols introduced in paragraph 2 we have for one individual isobar

$$p_{000} = p = \text{constant.}$$

The acceleration A_i of an element of the isobar along the x-axis is then obtained from **4** (6) by putting $p_{lmn} = p$. We then get:

$$A_i = -\frac{\frac{\partial^2 p}{\partial t^2} + 2\,C_i \frac{\partial^2 p}{\partial x \partial t} + C_i^2 \frac{\partial^2 p}{\partial x^2}}{\frac{\partial p}{\partial x}} \tag{1}$$

which is the general formula for the instantaneous acceleration along the x-axis of an element of the isobar.

It is convenient to choose the x-axis normal to the isobar. The various terms in (1) then have the following meanings:

$\frac{\partial p}{\partial x}$ is the total pressure ascendant.

$\frac{\partial^2 p}{\partial t^2}$ is the 'curvature' of the barogram (or more accurately, the local variation in tendency).

$\frac{\partial^2 p}{\partial x \partial t}$ is the component of the isallobaric ascendant normal to the isobar.

$\frac{\partial^2 p}{\partial x^2}$ is the 'curvature' of the pressure profile.

All quantities in (1), except $\frac{\partial^2 p}{\partial t^2}$, can be obtained from one single weather chart.

The acceleration, however, depends largely on the curvature of the barogram, which, unfortunately, is not contained in the international code for synoptic information. Over West-Europe, however, where three-hourly observations are common, $\frac{\partial^2 p}{\partial t^2}$ can be computed with fair accuracy from two consecutive weather charts.

8. **Discussion of the Preceeding Formulae.** (a) In the paragraphs 5 and 7 we have found expressions for the velocity and acceleration of the isobars. If these quantities were given as functions of time, the problem of predicting the pressure distribution would be completely solved. The formulae **5** (3) and **7** (1), however, give only the instantaneous velocity and acceleration. By means of these formulae, the instantaneous kinematical state of the pressure systems can be diagnosed. For the dynamical analysis of the weather charts, these formulae are indispensible.

The future position of the isobars may be extrapolated over a moderate interval of time by means of the formula

$$S = C_i t + \frac{1}{2} A_i t^2 \tag{1}$$

where S is the displacement along the initial normal, and t is the forecasting period.

(b) According to **5** (3) and **7** (1) we have

$$C_i = -Th \tag{2}$$

and

$$A_i = -\frac{\frac{\partial^2 p}{\partial t^2} + 2\,C_i \frac{\partial^2 p}{\partial x \partial t} + C_i^2 \frac{\partial^2 p}{\partial x^2}}{\frac{\partial p}{\partial x}} \tag{3}$$

Introducing as previously $\frac{\partial p}{\partial x} = \frac{1}{h}$, we get

$$\frac{\partial^2 p}{\partial x^2} = -\frac{1}{h^2}\frac{\partial h}{\partial x}$$

where h is the positive distance between two consecutive unit isobars.

Putting $\frac{\partial^2 p}{\partial x \partial t} = I_x =$ the x-component of the isallobaric ascendant, and substituting in (3), we get

$$A_i = -\frac{\partial^2 p}{\partial t^2} h - 2 C_i I_x h + \frac{C_i^2}{h}\frac{\partial h}{\partial x} \tag{4}$$

(c) *Uniformly changing pressure.* The term $\frac{\partial^2 p}{\partial t^2}$ depends on the curvature of the barogram. It is positive when the barogram is curved cyclonically, and negative when curved anticyclonically. When the pressure change is uniform it is zero.

Uniformly changing pressure generally occurs in places on the chart where there is no (or very slight) isallobaric gradient, or, in other words, in the centers of the isallobaric systems. In such areas we have $\frac{\partial^2 p}{\partial t^2} = 0$, and $I_x = 0$. From (4) we then get

$$A_i = \frac{C_i^2}{h}\frac{\partial h}{\partial x}$$

Substituting from (2), we get

$$A_i = T^2 h \frac{\partial h}{\partial x} \tag{5}$$

If, in such areas, the isobars are equidistant, we have $\frac{\partial h}{\partial x} = 0$, and hence:

$$A_i = 0.$$

This case frequently occurs in the front and in the rear of moving cyclones and anticyclones. It is in such areas that the isobar velocity is constant, in which case the extrapolation may be performed by means of the simple formula

$$S = C_i t = -Th\,t \tag{6}$$

Uniformly changing pressure generally also occurs in the warm sector, where the isobars are equidistant. We then have $\frac{\partial^2 p}{\partial t^2} = 0$ and $\frac{\partial h}{\partial x} = 0$. From (4) we then get

$$A_i = -2\,C_i I_x h = 2\,T I_x h^2. \tag{7}$$

If I_x is zero, there is no acceleration, and if $T = 0$, there is neither velocity nor acceleration.

(d) *Tendency equal to zero*: In such cases we have $C_i = 0$, and therefore

$$A_i = -\frac{\partial^2 p}{\partial t^2} h \tag{8}$$

This case generally occurs in the vicinity of the symmetry line in troughs and wedges, and also in the vicinity of a line through the pressure center and normal to the path of the center. In such areas formula (6) fails to be of any value for extrapolating the pressure distribution, the displacement then depending on the acceleration only.

In the next two chapters we shall develop some convenient formulae for calculating the pressure distribution in the vicinity of troughs, wedges and pressure centers. The difficulties arising in these areas where the term $\frac{\partial^2 p}{\partial t^2}$ is predominating, can thus be overcome.

9. Evaluation on the Weather Chart. Returning again to the complete equations for velocity and acceleration, we may endeavour to express the various quantities in terms which are most easily obtained from the weather chart.

The formula for velocity is most easily evaluated by means of 8 (2). The formula for the acceleration may be expressed in simple terms.

The term which is least easily obtained is the one which contains $\frac{\partial^2 p}{\partial t^2}$ (see f. inst. 8 (4)). This quantity may be obtained from two consecutive (preferably three-hourly) values of barometric tendency, viz[1]):

$$\frac{\partial^2 p}{\partial t^2} = T_1 - T_0 \tag{1}$$

or from three consecutive pressure observations, viz:

$$\frac{\partial^2 p}{\partial t^2} = (p_2 - p_1) - (p_1 - p_0). \tag{2}$$

It is recommended, whenever possible, to apply three consecutive pressure observations, because the barometer readings are much more reliable than are the estimates of the variations of the barograph.

[1]) In the following formulae for numerical differentiations we choose the time unit equal to the tendency interval (3 hours), and in accordance with common practice, we drop the notations for dimensions.

In most countries, the morning chart is the one that is the most important for the forecasting service. The time interval from the evening chart to the morning one is, however, too large for computing $\frac{\partial^2 p}{\partial t^2}$ as well as similar quantities in the equations of the succeeding chapters. It would, therefore, be an immense advantage if night observations, at least of pressure and tendency, were more common. Still more advantageous would be if the night observations were postponed to 4 o'clock G M T. In the morning, the forecaster would then have two complete pressure and tendency charts at intervals of three hours. From such charts, differentials could be obtained with sufficient accuracy.

The term $\frac{\partial^2 p}{\partial t^2}$ can also be obtained when the velocity of the isallobar can be evaluated with sufficient accuracy from two (preferably 3-hourly) weather charts. From **6** (1) we get

$$\frac{\partial^2 p}{\partial t^2} = -\frac{C_T}{H} \tag{3}$$

where C_T is the velocity of the isallobar, and H is the positive distance between two neighbouring isallobars.

The first component of the acceleration as given by 8 (4), may now be written in the alternative forms:

$$A_i' = \left\{ \begin{array}{l} -(T_1 - T_0)\, h \\ -(p_2 - 2p_1 + p_0)\, h \\ + C_T \frac{h}{H} \end{array} \right\} \tag{4}$$

The two other components of the acceleration can be computed from one single weather chart.

Putting $I_x = \frac{1}{H_x}$, where H_x is the distance between the points of intersection between the x-axis (which is normal to the isobars, see fig. 3) and two consecutive unit isallobars, we get for the second term in 8 (4)

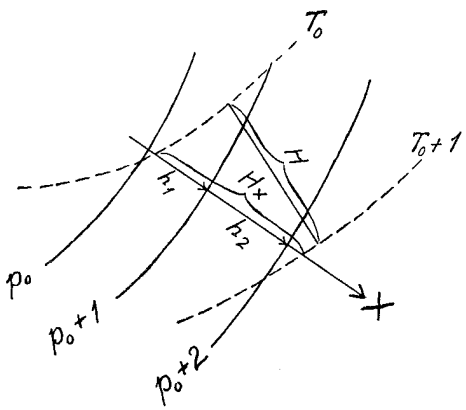

Fig. 3, showing the various quantities in the acceleration formula.

$$A_i'' = -2\, C_i \frac{h}{H_x} = 2\, T\, \frac{h^2}{H_x} \tag{5}$$

The third component is also easily evaluated. Let h_1 and h_2 be the distances between two consecutive pairs of isobars (see fig. 3). For the middle isobar $(p_0 + 1)$ we may put $h = \frac{1}{2}(h_1 + h_2)$ and $\frac{\partial h}{\partial x} = \frac{h_2 - h_1}{\frac{1}{2}(h_2 + h_1)}$. Furthermore:

$$C_i^2 = T^2 h^2 = T^2 \frac{(h_2 + h_1)^2}{4}.$$

Substituting we get:

$$A_i''' = T^2 (h_2 - h_1). \tag{6}$$

The total acceleration is then given by

$$A_i = A_i' + A_i'' + A_i'''. \tag{7}$$

In general, there are frequently simple areas on the chart where the displacement of the isobars may be computed without acceleration, or without some of the terms in the acceleration formula. It is, therefore, important to pick out the easy areas

and carry out the calculations there. In this way one can, in the majority of cases, get a good picture of the future pressure distribution without much computation.

The following table exhibits the various forms of the acceleration formula according to different types of pressure fields.

Table 1. Types of pressure fields and corresponding formulae for the acceleration of the isobars.

Description	Formula
Uniformly changing pressure.	$\frac{2Th^2}{H_x} + T^2(h_2 - h_1)$
Center of isallobars.	$T^2(h_2 - h_1)$
Center of isallobars on equidistant isobars.	Zero
Equidistant isobars.	$\left.\begin{matrix}(T_1 - T_0)\,h \\ C_T\frac{h}{H}\end{matrix}\right\} + 2T\frac{h^2}{H_x}$
On the zero-isallobar.	$(T_1 - T_0)h$ or $C_T\frac{h}{H}$

The writer is aware that the acceleration does not remain a constant. Equation 8 (1) gives only the first two terms in the series which can give accurate values for the displacement. Under present conditions the writer considers it useless to develop the terms of higher order. Even if such terms could be obtained, the series would converge only within a certain interval, and, at present, no estimate can be made as to the interval of convergence.

The formula for the velocity of the isobars gives by itself the actual instantaneous state of motion. By means of this simple formula only, a complete diagnosis can be carried out, and the evaluation of the instantaneous displacement of the pressure field is an important step from the completed physical analysis to the prognosis.

The accuracy which can be obtained depends largely on the accuracy of the observations. Accidental errors in the observations can generally be neutralized by a thorough analysis and an intelligent smoothing of the fields of pressure and tendency. It is, therefore, necessary that the observations should be critically analysed, and that the values which are put in the formulae, should be taken from the carefully drawn isolines, and not from the individual observations.

CHAPTER III.
THE MOVEMENT OF TROUGHS AND WEDGES.

10. Introduction. In the previous chapter we have seen how the future distribution of pressure may be computed by means of the equations for velocity and acceleration of the isobars. In the areas of the charts where the barogram has large curvature, some technical difficulties arise, because it frequently is difficult to obtain approximate values for the quantity $\frac{\partial^2 p}{\partial t^2}$. This quantity is particularly large during the passage of troughs, wedges and pressure centers. The aim of this chapter, therefore, is to develop some convenient means for computing the displacement of the pressure field in the vicinity of troughs and wedges. In chapter IV, pressure centers will be subjected to a similar examination.

The mathematical deductions being the same for troughs and wedges, it is inconvenient throughout to write both words. We shall, therefore, speak of *troughs* only, remembering that the results subsequently obtained, are applicable to both pressure formations.

The problem of calculating the displacement of a trough may be divided in two parts: (a) to compute the displacement of the trough line (which will presently be defined), and (b) to compute the variations in pressure in a system of co-ordinates which is fixed to the moving trough line. The second problem will be treated in chapter VI.

11. Definition of a Trough Line. Roughly speaking we may say that the pressure distribution exhibits a trough (or a wedge) when the isobars are curved in such a way that there is maximum of curvature along a line in the pressure field. We shall call this line the trough line.

In fig. 4 a and b are given two types of troughs. In fig. a the pressure gradient normal to the trough line is zero. In fig. b the pressure gradient normal to the trough line is different from zero. In both these cases we choose the x-axis tangential to the isobars with origin at the point of intersection between the isobar and the trough line.

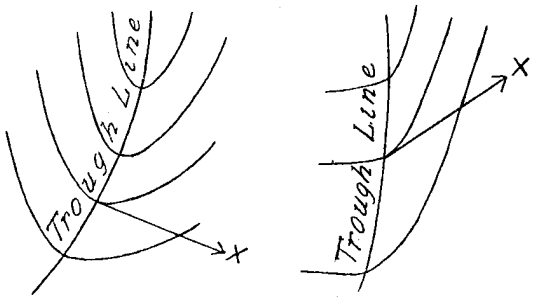

Fig. 4 a and b.

The trough line is then characterized by the following conditions:

$$(1) \qquad \frac{\partial p}{\partial x} = 0 \quad \text{and} \quad \frac{\partial^2 p}{\partial x^2} \gtrless 0 .$$

The second condition means that the isobars are not straight lines.

Troughs in the current sense of the word, are frequently accompanied by fronts, which cause a discontinuous distribution of pressure gradient and pressure tendency along the trough line. We shall here exclude these kinds of troughs, and treat them separately in chapter V. To the conditions previously stated we may, therefore, add one more, namely, that the quantities $\frac{\partial p}{\partial t}$ and $\frac{\partial p}{\partial x}$ shall be continuous functions of x in the vicinity of the trough line.

The conditions (1) are the necessary but not the sufficient conditions for having a pressure trough in the usual meaning of the word. The conditions are fulfilled for any line that cuts curved isobars, when the system of co-ordinates has been chosen as

specified above. We may, therefore, deduce equations for any such line and apply them to pressure troughs.

The trough is finally characterized by the condition that the pressure profile along the x-axis has maximum of curvature on the trough line.

Let σ denote the curvature of the profile. We may then write

$$\sigma = \frac{\frac{\partial^2 p}{\partial x^2}}{\left(1 + \left(\frac{\partial p}{\partial x}\right)^2\right)^{\frac{3}{2}}} = \frac{p_{200}}{(1 + p^2_{100})^{\frac{3}{2}}} \tag{2}$$

On the trough line, we have by definition, $p_{100} = 0$, and hence:

$$\sigma = p_{200}.$$

The condition of maximum or minimum of curvature is found from (2) by differentiating with regard to x, and equating to zero, viz:

$$\frac{\partial \sigma}{\partial x} = \frac{p_{300}(1 + p^2_{100}) - 3p^2_{200}p_{100}}{(1 + p^2_{100})^{\frac{5}{2}}} = 0. \tag{3}$$

Again we have as an initial condition that $p_{100} = 0$, and hence

$$\frac{\partial \sigma}{\partial x} = p_{300} = 0. \tag{4}$$

Summing up we get the following initial condition for a trough line:

(a) $p_{100} = 0$ and continuous
(b) $p_{200} \gtrless 0$ » »
(c) $p_{300} = 0$ » »

Condition (c) says that there is maximum or minimum of curvature along the trough line. For the deduction of the following equations it is immaterial whether there is maximum or minimum. This feature is worth noticing, because, in the next chapter we shall apply the equations to lines where there is minimum of curvature.

12. Velocity of Trough Lines. In order to obtain an expression for the velocity of a trough line, we must specify some permanent condition which the trough line shall obey during its motion. In order to do this we propose to develop an equation for the velocity along the x-axis of the point which always has maximum of curvature.

The condition of maximum of curvature is expressed by **11** (3), viz:

$$\frac{\partial \sigma}{\partial x} = \frac{p_{300}(1 + p^2_{100}) - 3p^2_{200}p_{100}}{(1 + p^2_{100})^{\frac{5}{2}}} = 0. \tag{1}$$

The permanent condition which the trough line must obey, therefore, is:

$$\frac{\delta}{\delta t}\left(\frac{\partial \sigma}{\partial x}\right) = 0. \tag{2}$$

The trough line thus corresponds to the definition of a characteristic line as given in paragraph 2. The velocity of an element of such a line, normal to its initial position, is obtained by substituting (2) in equation **4** (5)[1]), viz:

$$C_L = -\frac{\frac{\partial^2 \sigma}{\partial x \partial t}}{\frac{\partial^2 \sigma}{\partial x^2}} \tag{3}$$

[1]) See foot-note pag. 6.

From (1), we get:

$$\frac{\partial^2\sigma}{\partial x\partial t} = \frac{p_{301}(1+p^2_{100}) + p_{100}(2p_{300}p_{101} - 3p_{201}p_{101} - 3p_{200}p_{102}) - 3p^2_{200}p_{101}}{(1+p^2_{100})^{\frac{5}{2}}}$$

$$- 5\frac{p_{300} + p_{300}p^2_{100} - 3p_{200}p_{100}p_{101}}{(1+p^2_{100})^{\frac{7}{2}}} p_{101}p_{100}.$$

Introducing here the initial conditions: $p_{300} = p_{100} = 0$, we get:

$$\frac{\partial^2\sigma}{\partial x\partial t} = p_{301} - 3p^2_{200}p_{101}. \tag{4}$$

Likewise, we get by differentiating **11** (3) with respect to x and introducing the initial conditions:

$$\frac{\partial^2\sigma}{\partial x^2} = p_{400} - 3p^3_{200}. \tag{5}$$

Substituing in (3), we get:

$$C_L = \frac{p_{101} - \frac{p_{301}}{3p^2_{200}}}{p_{200} - \frac{p_{400}}{3p^2_{200}}} \tag{6}$$

which is the general formula for the instantaneous velocity of an element of the trough line along the chosen x-axis. If the trough is of the type given in fig. 4 a, the velocity is normal to the trough line. In any case the velocity is tangential to the isobar at the trough line.

Formula (6) contains two coefficients of high order, namely, p_{301} and p_{400}, both of which are exceedingly small. In relative units (which we shall explain in paragraph 14) p_{301} and p_{400} are of an order of magnitude 10^{-2} whereas p_{200} is of the order 10^1, and p_{101} is of the order 10^0.

We, therefore, get the following magnitudes:

$$p_{101} \sim 10^0$$
$$p_{200} \sim 10^1$$
$$\frac{p_{301}}{3p^2_{200}} \sim 10^{-4}$$
$$\frac{p_{400}}{3p^2_{200}} \sim 10^{-4}$$

Neglecting the terms of high order, we get from (6)

$$C_L = -\frac{p_{101}}{p_{200}} \tag{7}$$

which formula in all practical cases, may be applied without any noticeable inaccuracy.

Formula (7) is not only an approximate expression for the velocity of the trough line. It also has a stringent mathematical interpretation. Comparing (7) with the general formula **4** (5) for the velocity of a characteristic line, we see that formula (7) represents the velocity of a characteristic line defined by

$$p_{100} = \text{constant}.$$

At the initial instant we have $p_{100} = 0$, which only means that the isobar at the trough line is tangential to the x-axis. If the trough line moves without rotating, then would $p_{100} = 0$ hold at any instant for the trough line. This condition could then be taken as a permanent condition for the trough line. We would then get:

$$\frac{\delta p_{100}}{\delta t} = 0.$$

The velocity C'_L of this line would, according to **4** (5), be:

$$C'_L = -\frac{p_{101}}{p_{200}}. \tag{7'}$$

When the trough line rotates during its motion there would still be a line along which the condition $p_{100} = 0$ is a permanent condition, but this line would coincide with the trough line at the initial moment only. Formula (7), therefore, represents the velocity of the element of the isobar which is tangential to the x-axis.

Fig. 5 represents the trough line L and its position L_1 after an interval of time t. The line L' represents the position of the line defined by $p_{100} = 0$ at $t = t_1$. This line is in all practical cases hardly distinguishable from the trough line itself. The more pronounced the trough is, the closer does the line L follow the line L'. Noticeable discrepancies occur only when the trough is very indistinct because then p_{200} is small. In all practical cases we may, therefore, reckon with the simplified formula (7).

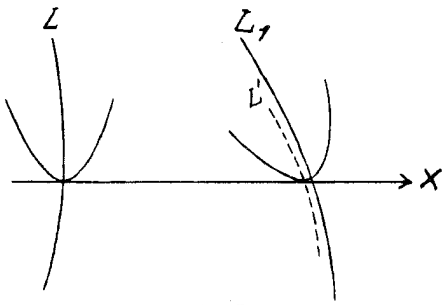

Fig. 5.

The quantities p_{101} and p_{200} as well as p_{301} and p_{400} are obtainable from one single weather chart. The velocity is, therefore, uniquely determined by the actual instantaneous state of affairs.

The coefficients in (7) and (7') may be interpreted in simple terms. p_{101} is the x-component of the isallobaric ascendant, or, approximately, the difference in tendency between the front and the rear of the trough. p_{200} is, as we have previously shown, the curvature of the pressure profile along the x-axis.

The formulae (7) and (7') are never indeterminate expressions, because, by definition we have $p_{200} \gtrless 0$, and neither p_{101} nor p_{200} are indeterminate at the trough line (see paragraph 11).

p_{200} is negative for wedges, and positive for troughs. A wedge, therefore, moves in the direction of the isallobaric ascendant, and a trough moves in the direction of the isallobaric gradient. The steeper the pressure profile, the slower the motion.

When the trough is accompanied by a front, p_{101} and p_{200} are discontinuous at the trough line. In chapter V we shall see that front troughs obey a formula similar to (7), the differentials p_{101} and p_{200} being then replaced by finite differences.

13. Acceleration of Trough Lines. In the last paragraph we have shown that the trough line corresponds to the definition of a characteristic line, defined by the permanent condition

$$\frac{\delta}{\delta t}\left(\frac{\partial \sigma}{\partial x}\right) = 0.$$

The acceleration of an element of such a line is then obtained from the general equation **4** (6)[1]) by substituting $\frac{\partial \sigma}{\partial x}$ for p_{lmn}. We then get:

$$A_L = -\frac{\frac{\partial^3 \sigma}{\partial x \partial t^2} + 2\,C_L \frac{\partial^3 \sigma}{\partial x^2 \partial t} + C^2{}_L \frac{\partial^3 \sigma}{\partial x^3}}{\frac{\partial^2 \sigma}{\partial x^2}} \tag{1}$$

[1]) See foot-note pag. 6.

The initial conditions of the trough line are, as stated in paragraph 12:

$$p_{100} = p_{300} = 0. \tag{2}$$

The curvature σ is given by **11** (2), viz:

$$\sigma = \frac{p_{200}}{(1 + p^2_{100})^{\frac{3}{2}}}. \tag{3}$$

From (3) we get some exceedingly long expressions for the various terms in formula (1). As our problem is to deduce a formula for the instantaneous acceleration at the initial moment, we may introduce the initial conditions (2). We then get:

$$\frac{\partial^3\sigma}{\partial x \partial t^2} = p_{302} - 12\, p_{201}\, p_{200}\, p_{101} - 3 p^2_{200}\, p_{102}. \tag{4}$$

$$\frac{\partial^3\sigma}{\partial x^2 \partial t} = p_{401} - 9 p^2_{200} p_{201}. \tag{5}$$

$$\frac{\partial^3\sigma}{\partial x^3} = p_{500}. \tag{6}$$

$$\frac{\partial^2\sigma}{\partial x^2} = p_{400} - 3 p^3_{200}. \tag{7}$$

In paragraph 12 we have shown that p_{400} is completely negligible in comparison with $3\, p^3_{200}$. Therefore, substituting (4)—(7) in (1), and writing down each term of (1) separately, we get:

$$-\frac{\frac{\partial^3\sigma}{\partial x \partial t^2}}{\frac{\partial^2\sigma}{\partial x^2}} = A'_L = \frac{p_{302}}{3 p^3_{200}} - \frac{4\, p_{201} p_{101} + p_{200} p_{102}}{p^2_{200}} \tag{8}$$

The first term on the right hand side is in the relative units mentioned in paragraph 12, of the order 10^{-4}, whereas the last term is of the order 10^{-1}. Neglecting the first term, we get:

$$A'_L = -\frac{4\, p_{201} p_{101} + p_{200} p_{102}}{p^2_{200}}. \tag{9}$$

The second term in (1) may be written, when we substitute for C_L by means of **12** (7):

$$-2 C_L \frac{\frac{\partial^3\sigma}{\partial x^2 \partial t}}{\frac{\partial^2\sigma}{\partial x^2}} = A''_L = -\frac{2}{3}\frac{p_{101}}{p^4_{200}} p_{401} + 6\frac{p_{201} p_{101}}{p^2_{200}}.$$

The first term on the right hand side is negligible in comparison with the second, because its order of magnitude is 10^{-5}, whereas, the second term is of the order 10^{-1}. Neglecting the first term we get:

$$A''_L = \frac{6\, p_{201} p_{101}}{p^2_{200}}. \tag{10}$$

The third part of formula (1) may be written, when we again substitute for C_L:

$$-C^2_L \frac{\frac{\partial^3\sigma}{\partial x^3}}{\frac{\partial^2\sigma}{\partial x^2}} = A''' = \frac{p^2_{100} p_{500}}{3 p^5_{200}} \tag{11}$$

If the pressure profile is symmetrical with respect to the trough line in its immediate vicinity, p_{300} is, as shown previously, equal to zero. This condition is identical

with the condition of maximum of curvature. If the symmetry exists apart from the immediate vicinity, the next odd derivative (i. e. p_{500}) must be equal to zero. For symmetrical troughs, therefore, $p_{500} = 0$. This condition corresponds to symmetry in curvature.

Even if p_{500} is of the same order of magnitude as p_{400}, which is negligible in comparison with $3p^3_{200}$, we get A'''_L of the order 10^{-6}, at most.

The three components of the acceleration as given by (9), (10) and (11), therefore, have the following orders of magnitude:

$$A'_L \sim 10^{-1}$$
$$A''_L \sim 10^{-1}$$
$$A'''_L \sim 10^{-6}$$

Neglecting the last component, we get instead of (1):

$$A_L = -\frac{p_{102}p_{200} - 2p_{101}p_{201}}{p^2_{200}} \tag{12}$$

which is the most convenient formula for calculating the acceleration of the trough line.

The coefficients in (12) may be interpreted in simple terms: p_{101} and p_{200} have the meanings explained in paragraph 12. p_{102} is the difference in tendency variations between the front and the rear of the trough. p_{201} is the difference in the x-component of the isallobaric ascendant between the front and the rear of the trough. The evaluation of the coefficients from the data of the weather charts will be demonstrated in paragraph 14.

Equation (12) has a very simple interpretation. If we, (as shown in fig. 5) instead of computing the acceleration of the trough line L, endeavour to calculate the acceleration of the line L', which defines the place where the isobars are tangential to the x-axis, we would have to put (as shown in paragraph 12), as a permanent condition of this line,

$$\frac{\delta p_{100}}{\delta t} = 0.$$

From the general formula **4** (6) for the acceleration of a characteristic line, we would get:

$$A'_L = -\frac{p_{102} + 2C'_L p_{201} + C^2_L p_{300}}{p_{200}} \tag{13}$$

At the initial moment this line coincides with the trough line where, by definition $p_{300} = 0$. We, therefore, get:

$$A'_L = -\frac{p_{102} + 2C'_L p_{201}}{p_{200}}$$

which after substitution from **12** (7') gives

$$A_L' = -\frac{p_{102}p_{200} - 2p_{101}p_{201}}{p^2_{200}} \tag{14}$$

which is identical with (12).

The equation **12** (7) and (12) give approximations of high order for the instantaneous velocity and acceleration of the trough line. Their stringent mathematical significance is explained above.

In the next paragraph we shall explain the facile evaluation of these formulae on the weather chart.

14. Evaluation on Weather Charts. The velocity and the acceleration of an element of the trough line are determined by 4 coefficients, which depend on the distribution of pressure and pressure tendencies. These coefficients are most accurately determined by graphical methods.

Fig. 6 represents the distribution of pressure and pressure tendencies in the vicinity of a trough, the full lines representing isobars and the dotted lines isallobars. L is the trough line. Draw the x-axis through the point P, tangential to the isobar or, in the present case, normal to the trough line.

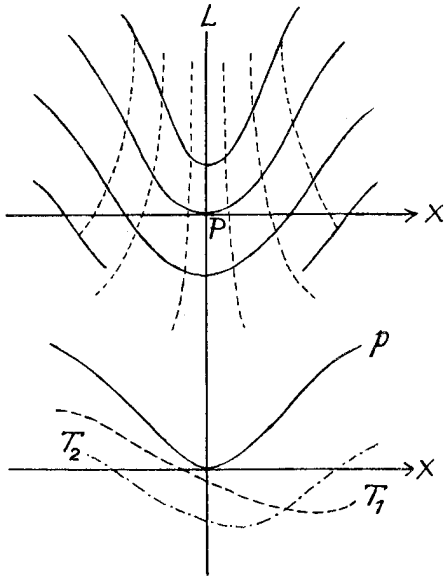

Fig. 6.

In fig. 6 below, the pressure profile along the x-axis is represented by curve p. Curve T_1 represents the distribution of tendencies along the x-axis at the instant of the chart above. Let curve T_2 represent the distribution of tendencies along the same line on the previous chart. We may then evaluate the four coefficients from these curves in the following manner:

p_{101} is obtained by graphical differentiation of curve T_1.

p_{200} by differentiating curve p twice.

p_{201} by differentiating curve T_1 twice.

p_{102} is finally obtained by differentiating graphically the difference between the curves T_1 and T_2.

In this way the most accurate results are obtained.

It is, however, quicker and sufficiently accurate to evaluate the coefficients by means of the well-known formulae for numerical differentiation.[1]) This differentiation is most easily performed in the following manner:

Choose an arbitrary unit of length, and mark the points (1,0), (1/2,0), (0,0), (— 1/2,0) and (— 1,0) on the chosen x-axis. Let p^{xy} and T^{xy} signify pressure and the three-hourly pressure tendency at the point (xy), and let $\triangle T^{xy}$ denote the three-hourly change in pressure tendency (or half of the 6-hourly change). With these notations we get the following approximate values for the coefficients:

$$\left.\begin{aligned} p_{101} &= T^{\frac{1}{2},0} - T^{-\frac{1}{2},0} \\ p_{200} &= p^{1,0} - 2p^{0,0} + p^{-1,0} \\ p_{102} &= \triangle T^{\frac{1}{2},0} - \triangle T^{-\frac{1}{2},0} \\ p_{201} &= T^{1,0} - 2\,T^{0,0} + T^{-1,0} \end{aligned}\right\} \quad (1)$$

It is important to choose a unit of length which is convenient in each particular case. In general, the length unit should be chosen as large as possible in order to neutralize the effect of inaccurate tendency values. Moreover, as the pressure tendencies are given as change per three hours, it follows, that the tendencies observed immediately behind the trough may be influenced by the pressure variation before and after the passage of the trough. For this reason also it is advantageous to choose the unit as large as possible.

On the other hand, the choice of length unit depends on the pressure and the tendency profiles. Let p represent the pressure profile and T the tendency profile

[1]) See Runge-König: Numeriches Rechnen. Berlin 1924.

along the x-axis (see fig. 7). The unit of length should be chosen in such a way that the approximate formulae for numerical differentiation give the closest approximations to the true differentials. We shall, therefore, have to choose the unit of length partly to satisfy the pressure profile and partly to satisfy the tendency profile. The question then arises: which of the profiles carry the largest weight for determining the displacement? The velocity is given by the formula **12** (7) viz:

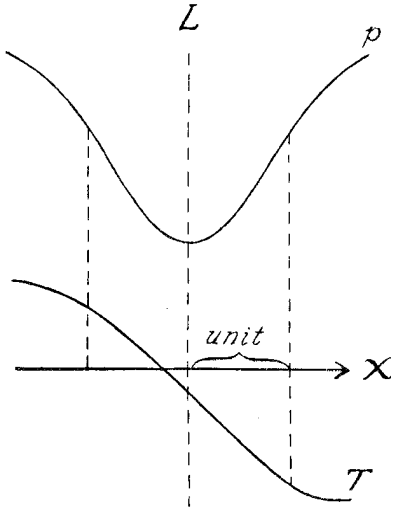

Fig. 7.

$$C_L = -\frac{p_{101}}{p_{200}}.$$

The variation in C_L with respect to p_{101} is:

$$\frac{\partial C_L}{\partial p_{101}} = -\frac{1}{p_{200}}.$$

Similarily we get the variation with respect to the value of p_{200}, viz:

$$\frac{\partial C_L}{\partial p_{200}} = -\frac{p_{101}}{p^2_{200}}.$$

Now, p_{101} is of the order 10^0 whereas p_{200} is of the order 10^1. We therefore get:

$$\frac{\partial C_L}{\partial p_{101}} \sim 10^{-1} \text{ and } \frac{\partial C_L}{\partial p_{200}} \sim 10^{-2}.$$

Thus p_{101} (the ascendant of the tendency) carries much more weight than does p_{200}. It is, therefore, recommended to choose the length unit in such a way that the most accurate value for p_{101} is obtained. Simultaneously the length unit should be chosen as large as possible in order to render the errors in the tendency values ineffective. In fig. 7 the most convenient unit is marked. As a general rule we may state that the length unit should, if possible, not be chosen smaller than 3 degrees latitude.

For practical reasons it is sometimes necessary to choose fairly small units. In such cases it is more advantageous to use another set of formulae for numerical differentiations, viz:

$$\left.\begin{aligned} p_{101} &= \tfrac{1}{2}(T^{1,0} - T^{-1,0}) \\ p_{200} &= p^{1,0} - 2p^{0,0} + p^{-1,0} \\ p_{102} &= \tfrac{1}{2}(\triangle T^{1,0} - \triangle T^{-1,0}) \\ p_{201} &= T^{1,0} - 2\,T^{0,0} + T^{-1,0} \end{aligned}\right\} \quad (2)$$

the advantages being that the tendency values are not taken from points which are immediately behind the trough line.

The two sets of formula (1) and (2) stand for the first approximations obtained from the general formulae for numerical differentiation (Runge-König, loc. cit.). The formulae thus correspond to differentiation after parabolic interpolation. The parabolic interpolation involves $p_{300} = 0$, which also is the condition for maximum of curvature, as previously stated.

When the velocity and the acceleration have been computed, we may extrapolate the displacement S of the trough line by combining velocity C_L and acceleration A_L, viz:

$$S = C_L t + \tfrac{1}{2} A_L t^2 \quad (3)$$

where t is the forecasting period.

It is understood that C_L and A_L are expressed in the arbitrarily chosen length unit, and three hours as unit of time (since the tendency is given as change per three hours). The forecasting period t, therefore, represents the number of 3-hourly intervals.

C_L and A_L represent instantaneous values only. Formula (3), therefore, gives only an approximation for the true displacement.

How far the displacement may be extrapolated depends on the particular case, and also on the accuracy of the observations. In chapter VII we shall see that the displacement may safely be calculated for 20 to 24 hours.

Formula (3) gives only the two first terms in a series, which can give exact values. Terms of higher order than acceleration are, at present, not obtainable from weather charts, and it is, therefore, of no interest to develop formulae for the instantaneous variation in acceleration. Even without the acceleration term, the displacement may be computed with sufficient accuracy for 12 or more hours.

It sometimes happens that the displacement may be calculated for two or three days in advance. In such cases, the series whose first two terms are given in (3), has a wide interval of convergence. At present no estimate with regard to the magnitude of the interval of convergence can be made. As a forecasting equation, formula (3), therefore, has no value outside the interval of time in which it is always (or in the large majority of cases) convergent. The present experience is that it may always be applied with advantage within 24 hours.

In chapter VI we shall develop methods for calculating the change in structure of moving troughs. In this way we can compute the future position of the trough line and the distribution of pressure in its vicinity. This method, therefore, is a valuable supplement to the method developed in chapter II.

CHAPTER IV.

THE MOVEMENT OF PRESSURE SYSTEMS.

In chapter II we have developed some formulae for calculating the instantaneous velocity and acceleration of the isobars and isallobars, and their future displacement. By means of these methods, it is possible to compute the future distribution of atmospheric pressure.

The pressure distribution in the vicinity of cyclones, anticyclones, and neutral points, are frequently of special interest. When for instance, a cyclone deepens, new isobars are created, and the methods developed in Chapter II do not furnish the necessary means for calculating the future distribution of the isobars which are going to be created. In order to overcome this difficulty, and for the purpose of deducing some convenient means for calculating the future pressure distribution, we propose to develop in this chapter some formulae for calculating the displacement of pressure systems. In chapter VI we shall demonstrate the methods for calculating the deepening or filling-up of pressure systems. In this way it is possible to predict the displacement and the change in structure of such pressure systems as cyclones, anticylones and neutral points.

15. Definition of Pressure Center and its Displacement. Let $p = p(x, y, t)$ represent the distribution of atmospheric pressure at sea level. A pressure center at any instant $t = t_1$ may be defined as the place where simultaneously:

$$\frac{\partial p}{\partial x} = \frac{\partial p}{\partial y} = 0 \tag{1}$$

and

$$\frac{\partial^2 p}{\partial x^2} \gtrless 0, \qquad \frac{\partial^2 p}{\partial y^2} \gtrless 0. \tag{2}$$

The definition thus comprises centers of cyclones, centers of anticyclones and neutral points. A cyclonic center is characterised by $\frac{\partial^2 p}{\partial x^2} > 0$ and $\frac{\partial^2 p}{\partial y^2} > 0$, an anticyclonic center by the opposite conditions. In the case of a neutral point, $\frac{\partial^2 p}{\partial x^2}$ and $\frac{\partial^2 p}{\partial y^2}$ have opposite signs, except in the direction of the asymptotes.

If the profiles of the pressure system have maximum of curvature in the center, we also have

$$\frac{\partial^3 p}{\partial x^3} = \frac{\partial^3 p}{\partial y^3} = 0. \tag{3}$$

Let S in fig. 8 be the path of the center, and S_1 and S_2 the positions of the center at two instants t_1 and t_2. Let $\triangle S$ be the secant that cuts the path at S_1 and S_2. Putting $t_2 - t_1 = \triangle t$, we may define the instantaneous velocity of the center as

$$C_c = \lim_{\triangle t \to 0} \left(\frac{\triangle S}{\triangle t} \right).$$

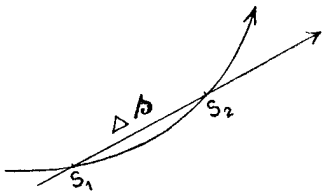

Fig. 8.

The acceleration of the path may be defined analogously as the change in velocity per unit time.

The velocity and the acceleration of the center is identical with the velocity and the acceleration of an individual particle that, during its motion, is forced to remain in the pressure center.

The acceleration may then be written:

$$A_c = \frac{dC_c}{dt}. \tag{4}$$

16. The Velocity of Pressure Centers. In order to obtain an analytical expression for the velocity of a pressure center, it is convenient to choose a system of co-ordinates (xy) whose origin is in the pressure center, and whose co-ordinate axes coincide with the lines where there is either maximum or minimum of curvature of the pressure profiles. These lines naturally coincide with the maximum or minimum of the curvature of the isobars. The co-ordinate axes need neither be straight nor orthogonal lines. If the center in question is circular, the axes may be chosen arbitrarily.

The center is then defined by the point of intersection between the two lines.

In all respects these lines correspond to the definition of trough lines. The equations which we have previously deduced for trough lines, are based on the condition that there is *either maximum or minimum* of curvature along the trough line. We can, therefore, apply these equations to the two lines which we have chosen to draw through the pressure center.

When the center moves, the two trough lines (we shall hereafter prefer to call them symmetry lines) will also move, and their point of intersection will always define the position of the center.

Relative to the chosen system of co-ordinates, the center has one component of velocity along the x-axis and one component along the y-axis. The two components of the velocity of the center are, therefore, equal to the velocity of the element of one sym-

metry line along the other. The two components are, therefore, identical with the velocities of trough lines, which we have developed in the previous chapter.

According to **12** (7) we may, therefore, write:

$$(1) \qquad \left.\begin{aligned} C_{cx} &= -\frac{p_{101}}{p_{200}} \\ C_{cy} &= -\frac{p_{021}}{p_{020}} \end{aligned}\right\}$$

which are the general expressions for the velocity of a pressure center.

p_{101} and p_{011} are respectively the x- and y-components of the isallobaric ascendant.

p_{200} and p_{020} are the curvatures of the x- and y-profiles respectively.

The velocity is proportional to the isallobaric ascendant, and inversely proportional to the curvature of the profiles.

It will be remembered from paragraph 12 that the velocity of a trough line does not depend on the condition that $p_{300} = 0$. Therefore, the velocity of a pressure center is also independent of this condition. The formulae (1), therefore, are valid for any kind of pressure center.

17. Acceleration of Pressure Centers. According to the considerations in the previous paragraph, we may apply the equations developed for trough lines, to the symmetry lines of pressure centers. The acceleration of a pressure center would have one component along the one symmetry axis, and one component along the other. Each component would represent the acceleration of an element of the one symmetry axis (trough line) along the other. In analogy with **13** (12), we may, therefore, write for the two significant components:

$$(1) \qquad \left.\begin{aligned} A_{cx} &= -\frac{p_{102}p_{200} - 2p_{101}p_{201}}{p^2_{200}} \\ A_{cy} &= -\frac{p_{012}p_{020} - 2p_{011}p_{021}}{p^2_{020}} \end{aligned}\right\}$$

In deducing equation **12** (12), we have assumed that there is maximum or minimum of curvature of the pressure profiles at the trough lines. The formulae (1), therefore, are subject to the same conditions, or, in other words, they are based on the assumption that $p_{300} = p_{030} = 0$.

In the same way as in paragraph 13, we may deduce formulae for the acceleration of a center where the co-ordinate axes do not coincide with the lines where there is maximum or minimum of curvature.

Formula **13** (13) gives the acceleration of a line in the pressure field where the only condition is that

$$p_{100} = 0.$$

As this condition is fulfilled for the co-ordinate axes, we get from **13** (13):

$$(2) \qquad \left.\begin{aligned} A_{cx} &= -\frac{p_{102} + 2C_{cx}p_{201} + C^2_{cx}p_{300}}{p_{200}} \\ A_{cy} &= -\frac{p_{102} + 2C_{cy}p_{021} + C_{cy}{}^2p_{030}}{p_{020}} \end{aligned}\right\}$$

Substituting for C_{cx} and C_{cy} by means of **16** (1), we get:

$$(3)\qquad \left.\begin{aligned} A_{cx} &= -\frac{p_{102}\,p_{200} - 2\,p_{101}\,p_{201} + p^2_{101}\,\dfrac{p_{300}}{p_{200}}}{p^2_{200}} \\ A_{cy} &= -\frac{p_{012}\,p_{020} - 2\,p_{011}\,p_{021} + p^2_{011}\,\dfrac{p_{030}}{p_{020}}}{p^2_{020}} \end{aligned}\right\}$$

The formulae (1) and (3) are identical, except for the terms which contain p_{300} and p_{030}, respectively. As in the last chapter, p_{101} and p_{011} are of the order 10^0, p_{200} and p_{020} are of the order 10^1, whereas p_{300} and p_{030} are at most of the order 10^{-1}, and are equal to zero if there is maximum or minimum of curvature. Consequently $p^2_{101}\,\frac{p_{300}}{p_{200}}$ and $p^2_{011}\,\frac{p_{030}}{p_{020}}$ are of the order of magnitude 10^{-2}, whereas the other terms in the numerators of (3) are (as shown previously) of the order 10^0. Neglecting therefore, the last terms in (3), we get the same formulae as (2). In all practical cases we may then reckon with formulae (2) as a sufficient approximation to the true instantaneous acceleration. It is, therefore, of very slight consequence whether the pressure center is symmetrical or not. The errors committed by neglecting the non-symmetrical terms are altogether smaller than are the errors due to inaccuracy in the observed tendencies. The interpretation of the various coefficients in (1), (2) and (3) need not be repeated here. The quantities have exactly the same meanings as stated in paragraph 13, the only difference being that we now have two co-ordinate axes instead of one as previously.

18. Determination of the Coefficients. The evaluation of the coefficients from the observations of the chart proceeds analogously with the methods described in paragraph 14, viz:

Draw the two co-ordinate axes, contingently along the symmetry axis of the pressure system (see fig. 9). Mark the points (1,0), (1/2,0) (0,0), (— 1/2,0), (— 1,0), (0,1), (0,1/2), (0, — 1/2) and (0, — 1). Writing as previously p^{xy}, T^{xy}, and $\triangle T^{xy}$ respectively for the values of pressure, tendency and tendency variation at the point $(x\,y)$, we get the following set of formulae for the numerical differentiation: (compare paragraph 14):

$$(1)\qquad \left.\begin{aligned} p_{101} &= T^{\frac{1}{2},0} - T^{-\frac{1}{2},0} && \text{or } \tfrac{1}{2}(T^{1,0} - T^{-1,0}) \\ p_{200} &= p^{1,0} - 2\,p^{0,0} + p^{-1,0} \\ p_{102} &= \triangle T^{\frac{1}{2},0} - \triangle T^{-\frac{1}{2},0} && \text{or } \tfrac{1}{2}(\triangle T^{1,0} - \triangle T^{-1,0}) \\ p_{201} &= T^{1,0} - 2\,T^{0,0} + T^{-1,0} \\ p_{011} &= T^{0,\frac{1}{2}} - T^{0,-\frac{1}{2}} && \text{or } \tfrac{1}{2}(T^{0,1} - T^{0,-1}) \\ p_{020} &= p^{0,1} - 2\,p^{0,0} + p^{0,-1} \\ p_{012} &= \triangle T^{0,\frac{1}{2}} - \triangle T^{0,-\frac{1}{2}} && \text{or } \tfrac{1}{2}(\triangle T^{0,1} - \triangle T^{0,-1}) \\ p_{021} &= T^{0,1} - 2\,T^{0,0} + T^{0,-1} \end{aligned}\right\}$$

where the alternative formulae are to used when the length unit is small.

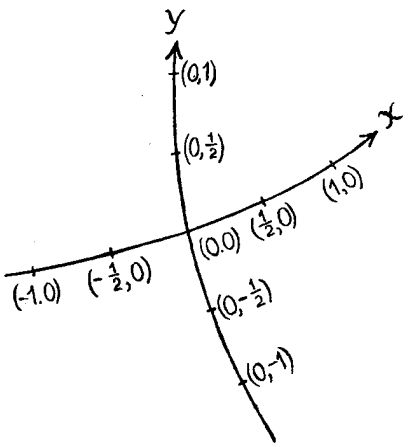

Fig. 9.

With respect to choice of length units etc., the reader is referred to paragraph 14. The statements made there, hold for pressure centers also.

When the velocity and the acceleration have been computed, the displacement of the center may be extrapolated by combining velocity and acceleration, viz:

$$(2)\qquad \left.\begin{aligned} S_x &= C_{cx}t + \tfrac{1}{2}A_{cx}t^2 \\ S_y &= C_{cy}t + \tfrac{1}{2}A_{cy}t^2 \end{aligned}\right\}$$

In paragraph 14 we have made some comments on the application of the corresponding formula for troughs. The same comments are true for pressure centers also.

19. The Path of Pressure Centers. The path of a pressure center is easily calculated from the velocity and the acceleration by means of the formula **18** (2).

Angervo[1]) has recently shown how the path of a center may be calculated more directly, when the center is symmetrical with respect to two axes. Angervo proceeds as follows:

Let $p = p(x, y, t)$ represent the pressure distribution at (say) sea level. Develop p in a series:

$$p = \sum_0^\infty \frac{1}{l!\,m!\,n!} p_{lmn}\, x^l y^m t^n$$

where

$$p_{lmn} = \frac{\partial^{l+m+n} p}{\partial x^l \partial y^m \partial t^n}.$$

Introducing the symmetry conditions and neglecting terms of 4th and higher order, he gets:

$$(1)\qquad \left.\begin{aligned} (p_{200} + p_{201}t)\frac{dx}{dt} + p_{101} + p_{201}x + p_{102}t &= 0 \\ (p_{020} + p_{021}t)\frac{dy}{dt} + p_{011} + p_{021}y + p_{120}t &= 0 \end{aligned}\right\}$$

The integration gives (for details see Angervo l. c.)

$$(2)\qquad \left.\begin{aligned} x &= -\frac{p_{101}t + \frac{1}{2}p_{102}t^2}{p_{200} + p_{201}t} \\ y &= -\frac{p_{011}t + \frac{1}{2}p_{012}t^2}{p_{020} + p_{021}t} \end{aligned}\right\}$$

where the coefficients have the same meaning as in paragraph 18.

Formula (2) is easier to work with than **18** (3) when the prohlem is to compute the path only. For the succeding considerations on the deepening and filling etc., of moving pressure systems, it is necessary to have separate expressions for the velocity and the acceleration. In chapter VII are given numerous examples showing the accuracy which can be obtained from Angervo's formulae compared with our formula **18** (3).

The discussion of the preceeding formulae offer corroboration of the following rules relating to the paths of cyclones:

(a) Round centers move in the direction of the isallobaric ascendant.

(b) Oblong centers most frequently move along the longest symmetry axis (or along 'the line of least resistance').

Newly formed wave cyclones invariably move in the direction of the warm sector current, which is parallel to the longest axis.

When the pressure center is circular, or nearly so, we may put $p_{200} = p_{020}$. Substituting in **16** (1), we get:

$$\tan\theta = \frac{C_{cy}}{C_{cx}} = \frac{p_{011}}{p_{101}}$$

[1]) Über die Vorausberechnung der Wetterlage für mehrere Tage. Gerlands Beitr. z. Geoph. Bd. 27. 1930.

where θ is the angle between the x-axis and the velocity of the center. Remembering that p_{101} and p_{011} are the x- and y-components of the isallobaric ascendant, we see that rule (a) necessarily must hold good. In paragraph 28 we shall see that this rule conforms with the rule that the center moves towards the area where the wind is most accelerated. (Guilbert's rule).

The velocity of a round center is obtained from **16** (1), viz:

$$C_c = \frac{\sqrt{p^2_{101} + p^2_{011}}}{p_{200}} = \frac{I}{p_{200}}$$

where I is the isallobaric ascendant. Thus, the velocity is proportional to the isallobaric ascendant and inversely proportional to the curvature of the profile of the pressure system. Therefore, centers whose profiles are very steep, generally move slowly.

Rule (b) holds good only conditionally. From **16** (1) we get:

$$\tan \theta = \frac{C_{cy}}{C_{cx}} = \frac{p_{011}\, p_{200}}{p_{101}\, p_{020}}.$$

Suppose that the pressure system is so oblong that p_{200} is negligible in comparison with p_{020}, we then see that θ approximates zero, unless p_{101} approximates zero. In general p_{101} and p_{011} are about equal, and, therefore, rule (b) generally holds good.

CHAPTER V.

THE MOVEMENTS OF FRONTS.

The movement of the fronts and the change in structure of their accompanying pressure fields are of crucial significance for the analysis of weather charts and for forecasting. In this chapter we shall only treat the movement of the fronts and kindred phenomena, leaving the deepening and filling to be investigated in chapter VI.

The mechanics of the fronts have recently been subjected to a thorough investigation by A. Giao.[1]) We shall, therefore, limit our investigation to a few points where Giao's investigations need supplementing.

20. Discontinuities and Layers of Transition. A front is generally defined as the line of intersection between a surface of discontinuity and a horizontal plane, at the ground or in the free atmosphere. The surface of discontinuity, which is supposed to be the surface of separation between air masses of different densities, must obey two conditions[2]):

(a) The pressure at both sides of the surface must be equal.

(b) The velocity components normal to the surface must be equal on both sides.

The first condition originates from the principle of equal action and reaction, and the second one is the well known kinematical surface condition, which states that no fissure can develop at the surface.

The front, being a line contained in the surface, must obey the first condition, but need not obey the second.

In the atmosphere, however, surfaces of discontinuities do not exist in the strict

[1]) A. Giao: La Mécanique Differentielle des Fronts et du Champ isallobarique. Memorial de L'Office Nat. Mét. No. 20. 1929.

[2]) See f. inst. V. Bjerknes: On the Dynamics of Circular Vortex etc. Geofysiske Publikationer Vol. II, No. 4. 1921.

mathematical sense of the word. The 'front surfaces' are layers of transition, in which density, temperature etc., vary continuously, but more or less rapidly. For the sake of clarity, we shall preliminarily use the phrases *surface of discontinuity* and *line of discontinuity* for mathematical discontinuities only, retaining *front surface* and *fronts* to designate layers and zones of transition.

The question now arises: Do the front surfaces obey the same surface conditions as do the surfaces of discontinuity? The question is a difficult one, and can hardly be answered satisfactorily. The following considerations, however, may help to throw some light on the matter.

The question whether a front surface can be treated as a surface of discontinuity is principally a matter of *scale.*

Let us, for example, consider the water content in a cloud. At a distance, the cloud may appear to be limited by a sharp surface. Examined at close distance, however, it will be found that there is a gradual transition from the saturated to the non-saturated air. Thus, the same cloud may be said to be limited by a surface of discontinuity or a layer of transition, according to the scale on which it is observed. If the surface of the cloud had to obey some mathematical law, one would have to find some such approximation as would suffice the accuracy which the scale of observation would necessitate.

Let ϱ_1 and ϱ_2 denote the densities of two adjacent air masses which are separated from one another by a surface of discontinuity. ϱ_1 and ϱ_2 may be functions of space and time. Let us consider the variation in density along a line (s) that intersects the surface (S). Let s measure length along the line s in such a way that $s = 0$ at the point of intersection. At this point the density (ϱ) will vary discontinuously, its value springing from ϱ_1 to ϱ_2. This discontinuous variation can be replaced by a continuous variation which, to any desired degree, approximates to the discontinuous one.

Writing:[1])

$$\varrho = \frac{\varrho_1 + \varrho_2 e^{ns}}{1 + e^{ns}} \tag{1}$$

we see that ϱ is a continuous function of s for finite values of n. When $n \to \infty$, ϱ is discontinuous for $s = 0$, its value then springing from ϱ_1 to ϱ_2. The number n may be said to measure the degree of approximation, and ϱ may be called the density of the approximated layer of transition.

Let us next consider a *real* layer of transition in which ϱ varies evenly from ϱ_1 to ϱ_2. Let s, in the same way as previously, measure length along a line that cuts through the layer of transition, and let m be the scale on which s is measured. We may then write:

$$d\varrho = (\varrho_1 - \varrho_2)\, m ds. \tag{2}$$

When $m \to \infty$, ϱ becomes discontinuous.

Differentiating (1) we get:

$$d\varrho = (\varrho_1 - \varrho_2)\, n ds \frac{e^{ns}}{(1 + e^{ns})^2}$$

which for $s = 0$, and for finite values of n, gives

$$d\varrho = (\varrho_1 - \varrho_2) \frac{n}{4} ds. \tag{3}$$

---

[1]) See f. ex. Webster-Szegö: Partielle Differentialgleichungen der mathematischen Physik. Leipzig 1930. p. 2.

Comparing (2) with (3) we see that m is equivalent to $\frac{n}{4}$. As (3), by suitable choice of n, approximates a discontinuity, it follows from (2), that a layer of transition, by suitable choice of scale (m), may be approximated by a discontinuity.

Fig. 10 represents the approximations. The full lines represent the discontinuous variation, the dotted line the approximation obtained by formula (2), and the thin line the approximation obtained by (1), which for $s = 0$, is equivalent to (3). Let ε be a given small positive number, and let δ_1, be the difference between the curves $a$and c, and δ_2 the difference between the curves a and b. It is easily seen that one can always find a value of n, so that

$$|\delta_2| < |\delta_1| < \varepsilon.$$

The same applies to m.

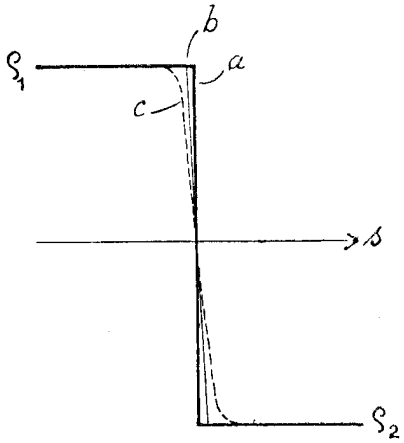

Fig. 10, showing the discontinuous and the approximated continuous variation.

In most cases m is given *à priori*, i. e. the scale of the chart. The question whether a layer may be treated as a surface, thus depends on whether the layer appears as a discontinuity on the scale on which the phenomenon is graphed. This leads to a closer definition of fronts and frontal zones, viz:

(c) A front is a zone of transition which, on the scale of reference, appears as a discontinuity.

(d) A frontal zone is a layer of transition which is so wide that it does not appear as a discontinuity.

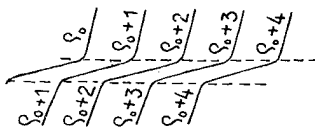

Fig. 11 a. Density varying rapidly in a layer of finite thickness.

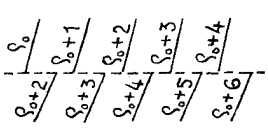

Fig. 11 b. Abrupt change of density at a front surface. (Scale m).

Fig. 11 a and b represent the distribution of density at a front surface, graphed on different scales.

21. Surface Conditions for Layers of Transition. The considerations in the previous paragraph now permit us to deduce surface conditions for layers of transition of finite thickness, analogous to the surface conditions of mathematical discontinuities.

Returning now to the surface conditions (page 31), we easily see that the alteration of the scale does not affect the continuity of pressure itself, and hence, the surface condition (a) holds good.

The second surface condition may be written:

$$(\boldsymbol{V}_1 - \boldsymbol{V}_2) \cdot \boldsymbol{N} = 0 \tag{1}$$

where $\boldsymbol{V}$ is the wind vector. Indices 1 and 2 denote two points on either side of the surface and infinitely near one another, and $\boldsymbol{N}$ stands for a unit vector perpendicular to the surface. Equation (1) may be written:

$$(u_1 - u_2)\,\alpha + (v_1 - v_2)\,\beta + (w_1 - w_2)\,\gamma = 0 \tag{2}$$

where u_1, v_1, w_1, are the components of $\boldsymbol{V}_1$, and u_2, v_2, w_2, the components of $\boldsymbol{V}_2$.

Let us now consider a layer of transition of finite thickness. Let U, V, W, be the velocity components in the layer of transition, in which U, V, and W vary evenly from U_1, V_1, W_1, to U_2, V_2, W_2, at the limits of the layer. Consider next a surface in the middle of the layer and a line which cuts the surface. Let s measure length

along this line in such a way that $s = 0$ at the point of the intersection. In analogy to **20** (2) we may write for the point $s = 0$:

$$(3) \qquad \begin{aligned} dU &= (U_1 - U_2)\, mds \\ dV &= (V_1 - V_2)\, mds \\ dW &= (W_1 - W_2)\, mds \end{aligned}$$

Let $\boldsymbol{N} = (\alpha, \beta, \gamma)$ be a unit vector normal to the surface. Multiplying (3) by α, β and γ respectively and adding, we get:

$$(U_1 - U_2)\,\alpha + (V_1 - V_2)\,\beta + (W_1 - W_2)\,\gamma = \frac{1}{m}\left(\frac{dU}{ds}\alpha + \frac{dV}{ds}\beta + \frac{dW}{ds}\gamma\right).$$

Remembering that U, V and W are continuous, and that $\frac{dU}{ds}, \frac{dV}{ds}$ and $\frac{dW}{ds}$ are finite values, we see that by suitable choice of scale (m), the expression on the right hand side of the equal sign may be made smaller than any small number ε. In such a scale we can write:

$$(4) \qquad (U_1 - U_2)\,\alpha + (V_1 - V_2)\,\beta + (W_1 - W_2)\,\gamma = 0$$

which is the surface condition of the layer of transition, which on the scale considered, is an apparent surface of discontinuity.

Equation (4) would hold good on any scale, if the velocity in the layer is parallel to the layer itself. If the layer expands or contracts, equation (4) holds good with an approximation which depends on the scale. In any case, if the scale of the chart is large enough to reduce the layer of transition to an apparent surface of discontinuity, we can apply equation (4) to the layer.

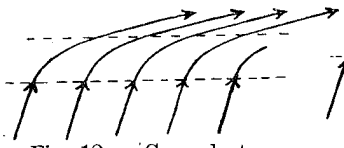

Fig. 12 a. Curved streamlines in a layer of finite thickness.

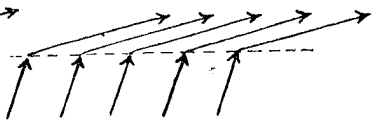

Fig. 12 b. Refracted streamlines at a front surface. (Scale m).

The following considerations on the movement of fronts proceed on the assumption that the surface conditions of front surfaces are the same as for surfaces of discontinuity. Fig. 12 a and b represent the stream lines on two different scales.

22. Definition of Velocity and Acceleration of Fronts. Let us consider the isochrones of a front. Let f_0 in figure 13 denote the position of the front at the initial instant $t = 0$, and let f_1 denote the position of the front after an interval of time Δt. Choose an arbitrary point P_0 on f_0 and draw an arbitrary line L. Let P_1 be the point of intersection, between L and f_1, and let $\Delta \boldsymbol{L}$ denote the vector from P_0 to P_1. The velocity of a curve element of the front f along the line L may then be defined as:

$$\boldsymbol{C}_f = \lim_{\Delta t \to 0}\left(\frac{\Delta \boldsymbol{L}}{\Delta t}\right).$$

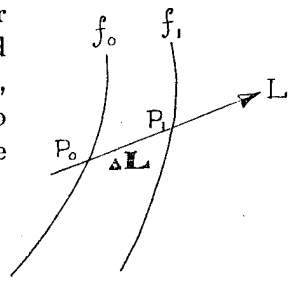

Fig. 13.

The velocity is thus defined as being co-axial with the line L at the point in question of the initial isochrone.

An imaginary particle which during its motion is forced to remain on the front and on the line L, would have a velocity equal to $\boldsymbol{C}_f$. The definition of the velocity of an

element of the front is identical with the definition of the velocity of a characteristic line (see paragraph 2).

The acceleration of an element of a front may be defined as the change in velocity per unit time of the individual front element. In the same way as in paragraph 2, we get:

$$A_f = \frac{dC_f}{dt}. \tag{1}$$

It is convenient to choose a system of co-ordinates with origin at P_0 and the positive x-axis directed along L. The element of the front has a velocity which is permanently directed along L, or along the x-axis. There can, therefore, never be any component of velocity or acceleration normal to the axis. We may therefore write:

$$A_f = \frac{dC_f}{dt} = \frac{\partial C_f}{\partial t} + C_f \frac{\partial C_f}{\partial x}. \tag{2}$$

When the line L is normal to the front, we get the normal velocity and the normal acceleration of the front element in question.

23. The Velocity of Fronts and Frontal Zones. In the previous paragraph we have seen that the definition of the velocity of a front is identical with the definition of the velocity of a characteristic line in the field of pressure. If we can find some pressure condition which must be fulfilled during the movement of the front, we may apply the general equation of paragraph 4 to the front.

The pressure condition that is permanently fulfilled at the front, is the dynamical surface condition, which, as we have seen in paragraph 21, holds also for front surfaces.

Let p_1 and p_2 be the values of pressure at two points 1 and 2 on either side of the element of the front which we consider. According to the surface condition we have:

$$p_1 - p_2 = 0. \tag{1}$$

In a system of co-ordinates which is fixed to the moving front element, we must, therefore, have:

$$\frac{\delta (p_1 - p_2)}{\delta t} = 0$$

which is the permanent condition that the front must obey. Substituting $p_{lmn} = p_1 - p_2$ in the general formula **4** (5), we get:

$$C_f = -\frac{\frac{\partial p_1}{\partial t} - \frac{\partial p_2}{\partial t}}{\frac{\partial p_1}{\partial x} - \frac{\partial p_2}{dx}} \tag{2}$$

which is the general formula for the instantaneous velocity of a front along the x-axis.

In general, it is most convenient to choose the x-axis normal to the front at the point in question.

Formula (2) is identical with the one which Giao (loc. cit.) has deduced for mathematical discontinuities.

The question now arises: Do the differences $\left(\frac{\partial p_1}{\partial t} - \frac{\partial p_2}{\partial t}\right)$ and $\left(\frac{\partial p_1}{\partial x} - \frac{\partial p_2}{\partial x}\right)$ exist at the front, or is formula (2) an indeterminate expression of the type $\frac{0}{0}$.

The surface condition (1) naturally holds good for any material surface in the air, whether there is a front surface or not. But, at a surface which is not a discontinuity

of some sort, we would have $\frac{\partial p_1}{\partial t} - \frac{\partial p_2}{\partial t} = 0$, and $\frac{\partial p_1}{\partial x} - \frac{\partial p_2}{\partial x} = 0$. In this case we may take the points 1 and 2 at finite distance from one another, divide $\left(\frac{\partial p_1}{\partial t} - \frac{\partial p_2}{\partial t}\right)$ and $\left(\frac{\partial p_1}{\partial x} - \frac{\partial p_2}{\partial x}\right)$ by Δx, and then let Δx converge to zero. We would then get:

$$C'_f = -\frac{\frac{\partial^2 p}{\partial x \partial t}}{\frac{\partial^2 p}{\partial x^2}} = -\frac{p_{101}}{p_{200}}. \tag{3}$$

which is identical with the formula for the trough line. When there is a front surface, we cannot differentiate through the discontinuity, and formula (2) will be appropriate to use in such cases.

The physical conditions for having a discontinuity in pressure tendency and pressure gradient may be studied by means of the well-known formula for the inclination of the front surface.[1]) When θ signifies the angle of inclination, we have:

$$\tan \theta = \frac{1}{g} \frac{\frac{\partial p_1}{\partial x} - \frac{\partial p_2}{\partial x}}{\varrho_1 - \varrho_2} \tag{4}$$

where ϱ is density, and g is the acceleration of gravity.

As the front velocity must be finite, we see from (2), that if $\frac{\partial p_1}{\partial x} - \frac{\partial p_2}{\partial x} = 0$, we must also have: $\frac{\partial p_1}{\partial t} - \frac{\partial p_2}{\partial t} = 0$. From (4) we then get that, if θ is different from zero, and $\frac{\partial p_1}{\partial x} - \frac{\partial p_2}{\partial x} = 0$, we must also have: $\varrho_1 - \varrho_2 = 0$, which is contradictory to our definition of a front (see paragraph 20). In this case, however, we may have a frontal zone, which according to the definition, does not exhibit a discontinuous distribution of density.

At the front surface we have by definition: $\varrho_1 \gtrless \varrho_2$, and since simultaneously $p_1 = p_2$, it follows that the temperature (τ) (disregarding the effect of humidity), must be discontinuous.

Summing up, we may state that the definition of a front also involves the following conditions:

$$p_1 = p_2$$
$$\varrho_1 \gtrless \varrho_2$$
$$\tau_1 \gtrless \tau_2$$
$$\frac{\partial p_1}{\partial x} \gtrless \frac{\partial p_2}{\partial x}$$

and $\frac{\partial p_1}{\partial t} \gtrless \frac{\partial p_2}{\partial t}$, unless the front is stationary.

A front, therefore, is always accompanied by angular isobars, and, if the front is not stationary, there will be an angle in the barogram. Formnla (2) may, therefore, be applied to the formations which we in paragraph 20 have defined as fronts. Formula (3) may be applied for calculating the velocity of frontal zones. This formula is, as previously stated, identical with the formula for a trough line. There is, therefore, no principal difficulty for computing the movement of fronts and frontal zones, because the

[1]) See J. Bjerknes: Exploration de quelques Perturbation etc. Geofysiske Publikasjoner Vol. IX, No. 9, where some similar questions are discussed.

above formulae are not deduced on the assumption of the existence of mathematical discontinuities.

The previous considerations may be transformed into some useful rules for the physical weather chart analysis.

(a) A front can never be drawn where there are no angular points in the isobars.

(b) A non-stationary front should never be drawn where there is no discontinuity in barometric tendency.

(c) Quickly running fronts are frequently accompanied by ill-defined pressure troughs, since the velocity is inversely proportional to the discontinuity in pressure gradient.

(d) Slowly moving fronts are, for the above reason, frequently accompanied by well marked troughs.

Some other interesting features regarding the velocity of atmospheric fronts, have been discussed by Giao (loc. cit.), and the reader is referred thereto.

The expression for the velocity of fronts, which we have developed and discussed, has been obtained from the dynamical surface condition. This expression is the only one that is applicable to the weather charts for calculating the displacement of the fronts. From the kinematical surface condition we can deduce another equation for the velocity of the front, but this equation is, owing to its structure, not applicable to the charts. It is, however, very useful for discussing the various conditions at fronts. We shall here only deduce the equations, and leave the discussion to a later paragraph.

We return to equation **21** (4), and choose a system of co-ordinates whose x-axis is normal to the front. Equation **21** (4) may then be written:

$$(U_1 - U_2)\,\alpha + (W_1 - W_2)\,\gamma = 0$$

or

$$W_1 - W_2 = (U_1 - U_2)\tan\theta \tag{5}$$

where θ denotes the inclination of the front surface.

Equation **21** (4) says directly that the discontinuity consists in a sliding motion parallel to the front surface. When $\boldsymbol{S}$ is the relative velocity of the two adjacent air masses, we may write:

$$\boldsymbol{S} \cdot \boldsymbol{N} = 0$$

where $\boldsymbol{N}$ is the normal vector of the surface.

The movement of each of the air masses relative to the front surface must also be tangential to the surface. When u_f denotes the normal velocity of the front,[1]) we may write:

$$U_1 - u_f = W_1 \operatorname{cotan}\theta$$
$$U_2 - u_f = W_2 \operatorname{cotan}\theta$$

or:

$$\begin{cases} W_1 = (U_1 - u_f)\tan\theta \\ W_2 = (U_2 - u_f)\tan\theta \end{cases} \tag{6}$$

From each of these equations we could compute the normal velocity of the front, if W, U and θ were known.

It is, however, easily understood, that owing to technical difficulties, the front velocity cannot be computed from these equations. The equations (5) and (6) are, however, useful for discussing the vertical velocity in the vicinity of front surfaces, and we propose to return to this subject in a later paragraph.

---

[1]) We prefer to write u_f here instead of previously C_f, which has a wider meaning. u_f is, however, indentical with C_f when the x-axis is normal to the front.

24. The Acceleration of Fronts and Frontal Zones. An analytical expression for the acceleration of a front may be deduced on the same principles as applied when deducing the formula for the velocity of fronts. The surface condition is $p_1 - p_2 = 0$. In a system of co-ordinates which is fixed to the moving front element, we must have

$$\frac{\delta (p_1 - p_2)}{\delta t} = 0.$$

Substituting $p_{tmn} = p_1 - p_2$ in the general equation **4** (6), we get:

$$A_f = - \frac{\left(\frac{\partial^2 p_1}{\partial t^2} - \frac{\partial^2 p_2}{\partial t^2}\right) + 2 C_f \left(\frac{\partial^2 p_1}{\partial x \partial t} - \frac{\partial^2 p_2}{\partial x \partial t}\right) + C_f^2 \left(\frac{\partial^2 p_1}{\partial x^2} - \frac{\partial^2 p_2}{\partial x^2}\right)}{\frac{\partial p_1}{\partial x} - \frac{\partial p_2}{\partial x}} \tag{1}$$

which is the general formula for the acceleration of a front element along the x-axis. When the x-axis is normal to the front, we get the normal acceleration.

Equation (1) is identical with the formula deduced by Giao (loc. cit.) for mathematical discontinuities, but, according to the considerations in the previous paragraphs, formula (1) also holds good for front surfaces as they are defined in paragraph 20.

According to the considerations in paragraph 23, the denominator in (1) is different from zero. The formula, therefore, is never indeterminate.

The surface condition $p_1 - p_2 = 0$ naturally holds good for any material surface, whether a front surface or not. Formula (1) would, therefore, also hold for a surface of air particles in a frontal zone. But in this case, we have by definition that there is no discontinuity in the various elements. A frontal zone is characterized by rapid but continuous variations of the meteorological elements. In this case formula (1) is indeterminate, because, according to the considerations in paragraph 23, $\frac{\partial p_1}{\partial x} - \frac{\partial p_2}{\partial x} = 0$, and A_f must be finite. In this case we may take the points 1 and 2 at finite distance (Δx), and divide the numerator and the denominator in (1) by Δx, and let Δx converge to zero. We would then get:

$$A'_f = - \frac{\frac{\partial^3 p}{\partial x \partial t^2} + C'_f \frac{\partial^3 p}{\partial x^2 \partial t} + C'^2_f \frac{\partial^3 p}{\partial x^3}}{\frac{\partial^2 p}{\partial x^2}} \tag{2}$$

or, with the notations applied in the previous chapters:

$$A'_f = - \frac{p_{102} + C'_f p_{201} + C'^2_f p_{300}}{p_{200}} \tag{3}$$

which is identical with the formula **13** (13) for the acceleration of a trough line.

The coefficients in (3) may be evaluated from the weather chart precisely as described in paragraph 14. The term which contains p_{300} is, as in paragraph 14, frequently negligible.

For the practical application there is no difference between the formulae for the accelerations of troughs, fronts and frontal zones, because the differentials p_{tmn}, which enter in the formulae for troughs and frontal zones, must be replaced by such finite differences as enter in the front formulae.

The various quantities in equation (1) are similar to the corresponding quantites in equation **7** (1), which express the acceleration of the isobar, and the various terms may be interpreted as shown in paragraph 7, with the exception that the x-axis now has a different orientation.

The kinematical surface condition could also be used for deducing an equation for the acceleration. Such an equation has been deduced by G i a o (loc. cit.) and the reader is referred thereto.

25. Types of Fronts. It should be emphasized at the outset that considerable difficulties are involved in computing the acceleration of the fronts. The difficulties arise from the circumstance that the quantities which are to be put into the formulae, are taken from the immediate vicinity of the fronts. For troughs and wedges etc., the problem is fairly simple, because, owing to the continuous variations of the various quantities, we may approximate the differentials by means of finite differences. In the case of a front this is not possible, because the first term in the acceleration depends on the curvature of the barogram, and this quantity cannot be determined by means of two consecutive tendency values, because the first of these two tendencies would have to be derived from that part of the barogram which gives the tendency before the front passage. For this reason we shall detail the discussion of formula **24** (1) in order to give rules for estimating the *sign* of the acceleration. Experience has shown, however, that when the front is accompanied by some sort of pressure trough, the formulae which we have previously developed forpressure troughs, give fairly accurate results for front troughs, when the discontinuity in pressure gradient and tendency is smoothed. These formulae may therefore be used for calculating the displacement of the front trough as a whole. The displacement of the front may, however, be slightly different from the displacement of the trough.

The discussion of the acceleration formula will also render valuable results for estimating the probable development of the cyclone to which the fronts belong. The analysis of weather charts has revealed various types of fronted cyclones, or patterns for characteristic steps in the development of individual cyclones. We shall first consider some frequent types of warm sector cyclones, and afterwards comment on the occluded ones.

In the previous paragraph we have developed a general equation for the acceleration of the front along an arbitrary line L, which we have chosen as x-axis. In general, it is most convenient to choose the x-axis normal to the front. In this paragraph we propose to discuss warm and cold fronts and their relative behaviour. It is then convenient to choose the x-axis along the warm-sector isobars, which, as a rule, are almost straight lines.

In order to avoid confusion of indices we shall throughout index the air masses in the following manner: Index 1 denotes the cold air in front of the front, index 2 the warm air in the rear of the warm front, index 3 the warm air in front of the cold front, and index 4 the cold air in the rear of the cold front.

Type A. Fig. 14 represents a warm sector cyclone whose main characteristics are the open warm sector and the symmetrical distribution of pressure.

The general formula for the acceleration is:

$$A_f = -\frac{\left(\frac{\partial^2 p_1}{\partial t^2} - \frac{\partial^2 p_2}{\partial t^2}\right) + 2\,C_f\left(\frac{\partial^2 p_1}{\partial x \partial t} - \frac{\partial^2 p_2}{\partial x \partial t}\right) + C^2{}_f\left(\frac{\partial^2 p_1}{\partial x^2} - \frac{\partial^2 p_2}{\partial x^2}\right)}{\frac{\partial p_1}{\partial x} - \frac{\partial p_2}{\partial x}} \tag{1}$$

where the subscripts 1 denote the air in front of the front, and the subscripts 2 denote the air in the rear of the front in question. With the indexing introduced above we may take equation (1) as the expression for the acceleration of the warm front. The

acceleration of the cold front is then obtained from (1) by substituting index 3 for 1, and index 4 for 2.

It is a fundamental property for all fronts that the denominator in (1) is always positive.[1])

Let us first consider the warm front at the point P_1. Since the x-axis falls along

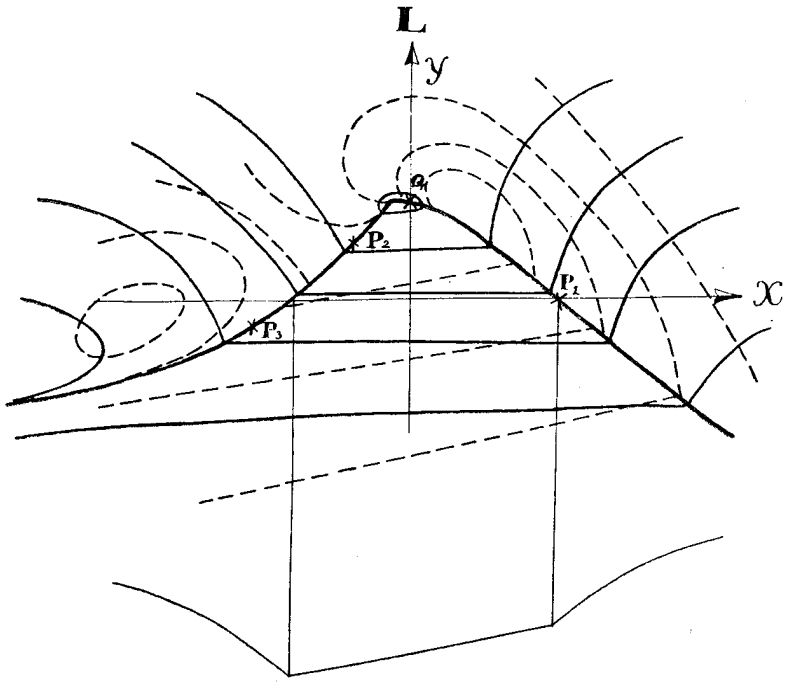

Fig. 14. Warm sector cyclone, type A. Continuous curves denote isobars. Broken curves denote isallobars. The curve below represents a barogram, reconstructed from the pressure variations at stations on the x-axis.

the warm sector isobar, we have $\frac{\partial p_2}{\partial x} = 0$, and $\frac{\partial p_1}{\partial x} > 0$. We prefer to discuss each term in (1) separately. We may then write for the first part of the acceleration:

$$A' = -\frac{\frac{\partial^2 p_1}{\partial t^2} - \frac{\partial^2 p_2}{\partial t^2}}{\frac{\partial p_1}{\partial x}}.$$

The inspection of the barograms shows that the tendency in the warm sector is almost invariably uniform (see also paragraph 34). We may therefore put $\frac{\partial^2 p_2}{\partial t^2} = 0$. Furthermore, at this type of warm front, the barogram in front of the warm front (and in the rear of the cold front) is almost invariably curved anticyclonically, i. e. $\frac{\partial^2 p_1}{\partial t^2} < 0$. We therefore get approximately:

$$A' = -\frac{\frac{\partial^2 p_1}{\partial t^2}}{\frac{\partial p_1}{\partial x}} > 0. \tag{2}$$

[1]) See Bjerknes—Bjerknes—Solberg—Bergeron: Physikalische Hydrodynamik. Springer 1932 p. 479—80.

The second term of the acceleration may be written:

$$A'' = -2\,C_f \frac{\frac{\partial^2 p_1}{\partial x \partial t} - \frac{\partial^2 p_2}{\partial x \partial t}}{\frac{\partial p_1}{\partial x}}.$$

Consulting the isallobars, we see that $\frac{\partial^2 p_1}{\partial x \partial t}$ is large and positive, whereas $\frac{\partial^2 p_2}{\partial x \partial t}$ is small and positive. Since C_f and $\frac{\partial p_1}{\partial x}$ are both positive, we get, when we neglect the small term $\frac{\partial^2 p_2}{\partial x \partial t}$:[1])

$$A'' = -2\,C_f \frac{\frac{\partial^2 p_1}{\partial x \partial t}}{\frac{\partial p_1}{\partial x}} < 0. \tag{3}$$

Finally, the third term of the acceleration may be written:

$$A''' = -C^2_f \frac{\frac{\partial^2 p_1}{\partial x^2} - \frac{\partial^2 p_2}{\partial x^2}}{\frac{\partial p_1}{\partial x}}.$$

Since the warm sector isobar is a straight line coinciding with the x-axis, we have $\frac{\partial^2 p_2}{\partial x^2} = 0$. Furthermore, $\frac{\partial^2 p_1}{\partial x^2}$ is negative. We therefore get:

$$A''' = -C^2_f \frac{\frac{\partial^2 p_1}{\partial x^2}}{\frac{\partial p_1}{\partial x}} > 0. \tag{4}$$

Returning now to equation (1) and discussing it in respect to the cold front (where the warm air is indexed by the number 3, and the cold air is indexed by the number 4), we get in the same manner:

$$\frac{\partial^2 p_3}{\partial t^2} = 0, \quad \frac{\partial p_3}{\partial x} = 0, \quad \frac{\partial^2 p_3}{\partial x \partial t} = 0, \text{ and } \frac{\partial p_4}{\partial x} < 0$$

and hence:

$$A' = -\frac{\frac{\partial^2 p_4}{\partial t^2}}{\frac{\partial p_4}{\partial x}} < 0. \tag{5}$$

For the second term we get, when the x-component of the isallobaric ascendant in the cold air is negative (i. e. directed away from the front):

$$A'' = -2\,C_f \frac{\frac{\partial^2 p_4}{\partial x \partial t}}{\frac{\partial p_4}{\partial x}} < 0,$$

---

[1]) The barometric tendency is frequently negative in the warm sectors, but in the majority of cases, the isallobars are almost parallel to the isobars. The term $\frac{\partial^2 p_2}{\partial x \partial t}$ can therefore be neglected, when the x-axis is chosen along the isobar.

and when the x-component of the isallobaric ascendant is positive (i. e. directed towards the front):

$$A'' = -2\,C_f \frac{\frac{\partial^2 p_4}{\partial x \partial t}}{\frac{\partial p_4}{\partial x}} > 0.$$

As mentioned previously, it is difficult to obtain an accurate picture of the distribution of the isallobars in the cold air close to the cold front. By means of the synoptic charts and equation 28 (3) we may determine the sign of the isallobaric ascendant. Equation 28 (3) gives the rule that the isallobaric ascendant is directed away from the front when the wind veers after the front passage, and it is directed towards the front when the wind backs after the front passage. Synoptic studies show that the first case most frequently occurs at the part of the front which is most distant from the center, whereas the second case most commonly occurs in the vicinity of the center. For this reason we have in fig. 14 marked two typical points P_2 and P_3, and in table 2 the acceleration is given for each of these points separately. We shall presently see the significance of the said distribution of isallobaric ascendant.

Returning to the above equation, we see that we get for the third term:

$$A''' = -C^2_f \frac{\frac{\partial^2 p_4}{\partial x^2}}{\frac{\partial p_4}{\partial x}} < 0,$$

since both $\frac{\partial^2 p_4}{\partial x^2}$ and $\frac{\partial p_4}{\partial x}$ are negative.

The results of the above discussion are comprised in the following table:

Table 2. Type A.

	Warm front	Cold front	
	at P_1	at P_2	at P_3
A'	$-\frac{\frac{\partial^2 p_1}{\partial t^2}}{\frac{\partial p_1}{\partial x}} > 0$	$-\frac{\frac{\partial^2 p_4}{\partial t^2}}{\frac{\partial p_4}{\partial x}} < 0$	$-\frac{\frac{\partial^2 p_4}{\partial t^2}}{\frac{\partial p_4}{\partial x}} < 0$
A''	$-2\,C_f \frac{\frac{\partial^2 p_1}{\partial x \partial t}}{\frac{\partial p_1}{\partial x}} < 0$	$-2\,C_f \frac{\frac{\partial^2 p_4}{\partial x \partial t}}{\frac{\partial p_4}{\partial x}} > 0$	$-2\,C_f \frac{\frac{\partial^2 p_4}{\partial x \partial t}}{\frac{\partial p_4}{\partial x}} < 0$
A'''	$-C^2_f \frac{\frac{\partial^2 p_1}{\partial x^2}}{\frac{\partial p_1}{\partial x}} > 0$	$-C^2_f \frac{\frac{\partial^2 p_4}{\partial x^2}}{\frac{\partial p_4}{\partial x}} < 0$	$-C^2_f \frac{\frac{\partial^2 p_4}{\partial x^2}}{\frac{\partial p_4}{\partial x}} < 0$

We thus see that the terms A' and A'', which depend on the curvature of the barogram and the curvature of the pressure profile respectively, are positive for warm fronts and negative for cold fronts. The second part of the acceleration is negative, except

at cold fronts where the isallobaric ascendant points from the cold side towards the front.

It is interesting to see that the southern part of the cold front of type A is retarded, all three terms being negative. In paragraph 26 we shall see that this kind of cold front is exposed to frontogenesis.

Another interesting feature is that the acceleration of both the warm and the cold fronts in the direction of the warm sector isobars, depends almost entirely on the conditions in the cold air. The retardation of the southern part of the cold front tends to prevent the southern part of the warm sector from occluding. It is a common experience that cyclones of this type occlude very slowly, and this observation concords with the results of the above discussion. Moreover, cyclones of this type proceed along the principal front more or less as waves without appreciably altering their structures. Such cyclones rarely develop into big affairs, however large the temperature differences may be.

An outstanding example of this type of cyclone has been described by Bergeron and Swoboda[1]) i. e. the wave cyclone marked A on the weather maps for October 10th and 11th 1923. The maps are reproduced at the end of the publication just mentioned. The cyclone travelled more than 4000 km. during 60 hours without occluding appreciably, thus approximating a *stable wave.*

Prima facie, it may appear difficult to understand that the cyclone can last for days, when the accelerations are distributed as described above. It should, however, be born in mind that the structure of the distribution of pressure and pressure tendencies in the vicinity of the center is somewhat different from the conditions described along the x-axis in fig. 14.

The general equation for the acceleration of the front permit us to obtain the acceleration along any line L. Let us now study the acceleration at a point Q near the center and slightly in front of it. It is now convenient to draw the line L normal to the warm sector current. We take L as co-ordinate axis, and, in order to prevent confusion, we let y measure length along this line L. The expression for the acceleration of the front element at Q along the y-axis is completely analogous to equation (1), when y is substituted for x. We then get:

$$A_{fy} = -\frac{\left(\frac{\partial^2 p_1}{\partial t^2} - \frac{\partial^2 p_2}{\partial t^2}\right) + 2\,C_{fy}\left(\frac{\partial^2 p_1}{\partial y \partial t} - \frac{\partial^2 p_2}{\partial y \partial t}\right) + C^2_{fy}\left(\frac{\partial^2 p_1}{\partial y^2} - \frac{\partial^2 p_2}{\partial y^2}\right)}{\frac{\partial p_1}{\partial y} - \frac{\partial p_2}{\partial y}}.$$

The denominator is positive, and so is C_{fy}, which stands for the velocity along the y-axis. Index 1 denotes the cold air, and index 2 the warm air. To the north of the front at the point Q, the barogram is curved cyclonically, and the curvature is generally large. $\frac{\partial^2 p_1}{\partial t^2}$ is, therefore, positive, and presumably much larger than $\frac{\partial^2 p_2}{\partial t^2}$. The first part of the acceleration is, therefore, negative.

It is easily seen that the other two parts of the acceleration are negative. These terms, however, carry less weight than does the first term, because the velocity of the warm front along the line L is exceedingly small.

Summing up, we get the following picture of the acceleration of the fronts of the cyclone represented in fig. 14: At P_1 the front is accelerated eastwards, at Q it is accelerated southwards and at P_3 it is accelerated westwards. The point P_3 will sooner or later come to a standstill, whereas the point at Q will move southwards and thus make

[1]) Wellen und Wirbel an einer quasistationären Grezfläche über Europa. Leipzig 1924.

up the rear of the cyclone. The center will move along the front. The resemblance to a stable wave is, after these considerations, even more pronounced.

In the said series of weather charts, Bergeron and Swoboda have treated the cyclone *B* which succeeded the cyclone *A*. It is easily seen from the charts, that the cyclone *B* represents a totally different type, its rear not being symmetrical with the front of the cyclone. This cyclone encountered a development totally different from that of the *A*. Cyklone *B* deepened quickly and occluded quickly. We shall presently see that Bergeron's *B*-cyclone represents a common type, whose main characteristic is that it occludes quickly.

The above considerations show *how utterly important it is to diagnose the structure of the cyclone, and how apparently minute differences in structure carry large weight for the future development.* The examples mentioned show the fundamental significance of an accurate physical analysis.

Returning again to the cyclone examplified in fig. 14, we may discuss the possibilities for occlusion by means of the formula for the front velocity. We index the air masses as previously, and we let C_w and C_c denote the velocities of the warm and the cold fronts respectively. According to **23** (2) we may then write;

$$C_w = -\frac{\frac{\partial p_1}{\partial t} - \frac{\partial p_2}{\partial t}}{\frac{\partial p_1}{\partial x} - \frac{\partial p_2}{\partial x}}$$

$$C_c = -\frac{\frac{\partial p_3}{\partial t} - \frac{\partial p_4}{\partial t}}{\frac{\partial p_3}{\partial x} - \frac{\partial p_4}{\partial x}}$$

According to the particular choice of x-axis, we have:

$$\frac{\partial p_2}{\partial x} = \frac{\partial p_3}{\partial x} = 0 .$$

Assuming the front and the rear of the cyclone to be symmetrical with regard to pressure distribution, we get:

$$\frac{\partial p_1}{\partial x} = -\frac{\partial p_4}{\partial x} > 0 .$$

Subtracting C_w from C_c we then get:

$$C_c - C_w = \frac{\frac{\partial p_1}{\partial t} - \frac{\partial p_2}{\partial t} - \frac{\partial p_3}{\partial t} + \frac{\partial p_4}{\partial t}}{\frac{\partial p_1}{\partial x}}$$

which is a measure for the rate at which the cold front overtakes the warm front.

In general, the barometric tendency in the warm sector is negative. We then see that negative tendency in the warm sector favours the occlusion. If the rise in pressure behind the cold front $\left(\text{i. e. } \frac{\partial p_4}{\partial t}\right)$, is larger than the magnitude of the fall in front of the warm front $\left(\text{i. e. } \frac{\partial p_1}{\partial t}\right)$, we also have favourable conditions for occlusion. The opposite conditions are in disfavour of occlusion.

The occlusion process naturally depends in the first instance on the occluding velocity. But the difference in velocity between the cold and the warm front is a result of acceleration, sinee the front originally was stationary. If we want to decide whether a warm sector cyclone is going to be long-lived or not, we should consult both velocity and acceleration.

Type B. Having detailed the discussion of the previous type A, we may now more briefly discuss the type B, which is represented in fig. 15. The main characteristic of this type is that the cold air isobars in the vicinity of the fronts are curved cyclonically.

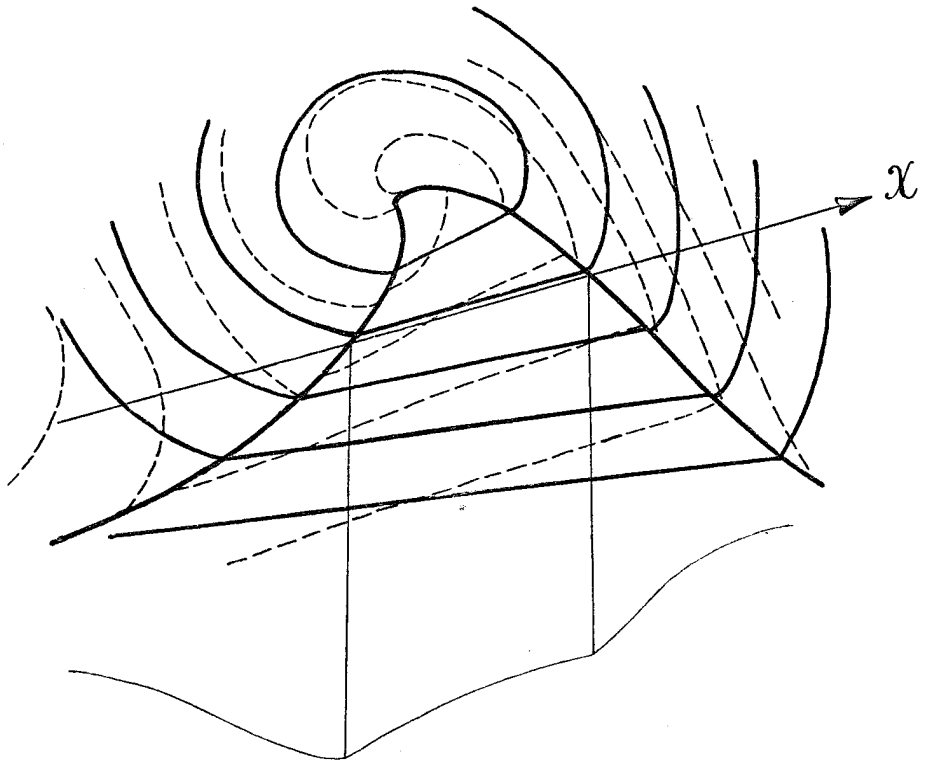

Fig. 15. Warm sector cyclone, type B. For symbols see fig. 14.

We index the air masses as shown under type A. The general equation 24 (1) then gives for the warm front:

$$A_f = -\frac{\left(\frac{\partial^2 p_1}{\partial t^2} - \frac{\partial^2 p_2}{\partial t^2}\right) + 2\,C_f\left(\frac{\partial^2 p_1}{\partial x \partial t} - \frac{\partial^2 p_2}{\partial x \partial t}\right) + C_f^2\left(\frac{\partial^2 p_1}{\partial x^2} - \frac{\partial^2 p_2}{\partial x^2}\right)}{\frac{\partial p_1}{\partial x} - \frac{\partial p_2}{\partial x}}.$$

Consulting the barogram, we see that $\frac{\partial^2 p_1}{\partial t^2}$ is positive, whereas $\frac{\partial^2 p_2}{\partial t^2}$ is zero or slightly negative. The denominator is, as previously positive, and $\frac{\partial p_2}{\partial x} = 0$. The first term of the acceleration may, therefore, be written:

$$A' = -\frac{\frac{\partial^2 p_2}{\partial t^2}}{\frac{\partial p_1}{\partial x}} < 0.$$

In the second term we have $C_f > 0$ and $\frac{\partial^2 p_1}{\partial x \partial t} > 0$ and $\frac{\partial^2 p_2}{\partial x \partial t} > 0$, but the isallobaric ascendant in the warm sector $\left(\text{i. e.} \frac{\partial^2 p_2}{\partial x \partial t}\right)$ is decidedly smaller than $\frac{\partial^2 p_1}{\partial x \partial t}$. We therefore get:

$$A'' = -2\, C_f \frac{\frac{\partial^2 p_1}{\partial x \partial t} - \frac{\partial^2 p_2}{\partial x \partial t}}{\frac{\partial p_1}{\partial x}} < 0.$$

In the third term we obviously have $\frac{\partial^2 p_2}{\partial x^2} = 0$ and $\frac{\partial^2 p_1}{\partial x^2} > 0$, and hence:

$$A''' = -C_f{}^2 \frac{\frac{\partial^2 p_1}{\partial x^2}}{\frac{\partial p_1}{\partial x}} < 0.$$

The acceleration of the cold front is obtained by substituting index 3 for index 1 and 4 for 2 in the general equation.

Consulting the barogram, we see that $\frac{\partial^2 p_3}{\partial t^2}$ is negative because the tendency increases towards the cold front. $\frac{\partial^2 p_4}{\partial t^2}$ is zero or slightly positive, and in any case smaller in magnitude than $\frac{\partial^2 p_3}{\partial t^2}$. In the denominator we have $\frac{\partial p_3}{\partial x} = 0$ and $\frac{\partial p_4}{\partial x} < 0$. The first term of the cold front acceleration may, therefore, be written:

$$A' = \frac{\frac{\partial^2 p_3}{\partial t^2} - \frac{\partial^2 p_4}{\partial t^2}}{\frac{\partial p_4}{\partial x}} > 0.$$

In the second term we have $\frac{\partial^2 p_3}{\partial x \partial t} > 0$ and $\frac{\partial^2 p_4}{\partial x \partial t} < 0$. We therefore get:

$$A'' = -2\, C_f \frac{\frac{\partial^2 p_3}{\partial x \partial t} - \frac{\partial^2 p_4}{\partial x \partial t}}{-\frac{\partial p_4}{\partial x}} < 0.$$

In the third term we have: $\frac{\partial^2 p_3}{\partial x^2} = 0$, and $\frac{\partial^2 p_4}{\partial x^2} > 0$, therefore:

$$A''' = -C_f{}^2 \frac{\frac{\partial^2 p_4}{\partial x^2}}{\frac{\partial p_4}{\partial x}} > 0.$$

Summing up, we get the following schedule for the distribution of front acceleration in a cyclone of type B.

Table 3. Type B.

	Warm Front	Cold Front
A'	$-\frac{\frac{\partial^2 p_1}{\partial t^2}}{\frac{\partial p_1}{\partial x}} < 0$	$\frac{\frac{\partial^2 p_3}{\partial t^2} - \frac{\partial^2 p_4}{\partial t^2}}{\frac{\partial p_4}{\partial x}} > 0$
A''	$-2\,C_f \frac{\frac{\partial^2 p_1}{\partial x \partial t} - \frac{\partial^2 p_2}{\partial x \partial t}}{\frac{\partial p_1}{\partial x}} < 0$	$2\,C_f \frac{\frac{\partial^2 p_3}{\partial x \partial t} - \frac{\partial^2 p_4}{\partial x \partial t}}{\frac{\partial p_4}{\partial x}} < 0$
A'''	$-C^2{}_f \frac{\frac{\partial^2 p_1}{\partial x^2}}{\frac{\partial p_1}{\partial x}} < 0$	$-C_f{}^2 \frac{\frac{\partial^2 p_4}{\partial x^2}}{\frac{\partial p_4}{\partial x}} > 0$

We thus see that the warm front is always retarded, whereas the cold front may be accelerated or retarded according to which of the three terms are predominating.

The formula for the velocity of the cold front may be written:

$$C_f = -\frac{\frac{\partial p_3}{\partial t} - \frac{\partial p_4}{\partial t}}{\frac{\partial p_3}{\partial x} - \frac{\partial p_4}{\partial x}}.$$

Again, $\frac{\partial p_3}{\partial x} = 0$ and $-\frac{\partial p_4}{\partial x} > 0$. Since the cold front of this type is accompanied by a very slight discontinuity in pressure gradient, simultaneous to a more pronunced discontinuity in pressure tendency, C_f is large. The type B is exactly the type that is generally recognized[1]) as a quickly running cold front. Since C_f is large, the third term of the acceleration is likely to carry larger weight than the other terms. A cold front of this type is, therefore, likely to be accelerated. Since simultaneously the warm front is retarded, we arrive at the conclusion that a *cyclone of type B occludes quickly*.

It would be easy to list a number of recent cyclones which belong to the type B. In fact, most warm sector cyclones belong to this type, at least with regard to the central region of the cyclone. The outskirts may exihibit other features, and we shall presently comment on such cases.

An excellent example of type B occured over the British Isles on January 23rd 1926 in the morning.[2]) The cyclone moved quickly and occluded at an enormous rate, developing a 'bent back' occlusion, which during 12 hours, grew to the length of about 600 km. A discription of this cyclone has been rendered by J. Bjerknes (loc. cit.) who has pointed out some other interesting features of this type of cyclone. We shall return to the same type of cyclone when dealing with frontogenesis and deepening and filling.

[1]) See f. inst. J. Bjerknes: Practical Examples of Polar-Front Analysis. Geophysical Memories No. 50. London 1930.

[2]) See example 11, chapter VII.

Type C. It frequently happens that the cyclone exhibits a warm front of type A and a cold front of type B (Fig. 16). In this case we get the following schedule for the distribution of acceleration.

Table 4. Type C.

	Warm Front	Cold Front
A'	$-\dfrac{\dfrac{\partial^2 p_1}{\partial t^2}}{\dfrac{\partial p_1}{\partial x}} > 0$	$\dfrac{\dfrac{\partial^2 p_3}{\partial t^2} - \dfrac{\partial^2 p_4}{\partial t^2}}{\dfrac{\partial p_4}{\partial x}} > 0$
A''	$-2\,C_f \dfrac{\dfrac{\partial^2 p_1}{\partial x \partial t}}{\dfrac{\partial p_1}{\partial x}} < 0$	$2\,C_f \dfrac{\dfrac{\partial^2 p_3}{\partial t^2} - \dfrac{\partial^2 p_4}{\partial t^2}}{\dfrac{\partial p_4}{\partial x}} < 0$
A'''	$-C_f{}^2 \dfrac{\dfrac{\partial^2 p_1}{\partial x^2}}{\dfrac{\partial p_1}{\partial x}} > 0$	$-C_f{}^2 \dfrac{\dfrac{\partial^2 p_4}{\partial x^2}}{\dfrac{\partial p_4}{\partial x}} > 0$

This type naturally occludes quicker than type A, but slower than type B. Type C exhibits some interesting features with regard to frontogenesis, deepening and filling etc. We shall return to this type later on.

Theoretically, it might be possible to combine a warm front of type B with a cold front of type A in one cyclone. Experience shows, however, that the case is extremely rare. We shall, therefore, not make any further comments on this type. Its properties with regard to acceleration are easily obtained by combining the results contained in the tables 2 and 3.

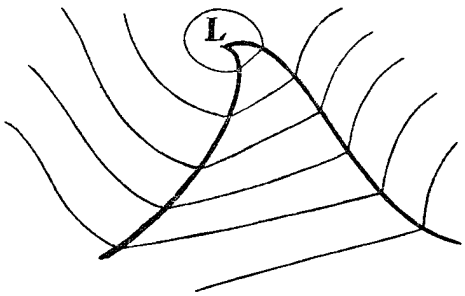

Fig. 16.

Type D. Most frequently the cyclones exhibit other combinations of types A and B. The most common case is that the northern parts of the warm and the cold fronts are of type B, whereas the southern parts are of type A. Most frequently the type B predominates on the cold front. This case is represented in Fig. 17.

Along the line L_1 we have the conditions represented by type B. Along the line L_2 we have type C, and along the line L_3 we have the conditions represented by type A. This frequent type of cyclone is charachterized by rapid occlusion near the center, and a remaining warm sector in the southern part. The southern part of the cold front, which is retarded, soon becomes stationary, simultaneously being exposed to the effect of frontogenesis, and under certain circumstances, cyclogenesis. We shall return to these questions in some later paragraphs.

Occlusions. The previous considerations on types of fronts refer to warm and cold fronts respectively. We have, however, not used temperature differences as arguments. The considerations are based on the structure of the pressure field only. The various

types of fronts mentioned above, are, therefore, representative for occlusions also, when the pressure field corresponds to any of the mentioned types. A word or two on occlusions may, however, be of some value.

In fig. 18 is drawn a partly occluded cyclone, which in structure is principally the same as the so-called *occlusion model* designed by Dr. Bergeron, and circulated in the Norwegian Weather Service as a professional note. The writer understands that the partly occluded cyclone will be subjected to a thorough examination by Dr. Bergeron in the second part of his *Dreidimensionale Wetteranalyse.* We shall, therefore, restrict our comments on occlusions to their properties with regard to acceleration.

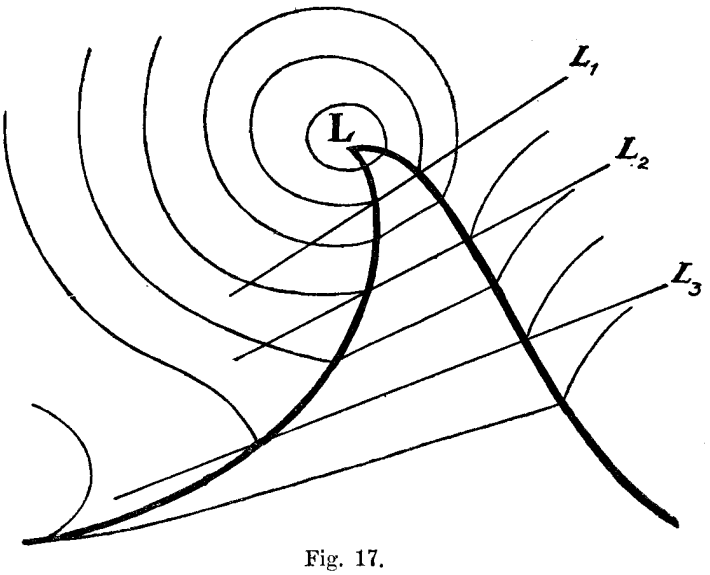

Fig. 17.

The various parts of the fronts in fig. 18 have features which correspond to either of the types mentioned previously. The arrows represent the acceleration of various typical parts of the fronts. The upper cold front, which is represented by the broken curve, may be accelerated or retarded according to the pressure conditions aloft. It is, however, most likely that it is accelerated in the vicinity of the junction point between the warm and the cold front, and retarded nearer the center.

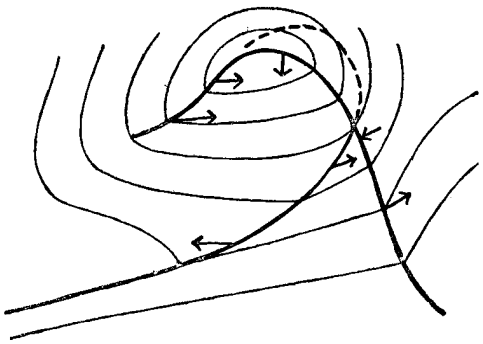

Fig. 18.

It is worth notice that the bent back occlusion in the rear of the center is equivalent to an accelerated cold front. It is easily understood that the distribution of velocity and acceleration along the occluded front may lead to a repeated occlusion process, which brings the bent back occlusion in contact with the primary occlusion, and that this process may lead to a new bent back occlusion of seemingly complicated structure.[1])

The types of fronts which we have discussed with regard to acceleration, should only be regarded as *tentative models.* A rational classification of fronts (with regard to acceleration, frontogenesis, rain intensity etc.) should be based on the study of a large number of authographic records. The writer hopes to be able to return to this subject in a later communication.

26. Frontogenesis and Frontolysis. Soon after the discovery of the fronts, it was realized that the fronts were subjected to processes which either diminished or increased

[1]) Only little is known as to the aerology of bent back occlusions. Frequently such fronts do not move with the air current at the ground. They should then be regarded as upper fronts — probably troughs of warm air — projecting from the varm sector at some altitude.

their intensities. Dr. Bergeron[1]) has proposed the phrases *frontogenesis* for the production of fronts and *frontolysis* for the destruction of fronts. A front is said to be exposed to frontogenesis when it develops towards increased intensity, and it is said to be exposed to frontolysis when it develops in the opposite direction.

According to Bergeron, the field of deformation produces a front along its stress-axis. In the régime of a neutral point in the pressure distribution, it is easy to locate the stress-axis, and to estimate the possibilities for formation of fronts.

In a moving cyclone f. ex, conditions are more complicated, and it is frequently impossible to estimate the whereabouts of the axes of deformation. It is, therefore, difficult to judge whether a ready made front is exposed to frontogenesis or frontolysis.

Giao has treated the problem of frontogenesis-frontolysis from a different point of view. The problem which has interested Giao is the following: What are the conditions which determine frontogenesis or frontolysis at a pre-existing front.

Let τ_1 and τ_2 denote the temperatures of adjacent air particles separated from one another by a front surface. The temperature variations on either side of a moving element of the front is obtained by applying the operator defined by **3** (6) to τ_1 and τ_2 viz:

$$\begin{aligned} \frac{\delta\tau_1}{\delta t} &= \frac{\partial\tau_1}{\partial t} + C_f\frac{\partial\tau_1}{\partial x} \\ \frac{\delta\tau_2}{\delta t} &= \frac{\partial\tau_2}{\partial t} + C_f\frac{\partial\tau_2}{\partial x} \end{aligned} \tag{1}$$

where C_f is the velocity of the front element along the chosen x-axis. The temperature discontinuity at the front element is $\tau_1 - \tau_2 = \Delta\tau$. The variation with time in $\Delta\tau$ at a moving front element is obtained from (1), by subtracting the one equation from the other:

$$F(\tau) = \frac{\delta\Delta\tau}{\delta t} = \frac{\partial\tau_1}{\partial t} - \frac{\partial\tau_2}{\partial t} + C_f\left(\frac{\partial\tau_1}{\partial x} - \frac{\partial\tau_2}{\partial x}\right). \tag{2}$$

The function $F(\tau)$ may then be taken as a measure of the intensity of the frontogenetical or frontolytical process in the field of temperature.

Equation (2) is not directly applicable to the weather charts, because the temperature tendencies are not known, and the temperature gradients obtained from the charts, are often misleading, because of the poor representativeness of surface temperatures. Neglecting the vertical velocity and performing various substitutions in (2), Giao derives the following equation:

$$F(\tau) = \frac{\tau_m}{p}\frac{C_p - C_v}{C_p}\frac{\partial p}{\partial y}(V_1 - V_2) - \left(V_1\frac{\partial\tau_1}{\partial y} - V_2\frac{\partial\tau_2}{\partial y}\right), \tag{3}$$

where τ_m is the mean value of τ_1 and τ_2. C_p and C_v are the specific heats respectively for constant pressure and constant volume. $(V_1 - V_2)$ is the discontinuity in wind velocity parallel to the front. $-\frac{\partial\tau_1}{\partial y}$ and $-\frac{\partial\tau_2}{\partial y}$ are the temperature gradients tangential to the front.

The first term on the right hand side represents the adiabatic change in temepera-ture, and the second term represents the 'transport of temperature' tangential to the front. Equation (3) expresses in simple terms some of the chief agents which produce frontogenesis or frontolysis. But, for reasons mentioned above, the equation is not applicable to the weather charts.

As the frontogenetical or frontolytical process causes variations in most quantities which characterize a front, we may define the measure for these processes in a more

[1]) Die dreidimensional Verknüpfende Wetteranalyse. Geofysiske Publikasjoner Vol. V, No. 6.

general way. Let s_1 and s_2 be some property at both sides of a front surface. We may then define the frontogenetical (or frontolytical) function as:

$$F(s) = \frac{\delta(s_1 - s_2)}{\delta t} = \frac{\partial s_1}{\partial t} - \frac{\partial s_2}{\partial t} + C_f \left(\frac{\partial s_1}{\partial x} - \frac{\partial s_2}{\partial x}\right) \tag{4}$$

because $\frac{\delta(s_1 - s_2)}{\delta t}$ measures the variations in the discontinuity in s at the moving element of the front. For density we would have, for instance:

$$F(\varrho) = \frac{\delta(\varrho_1 - \varrho_2)}{\delta t} = \frac{\partial \varrho_1}{\partial t} - \frac{\partial \varrho_2}{\partial t} + C_f \left(\frac{\partial \varrho_1}{\partial x} - \frac{\partial \varrho_2}{\partial x}\right). \tag{5}$$

We say that we have frontogenesis when the quantity in question $(s_1 - s_2)$ increases at the moving front element, and frontolysis when the discontinuity decreases.

As in paragraph 25, we choose the x-axis along the warm sector isobars so that C_f is positive both for warm and cold fronts. We then get the following schedule for the sign of F:

Table 5.

	Frontogenesis	Frontolysis
Warm Front	$F(\tau) < 0$ $F(\varrho) > 0$	$F(\tau) > 0$ $F(\varrho) < 0$
Cold Front	$F(\tau) > 0$ $F(\varrho) < 0$	$F(\tau) < 0$ $F(\varrho) > 0$

We shall now endeavour to express the effect of frontogenesis or frontolysis in terms of pressure only. This is so much more convenient, because pressure is the only element for which no question of representativeness arises.

According to the dynamical surface condition, there can be no discontinuity in pressure at the front. The time or space derivatives may, however, be discontinuous. In fact, the definition of a front involves discontinuity in the x-component of the pressure ascendant (see paragraph 23). We, therefore, propose to study the production or destruction of this discontinuity. Studying a number of fronts by means of autographic records, J. Bjerknes[1]) has shown that there is an intimate connection between the frontogenesis of the temperature field and the variations in the discontinuity in the pressure gradient at the front. Bjerknes understands that cold fronts become accelerated because of downward motion in the rear of the front. The downward motion causes adiabatic heating of the cold air and a decrease in the temperature discontinuity. Bjerknes' examination showed that cold fronts which were subjected to this development, developed into our type B, which we have previously described, whereas retarded cold fronts developed into our type A, simultaneously increasing in intensity. Moreover, it was found that there exists a close relation between the acceleration and the velocity on one hand, and the frontogenesis or frontolysis on the other.

Led by Bjerknes' ideas, we shall endeavour to express these rules in more concise forms.

According to the dynamical surface condition the pressure at both sides of the front must be equal. From this it follows that the pressure ascendant tangential to the front

[1]) Practical Examples etc. Loc. cit.

(the y-component) must be equal on both sides, because otherwise, the continuity in pressure could not be maintained. The discontinuity in pressure gradient at the front can, therefore, be represented by the discontinuity in the x-component of the pressure ascendant, or $\frac{\partial p_1}{\partial x} - \frac{\partial p_2}{\partial x}$. This quantity defines the pressure trough which accompanies the front. The expression for the frontogenesis or frontolysis of this quantity is then obtained from the general equation (4), by substituting $\frac{\partial p}{\partial x}$ for s, viz:

$$F\left(\frac{\partial p}{\partial x}\right) = \left(\frac{\partial^2 p_1}{\partial x \partial t} - \frac{\partial^2 p_2}{\partial x \partial t}\right) + C_f\left(\frac{\partial^2 p_1}{\partial x^2} - \frac{\partial^2 p_2}{\partial x^2}\right) \tag{6}$$

where the first term stands for the difference in the x-component of the isallobaric ascendant, and the terms in the last bracket give the difference in the curvatures of the pressure profiles at both sides of the front. Both these quantities are easily obtained from the weather charts (see paragraph 9). It is, therefore, easy to calculate the rate at which the discontinuity increases or decreases. The discontinuity increases when $F\left(\frac{\partial p}{\partial x}\right)$ is positive and decreases when it is negative, because $\left(\frac{\partial p_1}{\partial x} - \frac{\partial p_2}{\partial x}\right)$ is, by definition, positive.

Both terms in equation (6) are contained in the formula for the acceleration of the front. It is, therefore, only natural that the empirical investigations of B j e r k n e s have revealed some connection between frontogenesis and acceleration.

The relation, is, however, not a simple one.

As the front is accompanied by a discontinuity in pressure tendency, we may endeavour to express the production or destruction of this discontinuity in exact form. We would then have to apply the general definition of frontogenesis to the quantity $\frac{\partial p}{\partial t}$, which represents pressure tendency. Substituting $\frac{\partial p}{\partial t}$ for s in equation (4), we get:

$$F\left(\frac{\partial p}{\partial t}\right) = \left(\frac{\partial^2 p_1}{\partial t^2} - \frac{\partial^2 p_2}{\partial t^2}\right) + C_f\left(\frac{\partial^2 p_1}{\partial x \partial t} - \frac{\partial^2 p_2}{\partial x \partial t}\right), \tag{7}$$

where the terms in the first bracket depend on the curvatures of the barograms on either side of the front, and the terms in the last bracket give the difference in isallobaric ascendant. The terms in (7) are also contained in the general formula for the acceleration of a front (see equation **24** (1)). In fact, the equations (6) and (7) combined and compared with **24**, (1) give:

$$A_f = -\frac{F\left(\frac{\partial p}{\partial t}\right) + C_f F\left(\frac{\partial p}{\partial x}\right)}{\frac{\partial p_1}{\partial x} - \frac{\partial p_2}{\partial x}}, \tag{8}$$

which equation states the complete relation between the acceleration of the front and the frontogenesis of the field of pressure. As the denominator in (8) is positive, we see that the acceleration is negative when there is frontogenesis in pressure tendency and in pressure gradient.

The function $F\left(\frac{\partial p}{\partial x}\right)$ is more easily discussed in connection with weather charts than is the function $F\left(\frac{\partial p}{\partial t}\right)$. We shall, therefore, return to equation (6) and discuss it in detail. This equation is also the more important one, because it tells whether the front is going to increase or decrease in intensity.

It is most convenient to discuss formula (6) in connection with the types of fronts described in the previous paragraph. We start with a warm front of type A. We choose the x-axis along the warm sector isobar, and we index the air masses in the same way as previously. As shown in paragraph 25, we have:

$$\frac{\partial^2 p_2}{\partial x \partial t} = \frac{\partial^2 p_2}{\partial x^2} = 0, \quad \frac{\partial^2 p_1}{\partial x \partial t} > 0, \quad \frac{\partial^2 p_1}{\partial x^2} < 0$$

and therefore

$$F\left(\frac{\partial p}{\partial x}\right) = \left|\frac{\partial^2 p_1}{\partial x \partial t}\right| - \left|C_f \frac{\partial^2 p_1}{\partial x^2}\right|. \tag{9}$$

The two terms have opposite signs, and there is no general rule for the sign of $F\left(\frac{\partial p}{\partial x}\right)$. When the front is stationary or nearly so, it is likely that the first term is predominating. When the velocity is large, the second (negative) term is probably the larger one. The two terms are apt to balance one another, and fronts of this type are long-lived.

For the cold front of type A we have according to paragraph 25:

$$F\left(\frac{\partial p}{\partial x}\right) = -\frac{\partial^2 p_4}{\partial x \partial t} - C_f \frac{\partial^2 p_4}{\partial x^2}, \tag{10}$$

where $\frac{\partial^2 p_4}{\partial x^2} < 0$. Furthermore $\frac{\partial^2 p_4}{\partial x \partial t} > 0$ near the center, and $\frac{\partial^2 p_4}{\partial x \partial t} < 0$ along the more distant part of the front. For the more distant part of this cold front we get without exception:

$$F\left(\frac{\partial p}{\partial x}\right) > 0.$$

In paragraph 25 we found that the acceleration of this part of the cold front is negative. *The front is retarded and exposed to frontogenesis.*

The practical importance of this rule, which holds without exception, can hardly be overestimated. The reinforcement and simultaneous retardation of the cold front leads to a sharp stationray front, which in due time, may produce a new wave cyclone. The negative acceleration may lead to a retrograde movement of the cold front, and thus give birth to a new cyclone. (See paragraph 27).

The part of the cold front which is most distant from the center, is practically always of this type (see fig. 17 and 18). The retardation and reinforcement of this part of the front act in such a manner as *to link together the various members of the cyclone series.*

Looking again at the equations (9) and (10), we see that the frontogenetical and frontolytical processes depend only on the conditions in the cold air, since there are no terms of indices 2 or 3. The same rule may also be deduced from equation (2). Owing to the homogeneous conditions in the warm-sector air, we may neglect the terms $\frac{\partial \tau_2}{\partial t}$ and $\frac{\partial \tau_2}{\partial x}$ against the corresponding terms for the cold air. Examining some synoptic charts, J. Bjerknes[1]) found that the reinforcement of fronts was caused by processes in the cold air, notably adiabatic temperature variations.

Let us next consider a warm front of type B (fig. 15). According to the considerations in paragraph 25, we have:

$$\frac{\partial^2 p_1}{\partial x \partial t} - \frac{\partial^2 p_2}{\partial x \partial t} > 0, \quad \frac{\partial^2 p_1}{\partial x^2} > 0 \quad \text{and} \quad \frac{\partial^2 p_2}{\partial x^2} = 0.$$

[1]) Practical Examples, loc. cit.

We, therefore, get:

$$F\left(\frac{\partial p}{\partial x}\right) = \left|\frac{\partial^2 p_1}{\partial x \partial t} - \frac{\partial^2 p_2}{\partial x \partial t}\right| + \left|C_f \frac{\partial^2 p_1}{\partial x^2}\right| > 0. \tag{11}$$

Therefore: *A warm front of type B, is retarded (see paragraph 25) and exposed to frontogenesis.* The frontogenesis is, however, rarely as active at this type of warm front as it is at a cold front of type A, because, in general, none of the terms in (11) are as large as the corresponding terms in (10).

For a cold front of type B we have, according to paragraph 25:

$$\frac{\partial^2 p_3}{\partial x \partial t} - \frac{\partial^2 p_4}{\partial x \partial t} > 0, \quad \frac{\partial^2 p_3}{\partial x^2} = 0 \text{ and } \frac{\partial^2 p_4}{\partial x^2} > 0.$$

We then get

$$F\left(\frac{\partial p}{\partial x}\right) = \left|\frac{\partial^2 p_3}{\partial x \partial t} - \frac{\partial^2 p_4}{\partial x \partial t}\right| - \left|C_f \frac{\partial^2 p_4}{\partial x^2}\right|. \tag{12}$$

The two terms counteract one another. However, when the velocity is large, the last term predominates. Bjerknes' rule, that quickly running cold fronts of this type are exposed to frontolysis, thus seems corroborated.

The fronts of the types C and D, as well as occluded fronts mentioned in paragraph 25, belong in parts to type A and in parts to type B. The discussion of these types, therefore, would bring to light no further details.

A word or two may be said about the application of these equations to the weather charts. The function $F\left(\frac{\partial p}{\partial x}\right)$ is very easily evaluated. The four important equations (9), (10), (11), and (12) contain terms of two types, viz: $\frac{\partial^2 p}{\partial x \partial t}$ and $\frac{\partial^2 p}{\partial x^2} C_f$. The first quantity, which is an isallobaric ascendant, may be replaced by the reciprocal of the distance along the x-axis between two consecutive unit isallobars. The quantity $\frac{\partial^2 p}{\partial x^2}$ is the variation in $\frac{\partial p}{\partial x}$ along the x-axis. This quantity may be determined exactly as described in paragraph 9, by means of the two distances between three consecutive isobars.

The general equation (6) is very easily applied for studying frontogenesis and frontolysis at stationary fronts. We then choose the x-axis perpendicular to the front, and positive towards cold air, and let index 1 denote the cold air. For a stationary front, we have $C_f = 0$. Equation (6) then gives:

$$F\left(\frac{\partial p}{\partial x}\right) = \frac{\partial^2 p_1}{\partial x \partial t} - \frac{\partial^2 p_2}{\partial x \partial t} = I_{x_1} - I_{x_2} \tag{13}$$

when I_x denotes the x-component of the isallobaric ascendant.

Equation (13) shows that there is frontogenesis at stationary fronts when the isallobaric gradients ($-I_x$) are directed towards the front, and frontolysis when they are directed away from the front.

The results of the above discussions are comprised in fig. 19. Writting equation (6) in the following form:

$$F\left(\frac{\partial p}{\partial x}\right) = A + C_f B,$$

where

$$A = \frac{\partial^2 p_1}{\partial x \partial t} - \frac{\partial^2 p_2}{\partial x \partial t},$$

and

$$B = \frac{\partial^2 p_1}{\partial x^2} - \frac{\partial^2 p_2}{\partial x^2},$$

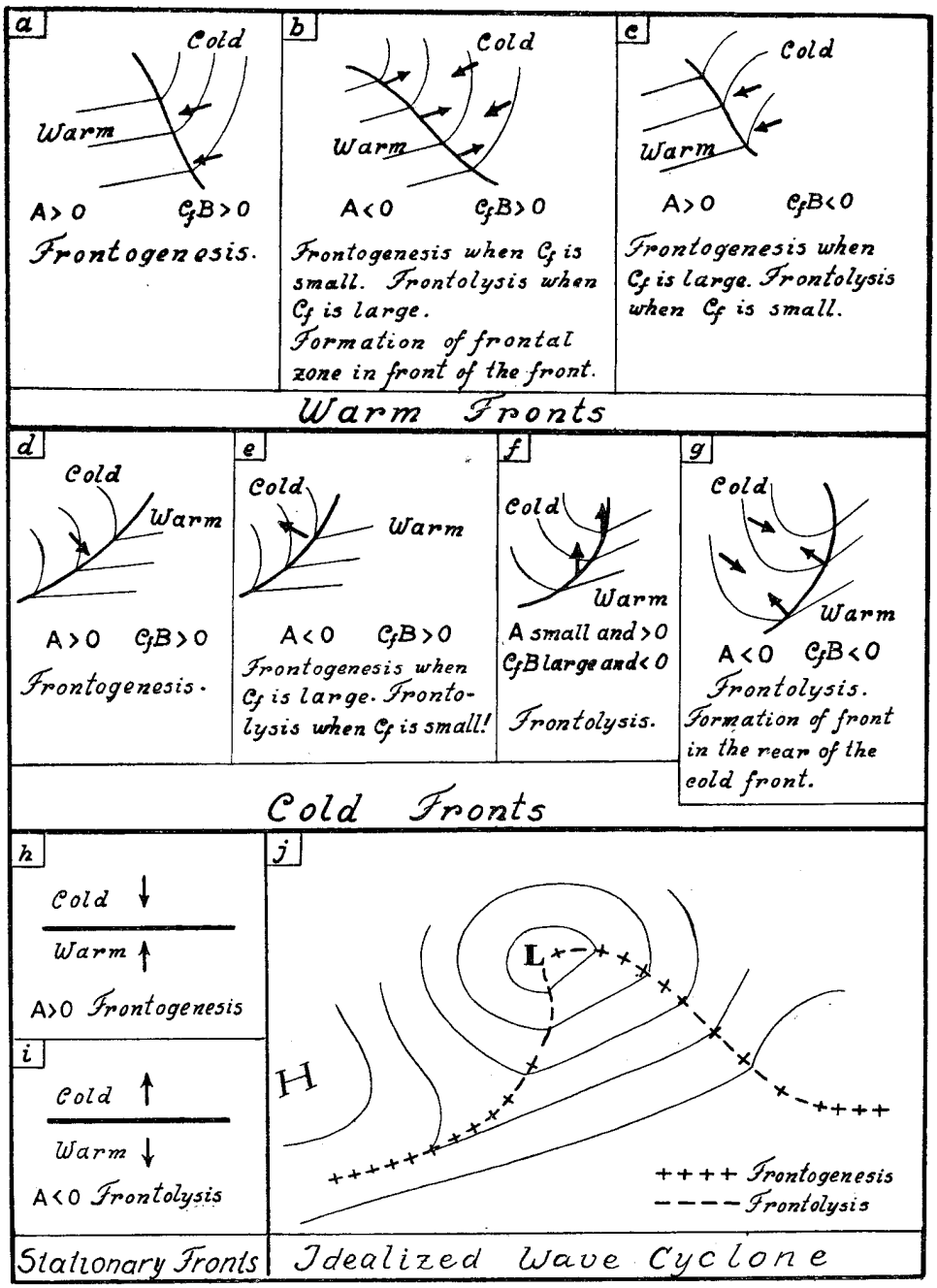

Fig. 19.

the symbols in fig. 19 give the possibilitis of frontogenesis or frontolysis at some frequent types of fronts. The small arrows indicate the directions of the isallobaric *gradients.* The x-axes are everywhere chosen along the warm sector isobars.

The idealized wawe cyclone in fig. 19 shows the normal distribution of frontogenesis along the front. It is interesting to see that the northern part of the warm front and the southern part of the cold front are exposed to frontogenesis. The occluded front, which results from such a cyclone, may, therefore, be a sharp one. Most frequently the northern part of the cold front and the southern part of the warm front are exposed to frontolysis. It is a common experience that cold fronts increase, and warm fronts decrease in intensity with distance from the cyclonic center.

In paragraph 29, we shall see that the convergence of the isallobaric gradient represents the convergence of the field of motion, and that frontogenesis depends largely on the convergence of the air currents.

We have in this paragraph given a quite general definition of frontogenesis, and shown how the increase or otherwise in the discontinuity of pressure gradient at a front can be calculated. *Prima facie,* it might seem as if the study of the function $F\left(\frac{\partial p}{\partial x}\right)$ has very little to do with frontogenesis or frontolysis in the current meaning of the word.

According to Bergeron[1]), frontogenesis gives concentration of the equiscalar surfaces of temperature at the front, and frontolysis gives separation of these surfaces. Moreover, frontogenesis means concentration of solenoids, and frontolysis dispersion of solenoids at the front. No such terms enter in our equations. If our function $F\left(\frac{\partial p}{\partial x}\right)$ is conform with frontogenesis—frontolysis in the current meaning, it must be because the pressure function contains the other arguments implicitly.

The connection between $F\left(\frac{\partial p}{\partial x}\right)$ and the variables which determine frontogenesis—frontolysis in the common meaning, could be obtained by substituting for p or $\frac{\partial p}{\partial x}$ in $F\left(\frac{\partial p}{\partial x}\right)$ by means of the equations of motion, the equation of condition or other convenient equations. A relation thus obtained, would, however, contain terms which are not discussable on the basis of the weather chart data. We shall, therefore, not enter into this discussion here, because it would fall outside the scope of this paper, which only deals with what is calculable from the weather charts. We shall here only show a simple relation between the function $F\left(\frac{\partial p}{\partial x}\right)$ and the function $F(\varrho)$, which gives the frontogenesis in density.

When $\tan\theta$ denotes the inclination of the front surface, we have[2])

$$\tan\theta = \frac{\frac{\partial p_1}{\partial x} - \frac{\partial p_2}{\partial x}}{g(\varrho_1 - \varrho_2)}$$

---

[1]) Die Dreidimensional verknüpfende Wetteranalyse, loc. cit.

[2]) See paragraph 23.

In a system of co-ordinates which is fixed to the front, we get by differentiation:

$$\frac{\delta\left(\frac{\partial p_1}{\partial x}-\frac{\partial p_2}{\partial x}\right)}{\delta t}=g\ \tan\theta\ \frac{\delta(\varrho_1-\varrho_2)}{\delta t}+g(\varrho_1-\varrho_2)\frac{\delta\tan\theta}{\delta t}$$

which compared to (5) and (6) gives:

$$F\left(\frac{\partial p}{\partial x}\right)=g\,F(\varrho)\ \tan\ \theta+g(\varrho_1-\varrho_2)\frac{\delta\ \tan\ \theta}{\delta t},$$

where $\frac{\delta\tan\theta}{\delta t}$ means the variation with time in the inclination of the moving element of the front surface. When θ is constant we have that $F\left(\frac{\partial p}{\partial x}\right)$ is directly proportional to $F(\varrho)$. The synoptical studies seem to indicate that the last term, which depends on the time variation in inclination, either is insignificant, or else acts in such a manner that $F\left(\frac{\partial p}{\partial x}\right)$ and $F(\varrho)$ always have the same sign. If this be so, we may consider $F\left(\frac{\partial p}{\partial x}\right)$ as expressive of the production or destruction of the density discontinuity. In this case $F\left(\frac{\partial p}{\partial x}\right)$ *is expressive of the intensity of the concentration or dispersion of solenoids at the front.* We shall return to these questions in a later paper.

27. Stationary Fronts. The formulae for the velocity and acceleration may be applied for discussing conditions at stationary fronts. It is then convenient to choose the x-axis normal to the front and positive from the warm towards the cold side.

We say that the front is stationary at the point in question, when the velocity normal to the front is zero. From **22** (2) we then get:

$$C_f=-\frac{\frac{\partial p_1}{\partial t}-\frac{\partial p_2}{\partial t}}{\frac{\partial p_1}{\partial x}-\frac{\partial p_2}{\partial x}}=0. \tag{1}$$

By definition we have $\frac{\partial p_1}{\partial x}-\frac{\partial p_2}{\partial x}\gtrless 0$ (see paragraph 23). From (1) we then get for a stationary front:

$$\frac{\partial p_1}{\partial t}-\frac{\partial p_2}{\partial t}=0. \tag{2}$$

The front is stationary when the tendencies are equal on both sides of the front.

It seems to be a general opinion that a front which is parallel to the isobars (for instance old occlusions) is stationary. This supposition does not hold, unless simultaneously (2) holds. A front which is parallel to the isobars, moves (as do all other fronts) towards the lowest tendency. This circumstance is particulary significant for the front at the tongue of cold air between two cyclones. Such tongues generally move southwards in spite of there being no isobars crossing the front. The southward displacement of the cold air tongue is due to the circumstance that the tendency is (algebraically) larger on the cold side than on the warm one.

Equation **24** (1) gives for a stationary front:

$$A_f=-\frac{\frac{\partial^2 p_1}{\partial t^2}-\frac{\partial^2 p_2}{\partial t^2}}{\frac{\partial p_1}{\partial x}-\frac{\partial p_2}{\partial x}} \tag{3}$$

The denominator is, by definition, different from zero, and it is positive, because the x-axis points towards the cold air, whose index is 1.

Equation (3) may be used for studying the conditions which produce a new wave on a stationary front. Let us consider a stationary front which runs (say) east—west. The questions then arise: (a) Is the new wave produced by a positive (northwards) acceleration of part of the front, or, (b) is the part of the front which makes up the rear of the cyclone accelerated southwards. Both processes are probably possible. From synoptic studies it is difficult to decide what actually happens at the moment of the birth of a new wave.

There is, however, sufficient evidence to show that the latter process (b) is by far the most common. The drawing of isochrones of fronts shows, that in most pronounced cases, the (say) western part of the stationary front becomes accelerated southwards. The rear of the cyclone thus born, then becomes stronger than the front part of the cyclone. Such cyclones quickly develop into formidable perturbations.

In other cases, even though uncertain, it seems as if the new wave is produced by a (say) northward acceleration of the stationary front. The wave thus born, seems to be extremely stable, travelling along the front without much increase in amplitude. Such waves frequently travel quicker than the air current.

We shall not enter into the synoptical evidences which we have already referred to, but only point out one important feature, which can be read off the pressure distribution in the vicinity of the stationary (or quasi-stationary) front.

Whether the new wave is produced according to the process (a) or (b), the acceleration which starts the phenomenon, is inversely proportional to the discontinuity in pressure gradient normal to the front (see equation (3)). As the front, by hypothesis, is stationary, the variation in the numerator of (3) cannot be caused by any displacement of the pressure field surrounding the front. The variations in the quantities $\frac{\partial^2 p_1}{\partial t^2}$ and $\frac{\partial^2 p_2}{\partial t^2}$, which represent the curvatures of the barograms on either side of the front, must then be due to processes which occur in each of the air masses. When $\frac{\partial^2 p_1}{\partial t^2}$ becomes different from $\frac{\partial^2 p_2}{\partial t^2}$, an acceleration is produced, one way or the other, which may cause a new wave. The resulting acceleration is, however, inversely proportional to the difference in pressure gradient normal to the front. We then see that the smaller this difference is, the larger is the resulting acceleration.

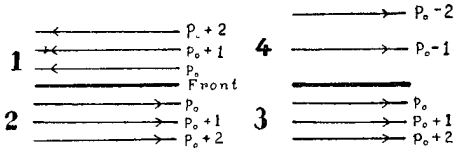

Fig. 20 a. Fig. 20 b.

Fig. 20 a and b represent two typical cases. In fig. a, the two currents are oppositely directed, and the difference in pressure gradient normal to the front is large. The acceleration resulting from a certain 'impulse' is then much smaller than in the second case (Fig. b), where the currents have the same direction. Say that the currents 1, 2 and 3 in fig. 20 have the same strength, and that the current 4 is only half of 3. We would then get that the acceleration resulting from a certain 'impulse', is in the second case four times larger than in the first case. The front surface in the first case, thus seems to be much more stable than in the second case.

These considerations would not hold good if there was any relation between the numerator and the denominator of equation (3) to the effect that the numerator and the denominator were proportional to one another. Apparently there is no such relation.

That two parallel currents of same direction more easily produce a wave than do currents of opposite directions, is a fact of experience obtained from empirical studies. Bergeron and Swoboda[1]) thus write: 'Auch an der Grenzfläche zwischen einer kalten und einer raschen bewegten warmen Westströmung kann Zyklogenese eintreten. Dieser Fall ist in Wirklichkeit sogar der häufigere.' J. Bjerknes[2]) also remarks that 'a polar westerly current in the north and a sub-tropical westerly current in the south is an almost unmistakable sign that a new disturbance in the shape of a young deepening disturbance is due to arrive'.

Formula (3) affords, at least, a qualitative means for estimating the stability of a front surface, and the rule stated above is uncommonly usefull in the weather service.

28. Convergence and Isallobaric Systems. In 1917 H. U. Sverdrup[3]) pointed out the dynamical significance of the field of isallobars, and showed that a very simple relation seemed to exist between the isallobaric gradient and the local acceleration of the air particles. Sverdrup found that the local acceleration is related to the isallobaric gradient in the same way as the geostrophic wind is related to the pressure gradient. Brunt and Douglas[4]) have more recently treated the question of the modification of the strophic balance caused by changing pressure distribution, and pointed out some highly interesting features which are of importance for our investigation. With due reference to the said authors, we proceed to develop the relation between the field of isallobars and the convergence of the field of motion.

Let the vectors $\boldsymbol{V}$ and $\dot{\boldsymbol{V}}$ denote wind velocity and acceleration respectively. Let ∇p, as previously, represent the pressure ascendant, and α specific volume. Put $\lambda = 2\ \omega \sin \varphi$, where ω is the angular velocity of the earth, and φ is the latitude. Let $\boldsymbol{k}$ denote a unit vector which is vertical and positive upwards. The equations of motion in the horizontal plane may then be written in the following form, when we disregard the effect of friction:

$$\dot{\boldsymbol{V}} = -\ \alpha\ \nabla p\ +\ \boldsymbol{V} \times (\lambda\ \boldsymbol{k})$$

Multiplying vectorially by $\boldsymbol{k}$, we get:

$$\boldsymbol{V} = -\ \frac{\alpha\ \nabla p}{\lambda} \times \boldsymbol{k} - \frac{\dot{\boldsymbol{V}} \times \boldsymbol{k}}{\lambda} \tag{1}$$

The first term on the right hand side of (1) is simply the geostrophic wind.

Differentiating (1) partially with respect to time, we get, when α is constant locally:

$$\frac{\partial \boldsymbol{V}}{\partial t} = -\ \frac{\alpha}{\lambda} \frac{\partial\ \nabla p}{\partial t} \times \boldsymbol{k} - \frac{1}{\lambda} \frac{\partial \dot{\boldsymbol{V}}}{\partial t} \times \boldsymbol{k} \tag{2}$$

According to the considerations of Sverdrup, Brunt and Douglas, the last term in (2) is negligible against the other. We, therefore, get:

---

[1]) Wellen und Wirbel etc., loc. cit. p. 63.

[2]) Practical Examples etc., loc. cit. p. 50 (19).

[3]) H. U. Sverdrup: Zur Bedeutung der Isallobarenkarten. Ann. d. Hydrogr. u. Mar. Met. 1917. Similar problems were also treated by Hesselberg, Sverdrup and Holtsmark, and published in Veröffentlichungen des Geophysikalischen Instituts, Leipzig.

[4]) Brunt and Douglas: On the Modification of Strophic Balance etc., Mem. of Royal Soc. Vol. 3, No. 22.

$$\frac{\partial \boldsymbol{V}}{\partial t} = -\frac{\alpha}{\lambda}\frac{\partial \nabla p}{\partial t} \times \boldsymbol{k} = -\frac{\alpha}{\lambda}\boldsymbol{I} \times \boldsymbol{k} \tag{3}$$

where $\boldsymbol{I}$ is the isallobaric ascendant. This equation shows that the local acceleration is related to the isallobaric gradient ($-\boldsymbol{I}$) in the same way as the geostrophic wind is related to the pressure gradient ($-\nabla p$). The local acceleration is tangential to the isallobars, with the lowest tendencies on its left hand side. *The isallobars, therefore, represent local acceleration in the same way as the isobars represent geostrophic wind.* Returning to equation (1), we may write

$$\dot{\boldsymbol{V}} = \frac{\partial \boldsymbol{V}}{\partial t} + \boldsymbol{V} \cdot \nabla \boldsymbol{V}$$

which combined with (3) gives:

$$\dot{\boldsymbol{V}} = -\frac{\alpha}{\lambda}\frac{\partial \nabla p}{\partial t} \times \boldsymbol{k} + \boldsymbol{V} \cdot \nabla \boldsymbol{V} \tag{4}$$

According to Brunt and Douglas (l. c. p. 32) the convective term in (4) is negligible against the others, except, when the curvature of the path is excessively large. Neglecting this term, and substituting in (1), we get:

$$\boldsymbol{V} = -\frac{\alpha \nabla p \times \boldsymbol{k}}{\lambda} - \frac{\alpha}{\lambda^2}\frac{\partial \nabla p}{\partial t}$$

or, when we introduce the geostrophic wind: $\boldsymbol{G} = -\frac{\alpha \nabla p}{\lambda} \times \boldsymbol{k}$, and the isallobaric ascendant: $\frac{\partial \nabla p}{\partial t} = \boldsymbol{I}$, we get:

$$\boldsymbol{V} = \boldsymbol{G} - \frac{\alpha}{\lambda^2}\boldsymbol{I} \tag{5}$$

The wind is thus composed of one component which is directed along the isobars, and one component directed along the isallobaric gradient ($-\boldsymbol{I}$). *The field of isallobars, therefore, represents the deviation of the wind from the geostrophic value.*

The simplifying assumptions, on which the deduction of the equations (3) and (5) is based, seem to be fully corroborated by the synoptical evidence brought to light by Sverdrup, Brunt and Douglas.

The divergence or convergence in the air masses and at their boundaries is a) question of crucial significance for the weather chart analysis and forecasting. To study divergence by means of the wind observations is of but little use, because of the poor representativeness of these observations. Equation (5), however, offers a means of expressing the divergence of the air current in terms of pressure only. Remembering that the geostrophic wind has no divergence, we get from (5):

$$\operatorname{div}(\varrho \boldsymbol{V}) = -\frac{1}{\lambda^2}\operatorname{div} \boldsymbol{I} \tag{6}$$

where ϱ is density. Disregarding again the slight horizontal variations in ϱ, we may interpret equation (6) in the following manner: *The convergence of the wind velocity is directly proportional to the convergence of the isallobaric gradient.*

The distribution of vertical velocity, which results from the convergence, may be obtained from the equation of continuity. Let $\boldsymbol{V}'$ be the three-dimentional wind vector, and let w be its vertical component. The equation of continuity may then be written:

$$\operatorname{div}(\varrho \boldsymbol{V}') = \operatorname{div}(\varrho \boldsymbol{V} + \varrho\, w\, \boldsymbol{k}) = 0$$

or

$$\text{div}\,(\varrho \boldsymbol{V}) + \frac{\partial\,(\varrho\, w)}{\partial z} = 0. \tag{7}$$

Combining (6) and (7) we get:

$$\frac{\partial\,(\varrho w)}{\partial z} = \frac{1}{\lambda^2}\,\text{div}\,\boldsymbol{I}$$

or, when we write $\text{div}\,\boldsymbol{I} = \text{conv}\,(-\boldsymbol{I})$, we get:

$$\frac{\partial\,(\varrho w)}{\partial z} = \frac{1}{\lambda^2}\,\text{conv}\,(-\boldsymbol{I}) \tag{8}$$

which gives the relation between the distribution of vertical velocity and the convergence of the isallobaric gradient $(-\boldsymbol{I})$. Since w vanishes at the surface of the earth (except at singular points or lines in the field of motion), we see that $(\varrho\, w)$ must increase with hight when the isallobaric gradients converge. Furthermore, since ϱ actually decreases with hight, it follows that w must increase with hight to such an extent that the variation in ϱ becomes over-compensated. The convergence of isallobaric gradients is, therefore, an unmistakable evidence for positive vertical velocity.

When, on the other hand, the isallobaric gradients diverge, as they do, for example, from a center of positive tendencies, $\frac{\partial\,(\varrho\, w)}{\partial\, z}$ is negative. Writing

$$\frac{\partial\,(\varrho w)}{\partial z} = w\,\frac{\partial \varrho}{\partial z} + \varrho\,\frac{\partial w}{\partial z}$$

we see that $\frac{\partial w}{\partial z}$ must be negative at the ground because w vanishes there. This means descending motion which increases with hight.

The above considerations may be applied to the weather charts for estimating the sign of w in areas where the isallobars are *closed curves*. It is a common experience that cloud systems and areas of precipitation occur in the centers of falling tendencies, whereas clearing weather occurs where the isallobaric gradients diverge from a center of positive tendencies. This coincidence between rain area and isallobaric low, seems sometimes to have lead to the misunderstanding that the rain-producing cloud system (Ast, Ast præcipitans, Nbst) is directly caused by the convergence towards the center of the isallobaric low, resulting in ascending motion. This conception, however, is at variance with the fact that (in case of a warm front), the isallobaric system belongs to the cold air, whereas the cloud system belongs to the warm air. A contingent ascending motion in the cold air cannot penetrate the front surface, and can therefore not produce the warm front cloud system. We shall return to this question in the next paragraph.

The equations (3) and (5) seem to corroborate the Guilbert's rule mentioned in paragraph 19. Equation (5) may be written:

$$\boldsymbol{G} - \boldsymbol{V} = \frac{a}{\lambda^2}\,\boldsymbol{I}$$

where the vector difference on the left hand side denotes the difference between the geostrophic wind and the true wind. This difference is directly proportional to the isallobaric ascendant. In paragraph 19 we have found that the velocity of a round pressure center is directed along $\boldsymbol{I}$. We may then say that the velocity of the pressure center is directed towards the area where the wind is most undernormal. Equation (3) expresses the same in terms of acceleration.

29. Remarks on the Distribution of Vertical Velocity in the Vicinity of Fronts. The discussion in this paragraph has no pretention of being a complete treatise of the subject. We shall here only discuss the sign and order of magnitude of the vertical velocity on the basis of the equations developed previously. In a later publication we shall endeavour to take up the problem of vertical velocity on a broader basis, and discuss it in full.

Equation **28** (8), which gives the relation between the vertical variation of vertical velocity and the convergence of the isallobaric gradient, is, as mentioned before, convenient to apply when the isallobars are *closed curves.* At a non-stationary front, however, the pressure tendency is discontinuous, because, otherwise the velocity of the front would be zero (see **23** (2)). The isallobars, therefore, either end at the front, or they run parallel to it. At the front itself the isallobaric gradient is indeterminate. This difficulty might be overcome by considering the front on a magnified scale, on which the front surface would be a layer of transition (see paragraph 20), However, since equation **28** (8) is deduced on the simplifying assumptions that the local variation in acceleration, and the convective term of the acceleration are negligible compared with the local variation in the wind velocity, we cannot apply equation **28** (8) to a layer of transition, where obviously, these quantities are large. We shall, therefore, choose to discuss the problem in a more indirect way.

It is well to note that the dynamical surface condition, which states that the pressure is continuous at the front, involves continuity in the pressure gradient *tangential* to the front. The geostrophic wind normal to the front would, therefore, be equal on both sides, except for the difference in density. Brunt and Douglas (l. c.) have shown that the slight discontinuity in densinty does not cause such discontinuity in the geostrophic wind normal to the front, that measurable amounts of precipitation could be accounted for. We must, therefore, take the acceleration into account in order to explain the rain intensities which usually occur.[1])

Let us, for sake of argument, consider a warm front as represented in fig. 14. We may now apply equation **28** (8) for discussing the convergence in each of the air masses, and equation **28** (5) for discussing the flux of air towards the front surface.

In the warm sector the isallobaric gradient is usually slight and is almost invariably directed towards the center of the cyclone. According to **28** (5), there is then in the warm sector a flux of air along the isobars (caused by the geostrophic wind), and a slight flux of air towards the pressure center. If the isallobars in the warm sector are straight and equidistant, there is no convergence (see **28** (8)), and there is, therefore, no vertical velocity. Precipitation can then only be caused by non-adiabatic cooling and expansion. The cooling by expansion may again be due to (a) the transport of air across the isobars, and (b) the local pressure variation. If the isallobaric gradients converge, there is ascending motion and increased precipitation.

On the cold side of the warm front, the isallobars generally run more parallel to the front (see fig. 14). There is then according to **28** (5), a fairly strong flux of air towards the front, which to some extent counteracts the flux of air away from

---

[1]) In a recent paper *A. Giao* means to have shown that the vertical velocity is of but slight significance for the production of precipitation. *Giao* understands that the rain is produced chiefly by the cooling due to the expansion caused by the local pressure variation $\left(\frac{\partial p}{\partial t}\right)$. *Giao* however, neglects the acceleration altogether. It is, therefore, not to be wondered at, that he arrives at the result that the vertical velocity is insignificant. Giao's theory can, therefore, have but slight bearing on the actual problem. See *Giao.* Essai D'Hydrométéorologie Quantitative, Gerlands Beiträge zur Geophysik. Köppen-Band III 1931.

the front, which is caused by the component of the geostrophic wind normal to the front. Again, if the isallobars are straight and equidistant, there is no convergence in the cold air, but the flux of air due to the isallobaric gradient, acts in such a way as to reduce the wind component in the cold air normal to the front relative to the same component in the warm air. Choose the x-axis normal to the front and let u_1, be the x-component of velocity in the cold air in front of the warm front, and let u_2 be the x-component in the warm air. We then see, that according to the above considerations, the distribution of the isallobars in fig. 14 corresponds to a case when u_1 is smaller than u_2. From the kinematical surface condition (see **23** (5)), we get:

$$w_1 - w_2 = (u_1 - u_2) \tan \theta. \tag{1}$$

The case discussed above thus involves that the warm air (index 2) is ascending *relative* to the cold air, becauce $\tan \theta$ is positive. This naturally need not mean that w_2 is positive, because it might happen that w_1 was negative and in magnitude larger than w_2.

The question now is: can we determine the sign of w_1? If so, we then also know the sign of w_2. Looking again at fig. 14 we see that the isallobars are most crowded at some distance in front of the warm front. *This is invariably the case with warm fronts.* Even though the tendency generally is larger near the front that at some distance from it, we invariably have that the inclination of the tendency profile is smaller near the front than at some distance from it. The maximum of isallobaric gradient is, therefore, always to be found at some distance from the warm front. On the right hand side (fig. 14) of the area where the isallobars are most crowded, we have divergence of isallobaric gradients and, therefore, also: $\frac{\partial (\varrho w)}{\partial z} < 0$ (see **28** (8)). Where the isallobaric gradient is maximum, we have: $\frac{\partial (\varrho w)}{\partial z} = 0$. To the left of the area where the isallobars are most crowded we have convergence of isallobaric gradients, and therefore: $\frac{\partial (\varrho w)}{\partial z} > 0$. According to the considerations in paragraph 28, there is then *descending* motion in the more distant part of the cold air, and *ascending* motion in the part which is nearer the front. It is a common experience that low clouds disolve under the front of a warm front cloud system, whereas low clouds form in the cold air near the warm front. These observations seem to concur with the above deductions. We may then take it for granted that the cold air near the front is ascending, or that w_1 in the above equation (1) is positive. We have previously seen that $\tan \theta$ is positive and $(u_1 - u_2)$ is negative. Equation (1) can, therefore, only hold when w_2 is positive, and in magnitude larger than w_1. We shall presently see that synoptical investigations have shown that this is so.

The above discussion leads to the conception of the vertical structure in the vincinity of the warm front surface which is represented in fig. 21: The velocity normal to the front is larger in the warm air than in the cold. The ascending motion is more intense on the warm side than on the cold. It is important to note that the sign of w is the same on both sides of the front. The difference in vertical velocity at both sides of the front may, therefore, be slight.

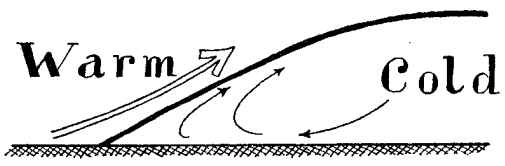

Fig. 21.

It is easily understood that this distribution of vertical velocity in general favours frontogenesis, because, if the temperature in the cold air decreases with distance from the front, the equiscalar surfaces of temperature will then be brought towards the front.

This case is frequent in winter when a warm front approaches the cold continent of Europe. In summer the revers conditions predominate, at least in the lower part of the atmosphere.

If the warm air ascends moist-adiabatically and the cold air dry-adiabatically, then would the distribution of vertical velocity described above, lead to frontogenesis which increases with hight. It is a common experience that warm fronts increase in intensity with hight[1]). It is, however, well to note that the southerly component of the air current in front of the warm front tends to bring warmer air northwards. This advective influence will then counteract the frontogenetical agents.

Let us next consider a cold front of type A as described in paragraph 25 (fig. 14). We choose the x-axis normal to the front and positive towards warm air. Tan θ is then negative, and u_1 denotes the x-component of the velocity of the warm air, and u_2 the same component of the cold air.

We consider first the flux of air, which according to **28** (5), is caused by the isallobaric gradient. In the warm air the isallobaric gradient is always directed towards the front. There is then a flux of warm air towards the front, and this flux subtracts from the geostrophic wind component. On the cold side the isallobaric gradient is directed away from the front in the vicinity of the center, but towards the front at the more distant part of the front. At the latter part there is then a flux of air towards the cold front both from the warm and from the cold side. Moreover, in the cold air the flux towards the cold front adds to the geostrophic wind, whereas in the warm air, it subtracts from it. Since the geostrophic wind normal to the front is approximately the same at both sides of the front, it follows, that u_2 must be larger than u_1.

Equation **23** (5) gives:

$$w_1 - w_2 = (u_1 - u_2) \tan \theta.$$

Since tan θ is negative, and u_2 is larger than u_1, it follows that *the warm air (index 1) must ascend relative to the cold air.*

In the vicinity of the center this rule need not hold, because the isallobaric gradient in the cold air may have opposite sign. For this part of the cold front no definite rule can be formed. It is even possible that the warm air may descend relative to the cold air.

The cold fronts of type B (paragraph 25) are characterized by very slight differences in tendencies. Moreover, since the isallobaric gradients are directed almost parallel to the front, there is but slight flux towards the front. These fronts are generally recognized for having no particular cloud system[2]). Their importance for weather forecasting is chiefly that they divide the areas of fog and drizzle from those of instable showery air.

We have here discussed the flux of air and the convergence by means of equations which have been derived from the the equations of motion without frictional force. The results are therefore subjected to such limitations as arise from this simplification. The investigations of B r u n t and D o u g l a s (loc. cit.), however, show that friction does not play an important rôle in the phenomena with which we are here concerned.

It is of considerable interest to determine the order of magnitude of the vertical velocity. It is a common practice to neglect vertical velocity in the vicinity of the ground. The common justification for neglecting vertical velocity is that it actually vanishes at the ground. It is then frequently assumed that the vertical velocity is negligible in the lower part of the atmosphere, say up to 100 or 200 meters. This simplification is frequently necessary for rendering the hydrodynamical equations agree-

[1]) See f. ex. B e r g e r o n, loc. cit.

[2]) See J. B j e r k n e s: Practical Examples, loc. cit. and Example **11** in chapter VII.

able for mathematical operations, but the supposition can hardly be said to have any foundation *in re*. It is easily seen, that if the vertical velocity is negligible up to 100 or 200 meters, a warm sector could not occlude. In the warm sector there is generally a flux of air towards the center. As there can be no piling-up of warm air at the top of the warm sector, it is necessary that the warm air must escape vertically. Moreover, if the cold front shall overtake the warm front, it is necessary that there is so much vertical velocity that the warm sector air can escape. It is reasonable to believe that the major part of this vertical velocity is concentrated at the fronts, where also the solenoids are concentrated. The vertical velocity is of course small, but it lasts a long time on the same air masses, and has, therefore, a large capacity for transforming the structure of the air masses. It is possible that the terms in the hydrodynamical equations which depend on the vertical velocity and vertical acceleration, are small compared with other terms, but, as the vertical velocity is necessary for the production of rain, the occlusion of cyclones etc., it is evident that the vertical velocity cannot be neglected when we deal with problems concerning weather forecasting.

It is frequently customary to neglect vertical velocity at the so-called earth fronts, because there can be no vertical velocity at the surface of the earth. The surface condition, which states that the velocity must be tangential to the surface of the earth, is only valid when there are no *singularities* in the field of motion. As the front is a formidable singularity, it is evident that the surface condition cannot be applied to the line of intersection between the front surface and the surface of the earth.

Even if it was allowed to assume the vertical velocity to be zero at an earth front, it is easy to show that the vertical velocity is likely to increase rapidly with height in the vicinity of the earth. According to **23** (6) we have:

$$(2) \qquad \begin{cases} w_1 = (u_1 - u_f) \tan \theta \\ w_2 = (u_2 - u_f) \tan \theta \end{cases}$$

where w is vertical velocity, u is the component of wind normal to the front, u_f is the velocity of the front along its normal, and $\tan \theta$ is the inclination of the front surface. Index 1 denotes, as previously, the air in front of the front, and index 2 the air in the rear.

Let s measure length along the line of intersection between the front surface and a vertical plane at right angle to the front. Differentiating the second of the above equations partially with respect to s, we get:

$$\frac{\partial w_2}{\partial s} = \frac{\partial u_2}{\partial s} \tan \theta - \frac{\partial u_f}{\partial s} \tan \theta + (u_2 - u_f) \frac{1}{\cos^2 \theta} \frac{\partial \theta}{\partial s}.$$

It is reasonable to suppose that the front velocity (u_f) is constant with height, and that the inclination of the front surface is constant. With these simplifications we get:

$$\frac{\partial w_2}{\partial s} = \frac{\partial u_2}{\partial s} \tan \theta,$$

or: the vertical velocity increases with height (along the front surface) in proportion to the increase with height in the x-component of the wind velocity. Suppose we have a warm front surface whose inclination is 1 in 100, and that the wind velocity increases from 3 m sec^{-1} at the ground to 5 m sec^{-1} at 5 meters above the ground. We then get: $\frac{\partial w_2}{\partial s} = 4.10^{-5}$ m sec^{-1} on an average near the ground. If w_2 is zero at the ground we get at 10 meters above the ground (i. e. $s = 1000$, because we measure along the front surface) $w_2 = 4$ cm sec^{-1}. This increase in vertical velocity is rapid near the ground

where the wind velocity increases rapidly with height. At larger height the increase is slow. In general the increase in wind velocity with height is more rapid than indicated above. The vertical velocity at the height of a well exposed anemometer may, therefore, easily exced 5 cm per second. This is also the value that Brunt and Douglas reckon with as a frequent value, admitting that larger values may occur frequently. We shall presently see that 5 cm sec.$^{-1}$ is the most common value at an ordinary station.

Returning to the first of equations (2), and discussing it in like manner, we see that $\frac{\partial w_1}{\partial z}$ must be positive at an earth front, and that $\frac{\partial w_1}{\partial z}$ and $\frac{\partial w_2}{\partial z}$ must be of the same order of magnitude, which agrees well with the results obtained previously.

Giao (loc. cit.) understands that the vertical velocity near the ground is negligible. According to **23** (5), we have:

$$w_1 - w_2 = (u_1 - u_2) \tan \theta.$$

Giao has examined the wind records at Utsira and found that $(u_1 - u_2)$ is approximately zero. Giao then concludes that both w_1 and w_2 must be equal to zero. This result of Giao's seems to be so largely at variance with the established ideas of the distribution of the velocity in the vicinity of fronts, that it was thought desireable to re-examine the question.

It is well to note that the meteorological station Utsira is situated at the top of a little island, the anemograph (Dines Pressure Tube with direction recorder) being 10.5 meters above the top of the hill, and 70 meters above sea level. It was, therefore, thought that the vertical velocity at the fronts would be of such an order of magnitude that a noticable difference between u_1 and u_2 might be recorded. In order to examine this question, a number of distinct front passages at Utsira were examined. During the years 1924 to 1932, 62 cases of sharp fronts were found when the orientation of the fronts could be determined with sufficient accuracy. The material thus examined includes the few cases examined by Giao. In order to avoid any ambiguity, the fronts examined were discussed by three synopticians of Værvarslingen på Vestlandet, the writer being one of them.

In table 6 is given the frequency of the quantity $\Delta u = u_2 - u_1$. Δu thus denotes the rate at which the warm air moves faster than the cold air at warm fronts (or occluded fronts whose rears are warm), or the rate at which the cold air moves faster than the warm air at cold fronts.

Table 6.

Δu (m sec.$^{-1}$)	Frequency
− 4 to 0	6
0 » 4	23
4 » 8	20
8 » 12	10
12 » 16	3
Sum	62

Out of 62 cases only 6 give negative values[1]) for Δu, whereas, 56 give positive values, which means that the warm air (both at warm and cold fronts), must ascend relative to the cold air.

[1]) The slight negative values may be due to slight errors in the orientation of the fronts.

If the inclinations of the front surfaces were known, we could calculate the relative vertical velocity of the two air masses by means of equation (3). We do not know the inclinations, but if we assume 1 in 100 to be a reasonable value, we would get that the frequency of the relative vertical velocities expressed in cm sec.$^{-1}$ would be equal to the frequency of Δu in table 6. A relative vertical velocity of about 5 cm per sec. would then be the most frequent value, but, as mentioned before, the absolute vertical velocity is likely to be larger, because both the cold and the warm air ascend.

During the working-up of the observations it was found that the sharpest fronts did not give the largest values of Δu. It was, therefore, thought that the value of Δu might depend on the wind velocity normal to the front. Table 7 gives the relation between the values of Δu and the values of wind velocity normal to the front and in the rear of it.

Table 7.

u_2 (m sec.$^{-1}$)	Δu m sec.$^{-1}$ (mean values)	Number of cases
0— 4	1.7	19
4— 8	3.5	21
8—12	6.7	15
12—16	7.3	3
16–20	13.6	2
20—24	6.3	1
24–28		
28–32	13.7	1

It is seen from the table that Δu is approximately proportional to the wind velocity in the rear of the front and normal to it. The values of Δu for high wind velocities are, of course, uncertain, owing to the small number of cases examined.

It appeared natural to test the above results by comparing the values of Δu with the intensity of the precipitation which occured during the front passages. Unfortunately, the pluviograph at Utsira had been out of order for long intervals of time. For this reason the records of the Bergen station had to be used. As, sometimes, some hours may elapse from the time the fronts passed Utsira until they passed Bergen, it was necessary to take the sum of precipitation during 6 hours. In this way we may, in some cases, risk to get incorrect amounts of precipitation, but there can be little doubt, that, on an average, the 6-hour sums of precipitation give some rational measure for the efficiency of the fronts in producing precipitation. The average amounts of rain in relation to the values of Δu are given in table 8.

Table 8.

Δu (m sec^{-1})	Precipitation during 6 hours
0— 4	4.6 mm
4— 8	6.8
8—12	7.6
12—16	8.6

It is seen that the rain intensity increases in proportion to Δu.

The above discussion shows that Δu is of the order 5 meters per second in anemometer level, and that the vertical velocity of the warm air relative to the cold air must be of the order of 5 cm sec.$^{-1}$. The absolute vertical velocity of the warm air may be larger than the relative velocity.

On page 65 we have shown that w increases rapidly with height in the vicinity of the ground. We found $\frac{\partial w}{\partial s} = 4.10^{-5}$ along the inclination of the front surface. With an inclination of 1 in 100 we would get 4.10^{-3} per unit vertical distance along the front surface. J. Bjerknes[1]) has frequently used the equation of continuity for discussing the conditions in the vicinity of the front. Bjerknes has shown that the equations of continuity for the air of the transitional layer may be written in the following form:

$$\frac{\partial w}{\partial z} = -\frac{\partial u}{\partial x}$$

In the 62 cases examined above, the average value of Δu is 4.5 m sec.$^{-1}$. The average duration of the front passages was 5 minutes. Say that the average velocity of the fronts was 48 km. per hour. The average thickness of the zone of transition would then be 4 km, which is a frequent value for sharp fronts. Assuming an inclination of 1 in 100, the average thickness of the transitional layer, would be 40 meters. The average increase in the x-component of wind velocity would then be $\frac{\partial u}{\partial x} = -\frac{\Delta u}{4}\ 10^{-3}$, (because Δu in the preceeding tables gives the difference between the rear and the front of the front). Substituting this value in the simplified equation of continuity, we get:

$$\frac{\partial w}{\partial z} = \frac{4.5}{4}\ 10^{-3}.$$

The increase from the bottom to the top of the layer of transition would then be approximately 4.5 cm sec.$^{-1}$, which agrees well with the values previously obtained. The absolute vertical velocity would then be this relative velocity plus the velocity of the cold air.

The statistical evidences given above clearly corroborate the theoretical deductions based on the equations **28** (5) and **28** (8). These equations may, therefore, be regarded as helpful means for estimating the intensity of the rain-producing processes at the fronts. It is, however, well to remember that only a *meticulous* analysis of the chart is capable of bringing out the details on which the prognosis should be based.

It would be natural to sub-divide the 62 cases treated above, in such under-groups as warm, cold and occluded fronts. The examination, however, showed that the number of cases was not large enough for such detailing, especially because the material comprised only 9 real warm fronts. It appeared, however, that Δu on an average was larger for warm fronts than for cold fronts. It was interesting to see that the extreme high values of Δu occured when the front surfaces became retarded against the store of cold winter air over Scandinavia.

We shall not here enter into further statistical discussion of the properties of fronts. A complete statistical discussion will be given in another paper which is hoped to be completed within a year or two. It will there be shown that the results obtained above for average values, also hold in individual cases. One such case is discussed in paragraph 41.

[1]) Practical Examples etc., and Exploration de quelques Perturbations Atmosphèrique etc., loc. cit.

CHAPTER VI.

DEEPENING AND FILLING.

30. Definition of Deepening and Filling. In the previous chapters we have given some formulae for the velocity, the acceleration and the displacement of such pressure systems as troughs, wedges, pressure centers and fronts. In this chapter we propose to develop equations for calculating the change in structure of the moving pressure systems.

The expressions *deepening* and *filling* are familiar to synopticians. A pressure center f. ex. is said to deepen when the pressure in the moving center decreases, and it fills-up when the pressure rises. Deepening and filling thus refer to the pressure in a moving system of co-ordinates which is fixed to the moving pressure system. For example, a ship furnished with barograph, and sailing in the center of a moving cyclone, would record the deepening or filling of the center. A number of ships evenly distributed round the center, and sailing with the velocity of the pressure center, would record the deepening or filling at the various points of the moving pressure system.

We shall now endeavour to develop equations which express the deepening or filling by means of the observations at a fixed station. According to the above considerations, we may define the instantaneous deepening or filling *intensity* as $\frac{\delta p}{\delta t}$, where p is pressure, and the differentiation refers to a system of co-ordinates which is fixed to the moving pressure system. The connection between the pressure variation in a moving system of co-ordinates and a fixed system is given by equation **3** (6), which writes:

$$\frac{\delta p}{\delta t} = \frac{\partial p}{\partial t} + \boldsymbol{C} \cdot \nabla p \tag{1}$$

This equation shows that the pressure variation at a fixed station is composed of two parts: (a) one which is caused by the movement of the pressure system, and (b) one which is caused by the deepening or filling, or in other words the *evolution* of the pressure system.

In the previous chapters we have shown how the velocity ($\boldsymbol{C}$) of the pressure system may be computed without the term $\frac{\delta p}{\delta t}$. Equation (1), therefore, permits of computing the deepening or filling of the pressure system.

The deepening or filling may vary from one point to another in the moving pressure system. By computing $\frac{\delta p}{\delta t}$ for a number of points and subsequent interpolation, the change in structure of the moving pressure formation may be calculated.

The deepening or filling may vary with time. The variation with time in the deepening or filling intensity is defined by $\frac{\delta^2 p}{\delta t^2}$, where the differentiation refers to the system of co-ordinates which follows the pressure formation (or part of it). The relation between $\frac{\delta^2 p}{\delta t^2}$ and the observations at a fixed station is given by equation **3** (7), viz:

$$\frac{\delta^2 p}{\delta t^2} = \frac{\partial^2 p}{\partial t^2} + 2\,\boldsymbol{C} \cdot \nabla \frac{\partial p}{\partial t} + \frac{\partial \boldsymbol{C}}{\partial t} \cdot \nabla p + \boldsymbol{C} \cdot \nabla (\boldsymbol{C} \cdot \nabla p) \tag{2}$$

The quantity $\frac{\delta p}{\delta t}$ may be called the deepening *celerity*, and the quantity $\frac{\delta^2 p}{\delta t^2}$ may

be called the deepening *acceleration* of the pressure system at the point considered. Both the celerity and the acceleration define instantaneous values.

Equation (1) is very easily applied, qualitatively and quantitatively, to any pressure formation. Equation (2) is seemingly more complicated. In the following paragraphs we shall specialize these equations for the various kinds of pressure systems.

At times, meteorologists have tried to calculate the future pressure distribution by developing the pressure function in a Mac-Laurin series. The results have, as a rule, been poor, owing to the irregular variations at a fixed station. The pressure variations in a system of co-ordinates which is fixed to the moving pressure formation, are, however, more regular and uniform, oscillating deepenings or fillings being rare exceptions. We shall, therefore, develop the pressure function in a moving system of co-ordinates, in order to study the deepening or filling of a moving pressure system. Let $\triangle p$ be the pressure variation at a point in the moving system during the time interval t. We then get:

$$\triangle p = \left(\frac{\delta p}{\delta t}\right)_0 t + \frac{1}{2}\left(\frac{\delta^2 p}{\delta t^2}\right)_0 t^2 + \ldots . \tag{3}$$

where index 0 denotes the initial values. With this in mind we may drop the indices as being superfluous. $\triangle p$ then defines the deepening or filling that takes place during the time interval t at the point considered.

Combining (1), (2) and (3), we get:

$$\triangle p = \left[\frac{\partial p}{\partial t} + \boldsymbol{C}\cdot\nabla p\right] t + \frac{1}{2}\left[\frac{\partial^2 p}{\partial t^2} + 2\,\boldsymbol{C}\cdot\nabla\frac{\partial p}{\partial t} + \frac{\partial \boldsymbol{C}}{\partial t}\cdot\nabla p + \boldsymbol{C}\cdot\nabla(\boldsymbol{C}\cdot\nabla p)\right] t^2 \tag{4}$$

where terms of third and higher order have been neglected.

The equations (1), (2) and (3) may be specialized and simplified, as will be shown in the succeeding paragraphs.

31. Deepening and Filling of Pressure Troughs. As in paragraph 10, we shall not distinguish between wedges and troughs when we treat general questions.

We choose the system of co-ordinates as shown in paragraph 11. The velocity of the point in question of the trough line is then given by **12** (7), viz:

$$C_L = -\frac{p_{101}}{p_{200}} \tag{1}$$

where p_{101} and p_{200} are given in paragraph 14. Since the velocity coincides with the x-axis, we may write:

$$\boldsymbol{C}_L\cdot\nabla p = C_L\frac{\partial p}{\partial x} = -\frac{p_{101}}{p_{200}}\frac{\partial p}{\partial x}$$

Substituting this in **30** (1), we get:

$$\frac{\delta p}{\delta t} = \frac{\partial p}{\partial t} + C_L\frac{\partial p}{\partial x} = \frac{\partial p}{\partial t} - \frac{p_{101}}{p_{200}}\frac{\partial p}{\partial x} \tag{2}$$

This equation may be applied at any point on the chosen x-axis. The coefficients p_{101} and p_{200} then refer to the trough line, whereas $\frac{\partial p}{\partial t}$ and $\frac{\partial p}{\partial x}$ refer to the point which

we consider. $\frac{\partial p}{\partial t}$ may be replaced by the observed barometric tendency, and $\frac{\partial p}{\partial x}$ may be replaced by the reciprocal value of the distance between unit isobars, or one fifth of the distance between two 5 to 5 isobars. The distance is reckoned positive from low to high pressure. When the displacement of the trough line has been computed, C_L is known, and the deepening intensity is then obtained without much reckoning.

It is important to note that $\frac{\partial p}{\partial x}$ is zero on the trough line itself. The deepening intensity is then simply equal to the barometric tendency. We then easily see, that when the zero tendency line is situated in front of the trough line, a wedge decreases (deepens) and a trough decreases (fills). When the zero tendency line is in the rear of the trough line, we have the reverse conditions. It is, therefore, easy to get a measure of the deepening or filling intensity without any calculations.

Since the time unit in the barometric tendency is three hours, equation (2) gives the deepening that takes place during three hours. The deepening for larger intervals of time may then be extrapolated by multiplying the tendency by the number of three-hour intervals.

More accurate results are obtained by applying equation **30** (2). This equation may be transformed as shown in paragraph 3. According to **3** (9) we have:

$$(3) \qquad \frac{\delta^2 p}{\delta t^2} = \frac{\partial^2 p}{\partial t^2} + 2 C_L \frac{\partial^2 p}{\partial x \partial t} + C^2{}_L \frac{\partial^2 p}{\partial x^2} + A_L \frac{\partial p}{\partial x}$$

where C_L and A_L are given by **12** (7) and **13** (12). All quantities in the above equations are evaluated in the same way as shown in paragraph 14. When the displacement of the trough line has been computed, C_L and A_L are known, and $\frac{\delta^2 p}{\delta t^2}$ is easily computed without much reckoning.

Returning now to equation **30** (4) and substituting by means of (2) and (3) we get for the total deepening or filling during the time interval t, t being the number of three-hour intervals:

$$(4) \qquad \triangle p = \left(\frac{\partial p}{\partial t} + C_L \frac{\partial p}{\partial x}\right) t + \frac{1}{2}\left(\frac{\partial^2 p}{\partial t^2} + 2 C_L \frac{\partial^2 p}{\partial x \partial t} + C^2{}_L \frac{\partial^2 p}{\partial x^2} + A_L \frac{\partial p}{\partial x}\right) t^2 + \cdots$$

This equation may be applied to any point on the chosen x-axis. Experience has shown, that in general, sufficient accuracy is obtained even if the term of second order is neglected. For points on the trough line, the second term is, however, obtained without any calculations except what is necessary for computing the velocity and the acceleration of the movement.

According to the definition of the trough line we have: $\frac{\partial p}{\partial x} = 0$. According to **12** (7) we have:

$$C_L = -\frac{p_{101}}{p_{200}}$$

For any point on the trough line we thus have:

$$\frac{\partial^2 p}{\partial t^2} = p_{002}, \quad \frac{\partial^2 p}{\partial x \partial t} = p_{101} \text{ and } \frac{\partial^2 p}{\partial x^2} = p_{200}$$

The last two of these quantities are contained in the formula for velocity, and the first one, is the auxiliary quantity $\triangle T$, (the difference between two consecutive tendency values), which is used for computing the acceleration (see paragraph 14). Putting

$\frac{\partial p}{\partial t} = T =$ the barometric tendency, and substituting the above values in (4), we get:

$$\triangle p = Tt + \frac{1}{2} \triangle T t^2 - \frac{1}{2} \frac{p_{101}^2}{p_{200}} t^2 \tag{5}$$

In chapter VII we shall give some examples which show the accuracy rendered by the above formulae.

32. Deepening and Filling of Pressure Centers. Expressions for deepening or filling of pressure centers are readily obtained from the general equations **30** (1), (2) and (4). By suitable choice of the points for which we want to calculate the deepening, the equations become much simplified. In chapter IV we have shown how the center may be defined by means of two lines along which there is either maximum or minimum of curvature of the pressure profiles. It was also shown that these lines in all respects correspond to the definition of trough lines. The movement of the pressure center could then be defined as the movement of the point of intersection between these two lines. Moreover, the said lines at the initial instant $t = 0$, were chosen as co-ordinate axes, and the quantities which enter in the formulae for velocity and acceleration of the center had to be evaluated at these lines. It is, therefore, natural to compute the deepening or filling at points which at the initial instant $t = 0$, are situated on the co-ordinate axes.

In general it suffices to compute the deepening or filling of five points, namely: the pressure center itself, and one point on each of the four semi-axes. The general equations may be applied to any point, but it saves labour to choose the points according to the above principles.

Let us first consider the pressure center. By definition we have $\bigtriangledown p = 0$. From equation **30** (1), we get:

$$\frac{\delta p}{\delta t} = \frac{\partial p}{\partial t} = T \tag{1}$$

The deepening or filling intensity at the center is simply equal to the barometric tendency. It is, therefore, important to note the position of the zero-isallobar relative to the center.

The deepening or filling that takes place in the center during the time interval t ($t =$ number of three-hour intervals), is obtained from the general equation **30** (4). Developing this equation and remembering that $\bigtriangledown p = 0$, we get:

$$\triangle p = \frac{\partial p}{\partial t} t + \frac{1}{2}\left(\frac{\partial^2 p}{\partial t^2} + 2\, C_x \frac{\partial^2 p}{\partial x \partial t} + 2 C_y \frac{\partial^2 p}{\partial y \partial t} + C_x^2 \frac{\partial^2 p}{\partial x^2} + C_y^2 \frac{\partial^2 p}{\partial y^2}\right) t^2$$

$$+ C_x\, C_y \frac{\partial^2 p}{\partial x \partial y} t^2$$

Owing to the particular choice of co-ordinate system, the last term vanishes.

Introducing the symbols defined in paragraph 18, and substituting for C_x and C_y by means of **16** (1), we get:

$$\triangle p = T^{00} t + \frac{1}{2}\left(\triangle T^{00} - \frac{p_{101}^2}{p_{200}} - \frac{p_{011}^2}{p_{020}}\right) t^2 \tag{2}$$

which gives the total deepening or filling that takes place during the time interval t. The quantities which enter in this equation are contained in the formulae for velocity

acceleration. The deepening or filling of the pressure center can, therefore, be computed without any additional labour.

Having completed the calculation of the deepening or filling of the pressure center itself, we proceed to calculate the deepening or filling at one point on each of the semi-axes of co-ordinates. Having done this, and having calculated the future position of the pressure center, we may easily draw the new isobars.

We have repeatedly stated that the co-ordinate axes have the properties of trough lines. We may, therefore, simply apply equation **31** (5) to any point of the co-ordinate axes. It is convenient to calculate the deepening or filling at the four points whose co-ordinates are (see paragraph 18 (1.0) (—1.0) (0.1) and (0.—1). For each of these points we may write an equation similar to **31** (5). This equation has been discussed previously, and no further comments are necessary.

33. Deepening and Filling of the entire Pressure System. In the previous paragraph we have seen how the deepening or filling may be computed at a number of points in the vicinity of a pressure center. It is frequently both useful and labour-saving to compute the integral of the deepening over certain areas of the chart. Looking at aquation **30** (1) we see that the deepening intensity depends largely on the velocity of the pressure center. For the deepening or filling at each particular point the convective term plays an important rôle. When we, however, consider the sum-total of deepening over certain areas of the chart, the convective term will disappear, so that we may evaluate the deepening or filling even without knowing the velocity of the center.

Let $d\sigma$ denote a surface element of the chart. The integral of deepening or filling per unit time over a surface σ is then given by:

$$\int \frac{\delta p}{\delta t} d\sigma = \int \frac{\partial p}{\partial t} d\sigma + \int \boldsymbol{C}_c \cdot \nabla p d\sigma \tag{1}$$

Choose a right hand system of unit vectors $\boldsymbol{r}$, $\boldsymbol{s}$ and $\boldsymbol{z}$, where $\boldsymbol{r}$ coincides with ∇p. We may then write $\nabla p = \frac{dp}{dh}\boldsymbol{r}$. Choosing $dp = 1$, dh becomes the distance between unit isobars. We may now write: $d\sigma = dhds$ where ds is a line element of the isobar. Substituting in (1), and remembering that $\boldsymbol{C}_c$ is a vector in common for all elements, we get for the last integral:

$$\int \boldsymbol{C}_c \cdot \nabla p \, d\sigma = \boldsymbol{C}_c \cdot \int \boldsymbol{r} \, ds \tag{2}$$

Integrating over the area bounded by two closed isobars, we get:

$$\int \boldsymbol{C}_c \cdot \nabla p \, d\sigma = 0,$$

because the last integral in (2) is the line integral of a closed curve. Substituting in (1) we get:

$$\int \frac{\delta p}{\delta t} d\sigma = \int \frac{\partial p}{\partial t} d\sigma \tag{3}$$

The deepening or filling over the area between two closed isobars is, therefore, equal to the planimetric value of the barometric tendency in the same area.

Adding up for all zones between consecutive isobars, we get the result that: *the deepening or filling inside a closed isobar is equal to the planimetric value of the barometric tendency.* The deepening or filling of pressure systems may thus be calculated without computing the velocity.

According to **30** (1) we have in any moving system of co-ordinates:

$$\frac{\delta p}{\delta t} = \frac{\partial p}{\partial t} + \boldsymbol{C} \cdot \nabla p.$$

In a system of co-ordinates that is fixed to the moving isobar, we have:

$$\frac{\partial p}{\partial t} = - \boldsymbol{C}_i \cdot \nabla p$$

where $\boldsymbol{C}_i$ is the velocity of the isobar.

Integrating this equation over an area between two closed isobars, we get:

$$\int \frac{\partial p}{\partial t} d\sigma = - \int \boldsymbol{C}_i \cdot \nabla p d\sigma \tag{4}$$

Substituting as above, we get:

$$- \int \boldsymbol{C}_i \cdot \boldsymbol{r} \, ds = - \frac{dA}{dt}$$

where, A is the area enclosed by the isobar. Summing up for all closed isobars in the pressure system, we get:

$$\int \frac{\partial p}{\partial t} d\sigma = - \sum \frac{dA}{dt} \tag{5}$$

where $\sum$ may be extended over the whole pressure system. Combining (5) and (3), we get:

$$\int \frac{\delta p}{\delta t} d\sigma = - \sum \frac{dA}{dt} \tag{6}$$

By means of this formula the deepening or filling may be estimated without tendency observations. The formulae (5) and (6) are, of course, less useful than (3). Over the ocean, however, where tendency values are not obtainable, the deepening intensity may be estimated by comparing two pressure charts.

34. Deepening and Filling at Fronts, in Warm Sectors etc. An expression for the deepening or filling intensity in the vicinity of fronts is obtained from the general equation **30** (1), which may be written in the following form:

$$\frac{\delta p}{\delta t} = \frac{\partial p}{\partial t} + C_f \frac{\partial p}{\partial x} \tag{1}$$

where C_f is the velocity of the front as given by equation **23** (2).

At the very front both $\frac{\partial p}{\partial t}$ and $\frac{\partial p}{\partial x}$ are discontinuous (see paragraph 23). Formula (1) can, therefore, only be applied in the vicinity of the fronts. Even though both $\frac{\partial p}{\partial t}$ and $\frac{\partial p}{\partial x}$ are discontinuous at the front, $\frac{\delta p}{\delta t}$ must be continuous, because otherwise, the dynamical surface condition would not hold. Since the deepening intensity is continuous, it must be equal at both sides of the front. If we, therefore, know the deepening at one side of the front, we also know it at the other side.

It is important to note that the velocity of the front (C_f) has been defined along an arbitrary line L which was chosen as x-axis. In the case of a warm sector cyclone, it is

convenient to choose the x-axis along the warm sector isobars. We then get for any point in the warm sector: $\frac{\partial p}{\partial x} = 0$, which substituted in (1), gives:

$$\frac{\delta p}{\delta t} = \frac{\partial p}{\partial t}.$$

The tendency in the warm sector, therefore, gives the deepening intensity. Since the deepening intensity must be equal at both sides of the front, we see that the warm sector tendency near the front expresses the deepening that takes place also at the cold side of the front. By simple inspection of the distribution of the warm sector tendencies, important results are obtained with regard to deepening and filling.

Outside the warm sector the convective term in (1) becomes important. Substituting for C_f by means of **23** (2), we get:

$$\frac{\delta p}{\delta t} = \frac{\partial p}{\partial t} - \frac{\frac{\partial p_1}{\partial t} - \frac{\partial p_2}{\partial t}}{\frac{\partial p_1}{\partial x} - \frac{\partial p_2}{\partial x}} \frac{\partial p}{\partial x} \tag{2}$$

It is important to note that p_1 and p_2 denote pressure at two points on the x-axis which are near one another and on each side of the front. p (without index) refers to the point whose deepening we want to calculate. Equation (2) may be applied to any point on the chosen x-axis. Index 1 denotes the air in front of the front, and index 2 the air in the rear. As we have chosen the x-axis along the warm seetor isobars, we have for warm fronts: $\frac{\partial p_2}{\partial x} = 0$ and for cold fronts: $\frac{\partial p_1}{\partial x} = 0$.

The variation with time in the deepening intensity is given by the general equation **30** (2). This equation is difficult to apply to fronts, because it is difficult to compute the acceleration of the front, (see terminus of paragraph 25). In the warm sector, however, the formula is simple. Since the velocity of the front is directed along the x-axis, we may write **30** (2) in the following form:[1])

$$\frac{\delta^2 p}{\delta t^2} = \frac{\partial^2 p}{\partial t^2} + 2\, C_f \frac{\partial^2 p}{\partial x \partial t} + C^2_f \frac{\partial^2 p}{\partial x^2} + A_f \frac{\partial p}{\partial x}$$

In the warm sector $\frac{\partial p}{\partial x} = 0$. Since the isobars in the warm sector are almost straight lines, we may write: $\frac{\partial^2 p}{\partial x^2} = 0$. We then get:

$$\frac{\delta^2 p}{\delta t^2} = \frac{\partial^2 p}{\partial t^2} + 2\, C_f I_x$$

where I_x is the component of isallobaric ascendant along the x-axis (the isobar). In general the isallobaric ascendant in the warm sector is slight and the isallobars run almost parallel to the isobars. For both reasons I_x is small. Furthermore, the pressure tendency in the warm sector is uniform, so that $\frac{\partial^2 p}{\partial t^2}$ is small. *We may, therefore, reckon with an almost unaccelerated deepening in the warm sector.* For reasons explained above, $\frac{\delta^2 p}{\delta t^2}$ must be equal at both sides of the front. We may, therefore, conclude that the deepening acceleration is slight in the cold air in the vicinity of the front. It is a common experience

[1]) Compare **3** (7) and **3** (9).

that the warm sector cyclones deepen with an almost constant intensity until they occlude. After occlusion, they may deepen with variable intensity. In chapter VII we shall see some examples which show the regularity of the deepening intensity of warm sectors.

Returning to the general equation **30** (1) for the deepening intensity

$$\frac{\delta p}{\delta t} = \frac{\partial p}{\partial t} + \boldsymbol{C} \cdot \nabla p, \tag{3}$$

we may give some qualitative rules for estimating the deepning or filling of warm sector cyclones. $\boldsymbol{C}$ in the above equation denotes the velocity of the system of co-ordinates in which $\frac{\delta p}{\delta t}$ is recorded. We may then take $\boldsymbol{C}$ as the velocity of the center of the cyclone. Warm sector cyclones invariably move in the direction of the warm sector current. We then have $\boldsymbol{C} \cdot \nabla p = 0$, and the deepening intensity at the center is equal to the tendency at the top of the warm sector. This rule holds with such accuracy that it may safely be applied.[1])

Let us next see how the convective term influences on the deepening intensity.

We consider first a round and symmetrical cyclone (fig. 22 a) whose velocity is $\boldsymbol{C}$. In the direction of $\boldsymbol{C}$ the convective term $(\boldsymbol{C} \cdot \nabla p)$ has maximum, and it is positive in front of the cyclone and negative in the rear. The convective term thus counteracts the negative tendency in front of the cyclone, and the positive tendency in its rear. At right angle to $\boldsymbol{C}$, the convective term is zero, and the deepening along this line depends entirely on the tendency. In a round cyclone the convective term will more strongly counteract the tendencies than in other cyclones.

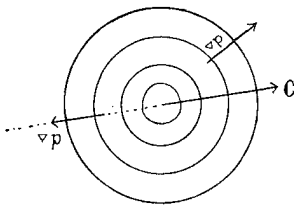

Fig. 22 a

Let us next consider a new warm sector cyclone as given in fig. 22 b. The convective term is positive in front and negative in the rear of the cyclone. But since ∇p is small and deflected from $\boldsymbol{C}$, we see that the convective term is of slight significance. The tendencies, therefore, carry larger weight for the deepening of this cyclone than in the previous case of a round one. Moreover, since the rear and the front are symmetrical with respect to pressure distribution (∇p), it follows that the convective term plays the same part in the front and in the rear. The convective term, therefore, does not help to deform the cyclone. This is exactly the type A, which we have described in paragraph 25. Such cyclones are generally long lived. They travel along the principal front more or less as stable waves (see paragraph 25).

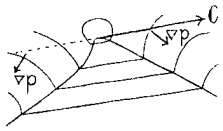

Fig. 22 b

Let us next consider the cyclone represented in fig. 22 c. The convective term in front of the cyclone is small and positive, whereas, in the rear, it is large and negative. This type of cyclones invariably deepen quickly, chiefly in the rear. The warm sector occludes quickly and the fronts become rolled up.

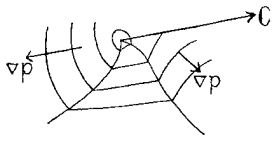

Fig 22 c

It sometimes happens that a warm sector occludes partially, and develops a secondary low at the top of the remainder of the warm sector. The classical example of this type is the so-called Skagerakk-cyclone described by J. Bjerknes and H. Solberg.[2]) The development of such a secondary, naturally,

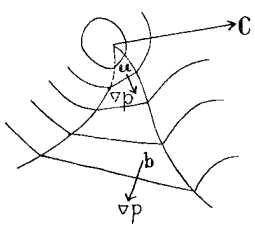

Fig. 22 d

[1]) See examples in chapter VII.

[2]) Life Cycle of Cyclones. Geofysiske Publikasjoner Vol. III, No. 1.

is a tricky thing to forecast, and the writer has spent some time in exploring the structure of such cyclones before they develop the secondary low. It was found that these cyclones invariably had warm sector isobars which diverge from the cold to the warm front. Let us, therefore, examine the influence of the convective term on such a warm sector. Consider the convective term at two points a and b in fig. 22 d. At a, the convective term is positive and, therefore, counteracts the negative tendency in the warm sector. At b, the same term is negative, and thus adds to the negative tendency. The distribution of the convective influence thus favours deepening in the southern part of the warm sector. Whether a secondary develops or not, depends on the distribution of tendency, but it has never been recorded that a secondary has developed without diverging warm sector isobars. In each particular case the deepening is easily calculated numerically.

The reader will probably think that the amount of work involved in the calculations of the displacement and the deepening or filling of pressure systems is so large that it cannot be overcome in the daily weather service. This conception may be right if the forecaster concerns himself with every detail which the pressure distribution exhibits. It is, however, well to remember that in each particular case, the forecast depends chiefly on the movement and the development of one single pressure system. Again, the movement of the pressure system is generally much more important than the development, and the displacement is easily calculated in 30 minutes. The deepening in the center of the system is obtained without additional labour.

It should also be remembered that it depends on the particular weather situation which method is best adapted for the numerical operations. In some cases it pays to calculate the displacement of the isobars, in other cases it pays to calculate the movement of the center, and so on. It is not easy to give general rules for when each method is most advantageously applied. Experience only can tell. Even without any computation, a mere qualitative discussion of the chart, based on the principles developed in these chapters, will render valuable results.

CHAPTER VII.

PRACTICAL EXAMPLES.

35. Introduction. In this chapter we propose to give some examples of the application of the preceeding formulae to the weather charts, the aim being to give an idea of the average accuracy which can be obtained by numerical methods.

In order to be able to publish a fairly large number of cases, the writer has had to publish the results in a somewhat condensed form. For this reason, the charts showing the physical analysis on which the calculations are based, had to be left out. Readers, who would like to study each particular case, are recommended to compare the examples given below with the daily weather maps issued by Værvarslingen på Vestlandet. The reader will then see that the cases treated below are not 'simple' cases. In fact, many of the cases treated below have been chosen because of their complicated structures.

It was thought to be of particular interest to examine some cases where the forecasts (which were based on usual estimations) were erroneous, in order to see if numerical methods would have given better results. Some such cases will be mentioned below, and it will be clearly seen that numerical methods would have given correct forecasts.

A word or two may be said about some technical difficulties in calculating the

movement and the development of the pressure systems. The velocity of any pressure system depends on quantities of the following forms:

$$\frac{\partial^2 p}{\partial x \partial t} \text{ and } \frac{\partial^2 p}{\partial x^2}$$

The last quantity, which is the denominator in the expression for velocity, is obtained with great accuracy from the pressure chart. The first quantity, which is the numerator in the said expression, is inaccurate for two reasons: (a) because $\frac{\partial p}{\partial t}$ must be replaced by the mean pressure variation during 3 hours, and (b) because $\frac{\partial^2 p}{\partial x \partial t}$ must be replaced by the difference between the tendencies in front and in the rear of the pressure system. The three-hour tendency which is observed in the rear of a pressure system, is in general more erroneous than is the one in front of the system. The tendency in the rear of a cyclone, for instance, is in general too small, because the three hour variation depends on the pressure variation during the passage of the cyclone. For this reason $\frac{\partial^2 p}{\partial x \partial t}$ is generally too small, and, therefore, the instantaneous velocity thus computed, is somewhat smaller than the true velocity.

On the other hand, the inadequacy of the rear tendency of a cyclone causes a computed acceleration which is slightly larger than the true acceleration. The two errors thus compensate one another, but, as the acceleration is multiplied by the square of time, the error in the acceleration, therefore, causes too large displacement for large values of time. This feature is predominating practically in every case treated below.

It will be seen from the succeeding examples that the accuracy obtained for the displacement during 24 hours is altogether satisfactory. The discrepancies which occur, are chiefly caused by the inaccuracy in the pressure tendencies.

Another difficulty is that the quantity $\frac{\partial^3 p}{\partial x \partial t^2}$, which enters in the expression for acceleration, has to be determined by means of 6-hour differences. Even slight errors in the acceleration may cause considerable discrepancies when the forecasting period is large. The succeeding examples show that fair accuracy is obtained for 24 hours ahead, even with the rough methods for determining $\frac{\partial^2 p}{\partial x \partial t}$ and $\frac{\partial^3 p}{\partial x \partial t^2}$. It is, therefore, reasonable to believe that better accuracy could be obtained even for longer periods, if the tendencies were more accurately observed, and if the time interval between the weather charts was smaller[1]).

36. Examples of Troughs, Wedges and Fronts. *Example 1.* Fig. 23 shows the symmetry line of a well developed wedge, which on Nov. 30th 1927 at 14 M E T extended from a central High over the British Isles towards The Barents Sea. Simultaneously a front with a well developed pressure trough extended from a depression near Novaya Sembla towards east Germany. Both the front and the wedge moved towards SE. The movement was calculated for 24 hours ahead. The broken lines show the computed positions. It is seen from the chart that the discrepancy between the calculated and the observed displacement is nowhere larger than 100 km. The front moved with a velocity averaging 30 km per hour. The error of 100 km after 24 hours thus means that the front arrived at the calculated place 3 hours too early. An error of 3 hours in 24 is generally considered to be slight.

[1]) The writer is preparing a memorandum on the technical arrangements which a quantitative forecasting service would necessitate.

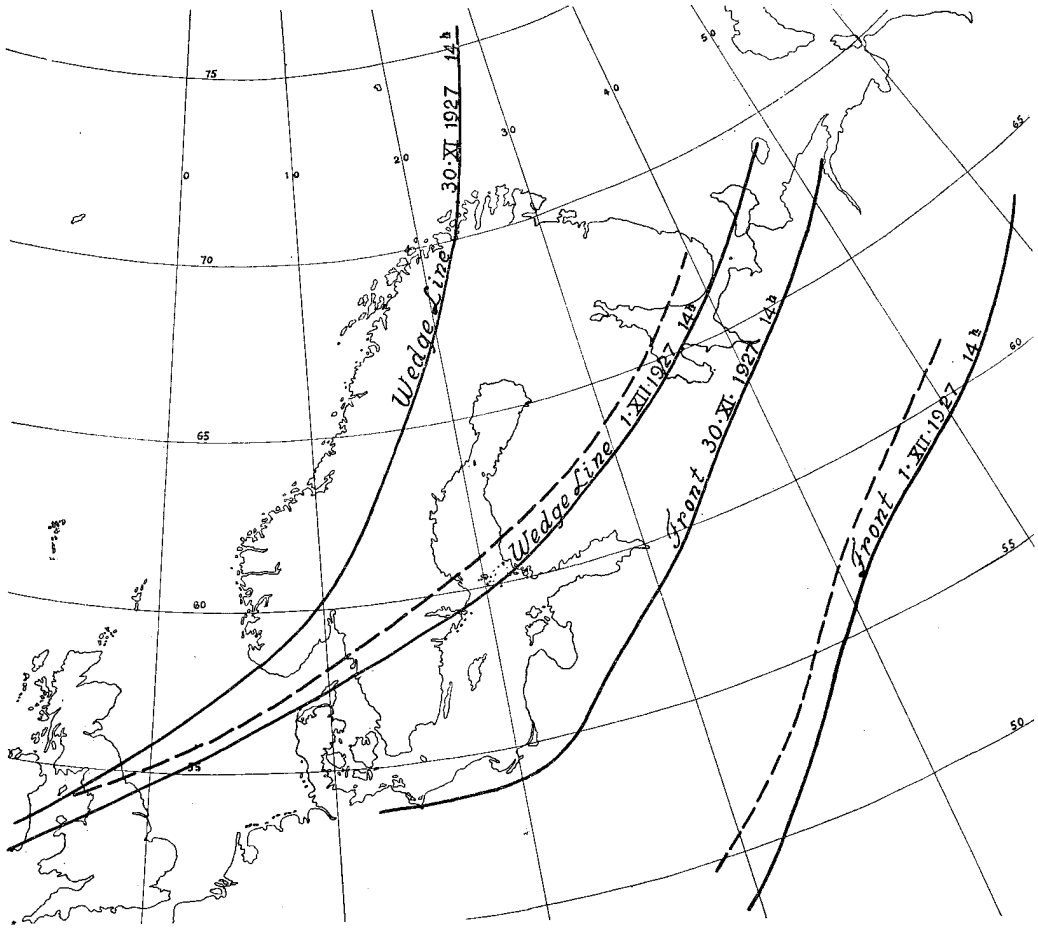

Fig. 23. Full lines observed positions. Broken lines computed positions.

The wedge line remained stationary over the British Isles and moved with large velocity in the northern part. The agreement between the observed and the calculated positions is altogether satisfactory. There can be little doubt that such accuracy could not be obtained by guessing the movements.

Example 2. Fig. 24 shows the symmetry line of a well developed wedge, which on Nov. 11th 1932 at 14 M E T extended from a central High over South Norway to half way between Bear Island and Jan Mayen. The position of the wedge line was calculated for 5, 18 and 24 hours ahead. The chart shows that there is perfect agreement between the computed and the observed positions, except over North Finland, where the wedge arrived 3 hours too early on the following morning. The calculations show that

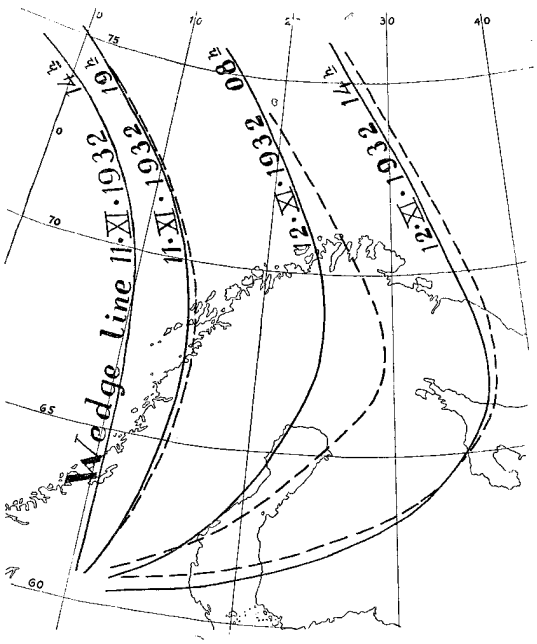

Fig. 24. Full lines observed positions. Broken lines computed positions.

the central High over South Norway would remain stationary. The rapid movement eastwards in the northern part was due to an approaching depression over Iceland. The movement of this cyclone could not be calculated because of lacking informations. It was, however, concluded that the accelerated movement of the wedge would be correlated to the movement of the said cyclone. The development took place as expected, and the next day there was a gale in North Norway, while South Norway still was under the influence of the Central High. This case is particularly interesting because the calculations were carried out before the forecasts were issued.

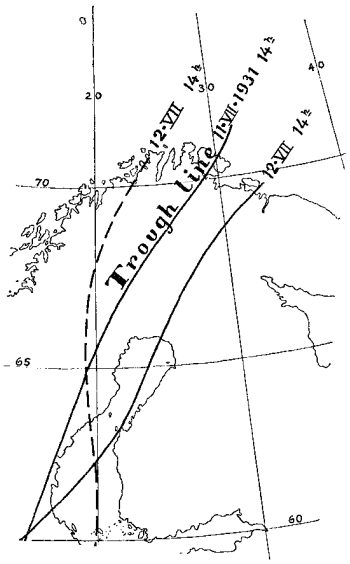

Fig. 25. Full lines observed positions. Broken line computed positions.

Example 3. Fig. 25 shows a trough line which on July 11th 1931 ran from East Finmarken to South Sweden. The trough line first moved slowly eastwards and than returned. The calculations gave the same result, except that the trough in the northern part returned slower than calculated. It is difficult to say whether this calculation would have improved a forecast based on guessing. On the whole the trough remaind stationary, and the writer does not think that a forecast based on these calculations, would be substantially wrong. The example is included here to show what inaccuracy one may experience in difficult cases.

Example 4. Fig. 26 shows a front which on the 12th of March 1932 at 8 M E T had passed the west coast of Norway. The same morning there was no pressure gradient over the Baltic. The wind was everywhere slight. The velocity of the front was calculated for two points indicated by arrows on the chart. The displacement was computed to 19 M E T (the broken line). The agreement was perfect.

In order to see what winds were likely to occur over the Baltic area, the velocity of the isobars were calculated. (Accelerations were not obtainable). The computed isobars at 19 h are given on the map, and the winds observed at 19 h are plotted. The calculations show that the wind would increase from 2 or 3 B to 7 B, which also occured. The computed pressure distribution differed from the observed one by 3 to 5 mb., but the distribution of gradient and wind was fairly accurate.

Example 5. On January 12th 1932 a strong depression approached The British Isles. The front and the center was off the coast so that no calculations could be made until 19 h. At this hour part of the depression covered Scotland and Ireland. The displacement of the isobars were calculated for the area over West Scotland, where the pressure distribution was such that the calculations were easy.

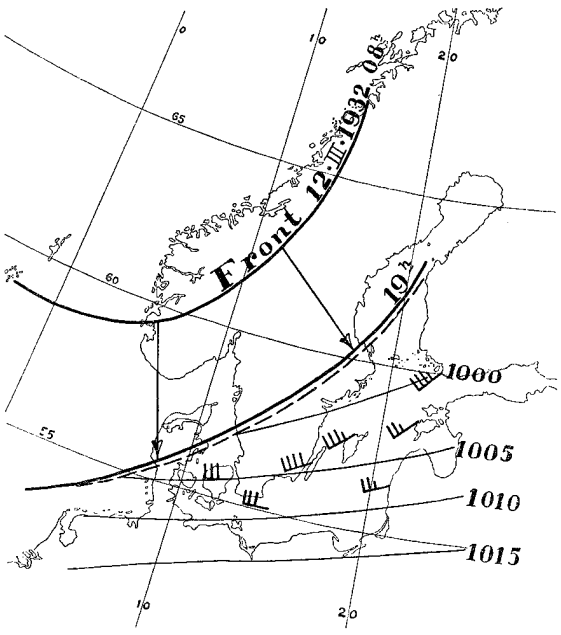

Fig. 26.

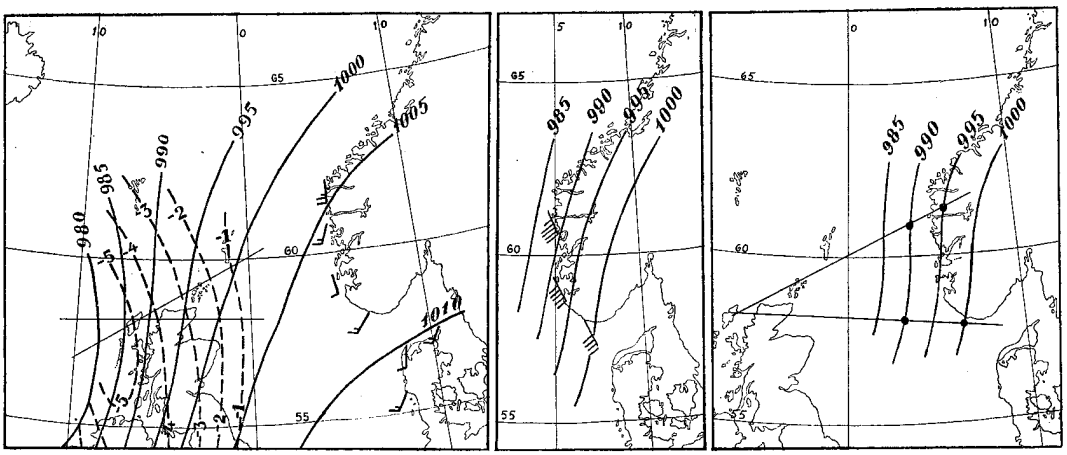

Fig. 27.

The first map in fig. 27 gives the pressure distribution and wind observations over West Norway on the 12th at 19h. The second map gives the observed pressure distribution and the observed winds 18 hours later, and the third map gives the pressure distribution calculated 18 hours ahead. It is seen that the pressure gradient agrees well with the calculations, and that a wind forecast, based on the calculations of the furture pressure distribution, would have given the observed wind velocities. The actual forecast for the 13th was: SSE 9 to 10 Beaufort. The forecast was founded on calculations.

37. Examples of Pressure Centers. The following examples of pressure centers show 9 cases where the movements of the centers have been calculated. The full lines represent the observed paths, the broken lines give the paths calculated according to formula **18** (2), and the dotted lines show the paths computed by means of A n g e r v o's formulae **19** (2). Each center has been calculated for 24 hours in advance. For the centers indicated by numbers 1 to 8, the calculations proceed from 14 to 14 o'clock. The first point, where all three paths unite, is the position of the center at the beginning of the calculation. The second point on each path denote the position of the center (observed or calculated) the same day at 19 h. The third point gives the position the next day at 8 h, and the last point gives the position at 14 h the second day.

Each center is indicated by a number. We shall return to the same centers in paragraph 38, where the dates will be given in the tables 11 and 12.

Example 6. Fig 28 shows the eight centers mentioned above. It is seen from the maps that the agreement between the computed and the observed paths on the whole is good. No. 1 exhibits a considerable discrepancy which was caused by the approach of a secondary perturbation. In view of the fact that it is not always easy to locate the position of a pressure center with larger accuracy than 50 to 100 km, the discrepancies in the above examples are insignificant.

The examples show that the writer's formula for the path of the center renders larger accuracy than does A n g e r v o's formula. Experience has, however, shown, that A n g e r v o's formula gives larger accuracy for 24 to 48 hours.

It is seen from the above examples that the accuracy obtained is as large for quickly running centers as for slowly moving ones.

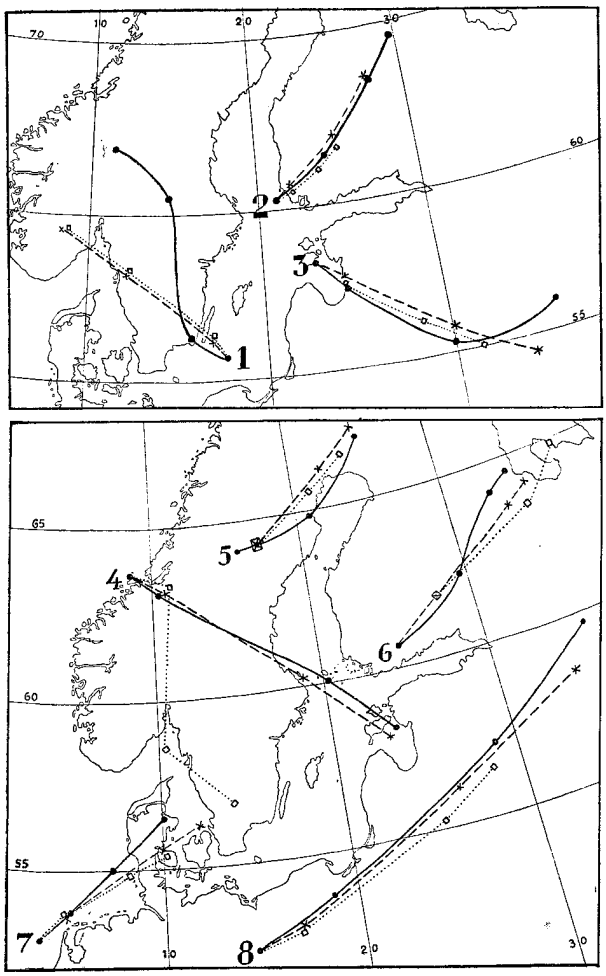

Fig. 28. Full lines observed paths. Broken lines paths computed from the writer's formulae. Dotted lines paths computed by means of Angervo's formulae. All paths are calculated 24 hours ahead, and the positions corresponding to the intermediate weather charts are indicated.

Example 7. An interesting depression occured over the Irish Sea, on the 22nd of October 1932 at 8 M E T (see fig. 29). There was no time forthe forecaster to compute the path of the center. The forecast for the next day was based on the assumption that the center would move quickly and keep off the west coast of Norway. Southerly gales were forecasted. Even at 19h, the forecaster believed that the center would move close off the west coast. The next morning the forecaster was rather surprised to see that the center had crossed the coast of the southern part of Norway.

The path of the center was calculated afterwards in order to see whether the forecast might have been improved upon by numerical labour. It was then found that the path of the center could be computed with an error which nowhere exceeded 100 km. The average velocity of the center was 70 km per hour. An inaccnuracy of 100 km would then mean that the center arrived at (say) the SW coast of Norway 1 hour and 20 minutes, as it was, too early. This inaccuracy is of course of no consequence for practical purposes. Again, the A n g e r v o path is less accurate than the one calculated from the writer's formula. But, if the path had been calculated for 48 hours or more, A n g e r v o's formula would have given more accurate results for the second half of the path.

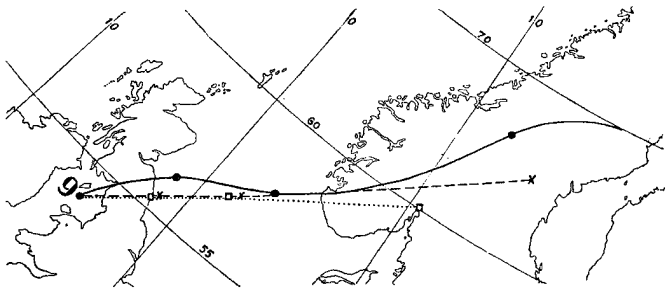

Fig. 29. Symbols as in fig. 28.

In the introduction to this chapter we have pointed out that the computed velocity is slightly too small, and the computed acceleration is slightly too large. In the majority of cases, the two errors seem to neutralize one another after a time interval of 18 to 24 hours. After 24 hours it is generally found that the error in the acceleration predominates. If the tendencies were observed with larger accuracy, the formula would probably hold for much larger intervals of time.

The depression mentioned above, deepened quickly. In the next paragraph we shall see that the calculations also give accurate values for the increase in intensity.

38. Examples of Deepening and Filling. In chapter VI we have given the general principles for calculating the deepening and filling of pressure systems. We shall here show some cases where the various formulae developed in chapter VI, have been applied to pressure centers.

In paragraph 34 we have shown that the deepening intensity of a warm sector cyclone is simply equal to the pressure tendency at the top of the warm sector, the deepening acceleration being negligible. This rule has been subjected to a thourough test by examining a large number of warm sector cyclones. During the winter 1931—32, 25 warm sector cyclones were examined and the deepening calculated for as long intervals of time as the centers could be identified. The results of these computations, compared with the actual development of the cyclones, are given in the following tables. 7 out of the 25 cases occured on evening charts, and 7 others occured on noon charts. Therefore, only 18 could be checked after 6 and 12 hours respectively.

Table 9. Frequency of Errors in the calculated Deepening for Warm Sector Cyclones.

Error (mb)	After 6 hours	After 12 hours	After 18 hours	After 24 hours
0	7	2	2	1
1	7	5	3	1
2	1	6	2	2
3	3	3	—	2
4	—	2	1	—
5	—	—	1	—
6	—	—	1	1
7	—	—	—	1
8	—	—	1	—
11	—	—	1	—
15	—	—	—	1
Number of cases . .	18	18	12	9

Table 10. Actual Deepening and Error in the Calculations.

After 6 hours		After 12 hours		After 18 hours		After 24 hours	
Deepening	Error	Deepening	Error	Deepening	Error	Deepening	Error
0	0	0	0	0	0	0	1
0	0	2	2	1	1	0	1
1	1	3	1	7	8	6	5
1	1	4	3	8	1	9	3
2	0	4	3	8	2	9	15
2	2	5	5	9	0	13	2
3	3	9	0	10	6	20	2
3	1	9	1	14	4	21	3
3	3	9	2	17	1	24	0
4	1	9	2	17	2	—	—
4	1	10	1	18	5	—	—
5	0	10	1	25	11	—	—
6	0	10	1	—	—	—	—
7	0	10	2	—	—	—	—
7	1	10	3	—	—	—	—
8	1	12	2	—	—	—	—
8	3	12	2	—	—	—	—
10	0	17	4	—	—	—	—
Mean 4 mb	1 mb	M 8 mb	2 mb	11 mb	3 mb	11 mb	4 mb

Out of 25 cases only 2 showed appreciable discrepancies from the calculated values. The one showed an error of 8 mb, and the second an error of 11 mb after 18 hours. Both these cases were disturbrd by secondary perturbations which caused accelerated deepenings. After 12 hours the majority of cases have an error of 1 to 2 mb, and in no case did the error exceed 4 mb.

It is of greater interest to see how the errors are distributed relative to the amount of deepening that actually took place. Table 10 shows this.

It is seen from the table that the errors are independant of the actual deepening that takes place. The large deepenings are calculated with the same accuracy as the small ones. The error is proportional to the time interval, and increases with 1 mb pr. 6 hours. It is, therefore, to be believed that the errors are almost entirely due to errors in the observed tendencies, because the deepening has been calculated by multiplying the initial tendency by the number of 3-hour intervals.

In the above tables we have written down the magnitudes of the errors regardless of their signs. If we compute the algebraic means of the errors, we get:

Interval (hours)	6	12	18	24
Mean Error	— 0.4	— 0.3	— 1.2	— 1.2

The algebraic means of the errors are exceedingly small. We may, therefore, conclude that the errors in table 10 are more likely to be due to inaccuracy in the observed tendencies than to any systematic error in the applied method.

If we exclude the said two cases, when secondary perturbations disturbed the development of the warm sector cyclones, we may form the following rule: *Warm sector cyclones deepen with an almost constant celerity, which is determined by the tendency at the top of the warm sector* (see also paragraph 34).

When the occlusion progresses, the deepening is more irregular, and the intensity varies. When the path of the center has been computed, the deepening is easily calculated by means of the formulae developed in chapter VI.

The deepening or filling has been computed for all the centers whose paths we have described in paragraph 37. These are the results obtained:

Table 11. Deepening calculated by means of Formula **32** *(2) for the 8 Pressure Centers (No. 1 to 8) referred to as Example 6 in Paragraph 37. (Calculated pressures in brackets).*

No.	Dates	Initial Pressure	After 6 hours	After 18 hours	After 24 hours
1	22. IV. 1932. 14h . . .	987	986 (986)	993 (996)	996 (1006)
2	20. X. 1931. 14h . . .	970	967 (966)	973 (968)	? (972)
3	15. XII. 1931. 14h . . .	964	962 (960)	968 (966)	975 (976)
4	14. XII. 1931. 14h . . .	993	987 (988)	970 (969)	965 (965)
5	22. VI. 1931. 14h . . .	988	986 (984)	983 (980)	983 (983)
6	13. III. 1931. 14h . . .	982	982 (983)	983 (983)	986 (982)
7	15. VII. 1931. 14h . . .	994	996 (995)	996 (995)	998 (994)
8	24. X. 1931. 14h . . .	982	980 (978)	978 (975)	976 (972)

Table 12. Deepening of the Pressure Center referred to as Example 7 in Paragraph 37.

	Dates	Initial Pressure	After 6 hours	After 11 hours	After 24 hours
No. 9	22. X. 1932. 8^h	990	988 (988)	987 (986)	982 (982)

It is seen from the two tables that the 9 centers are mostly very deep centers. 7 out of 9 centers were old occluded cyclones, whose future developments were not easily estimated. No. 1 shows a considerable discrepancy between the calculated and the observed pressure after 24 hours. Otherwise the results of the calculations are satisfactory. It is seen that some centers deepen throughout the period of 24 hours, others deepen and then fill-up, and others fill-up the whole time. The calculations show the same march.

It is interesting to see that No. 1, whose deepening was imperfectly calculated, also showed considerable discrepancy with regard to the calculated path. The calculated pressures, however, agree well with what is observed along the calculated path.

The 34 cases of deepening and filling, treated above, show such correspondance between observations and calculations, that there can be little doubt that the calculation of the paths and the development of pressure systems would largely increase the accuracy of weather forecasting.

39. The Hurricane Center of October 22nd 1921. *Example 8.* The writer does not know any pressure center which has developed more unexpectedly, attained such strength, and caused such damage, as did the pressure center that developed over England on the 22nd of October 1921. It was, therefore, thought to be of particular interest to see if this master cyclone could be forecasted with sufficient accuracy by means of numerical methods.

The story began with a quasistationary front over South England which, in the morning of the 22nd, developed a tiny center. At 14^h the same day the center was situated over Lancashire. The distribution of pressure and pressure tendencies at this hour is given in fig. 30. It is seen that the center is not a strong one. This chart, and the tendency chart at 8^h the same morning (fig. 31), form the basis for our calculations. The system of co-ordinates and the chosen length units are marked in fig. 30.

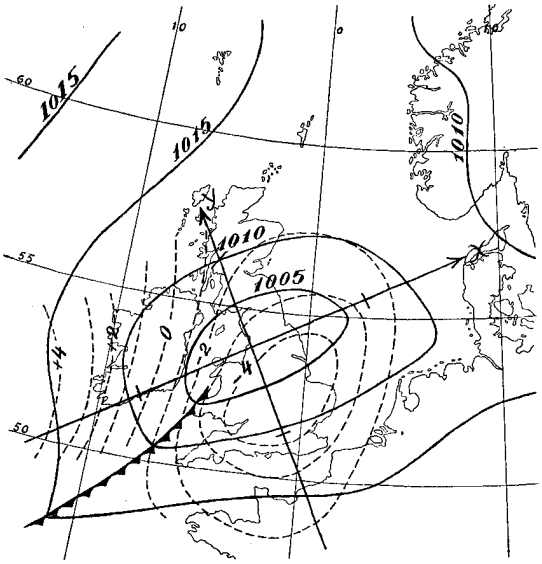

Fig. 30.

From these two charts we get: (see paragraph 18):

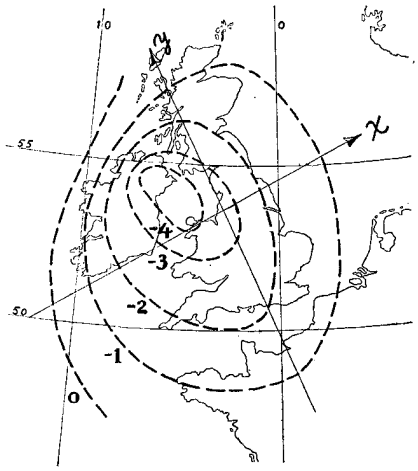

Fig. 31.

T^{00}	$= -3.3$	$\triangle T^{00}$	$= 0.15$
p_{101}	$= -1.6$	p_{011}	$= 1.05$
p_{200}	$= 13.0$	p_{020}	$= 18.0$
p_{102}	$= -1.75$	p_{012}	$= 0.58$
p_{201}	$= 4.40$	p_{021}	$= 3.3$

The length unit is 4 cm (scale of the chart 10^{-7}) along the x-axis, and 3 cm along the y-axis. Transferring the above coefficients to cm-distances on the chart, and substituting in **16** (1), we get for the velocity of the center:

$$C_x = 0.48, \; C_y = -0.17.$$

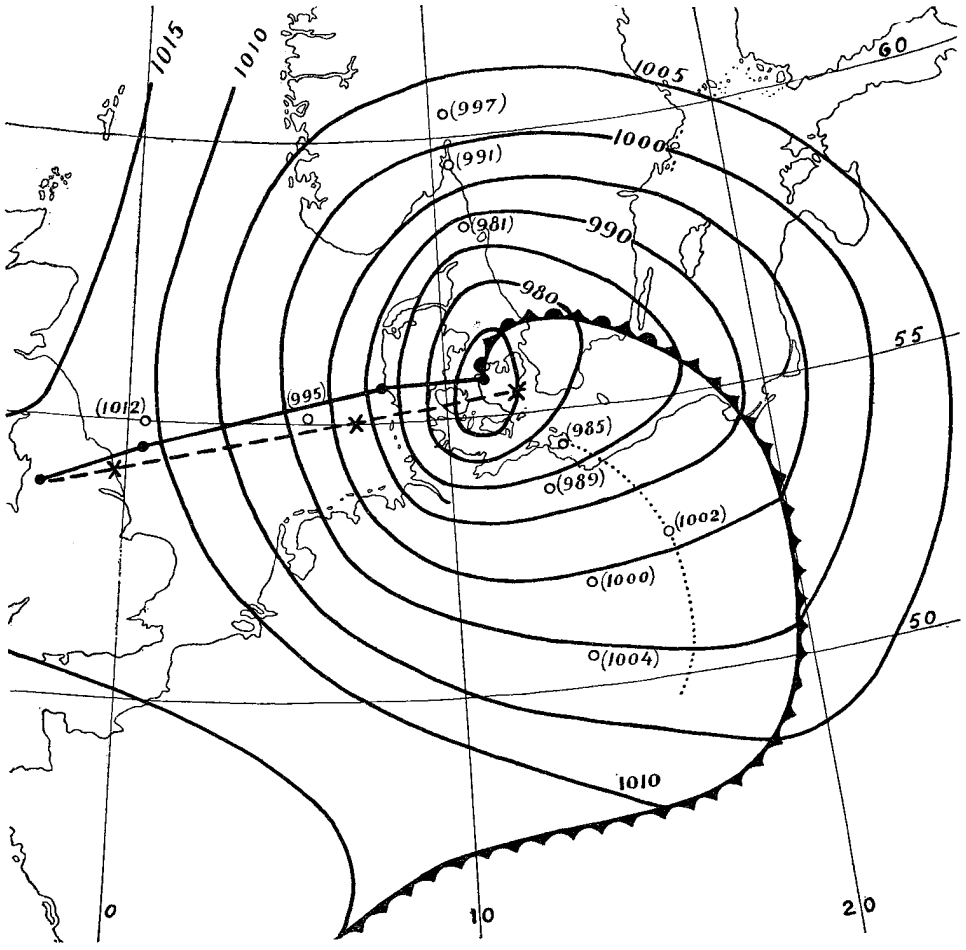

Fig. 32.

The hurricane center October 23rd, 1921, 14 h. The isobars represent the actual pressure distribution. Small circles indicate points for which pressure has been computed. The dotted line represents the computed position of the cold front. The actual path is drawn as a full line, the computed path as a broken line. The points marked on the paths, give the positions on the the preceeding charts.

According to **17** (1) we get for the acceleration:

$$A_x = 0.188, \quad A_y = - 0.030.$$

Substituting in **18** (2), we get for the co-ordinates of the center:

(1)
$$S_x = 0.48\ t + 0.094\ t^2$$
$$S_y = - 0.17\ t - 0.015\ t^2$$

Substituting in **32** (2), we get for the deepening of the center:

(2)
$$\triangle p = - 3.3\ t - 0.054\ t^2$$

The position of the center has been computed for the same evening at 19^h, the next day at 8^h and 14^h. Fig. 32 shows the computed path compared with the actual path. The center was easy to locate, and the agreement between calculations and observations is so pronounced that the slight discrepancies which occur are of no practical significance whatever. The calculations thus show that the path of the center could have been computed with abundant accuracy.

In this case it is, however, of equal importance to decide if the deepening of the center could have been predicted. Evaluating the above expression for $\triangle p$, we get for the pressure in the center:

Table 13.

Dates	Observed pressure	Calculated pressure
22. Oct. 14^h	1001	—
22. » 19^h	994	995
23. » 8^h	975	979
23. » 14^h	971	971

It is seen that the calculations give an accuracy which is far superior to what is required for a correct forecast.

The next question of considerable interest is: Could the pressure gradient in the surroundings of the center have been forecasted? In order to decide this we must calculate the deepening at some points round the center. Looking at equation (2), we see that the deepening celerity is about 60 times larger than the deepening acceleration. It is, in the present case, difficult to compute the deepening acceleration outside the center. Since the deepening acceleration in the center is small compared with the deepening celerity, we may expect to obtain fair accuracy by computing the deepening celerity at a number of points in the vicinity of the center.

The deepening during 24 hours has been computed for a number of points, which are marked by circles on the chart fig. 32. The computed pressures are written in brackets. It is seen that the computed pressures differ from the observed pressures by 1 to 7 mb. This is what we have expected, because we have not taken the deepening acceleration into account. The agreement between the computed and the observed pressures is, however, so good that no appreciable error would result in the distribution of gradient.

The displacement of the cold front trough, indicated in fig. 30 was also computed. The dotted line indicated in fig. 32, shows the computed position after 24 hours. The error in the computation is 200 km. after 24 hours. Since the velocity of the front on an average is 72 km., the error in the computation involves that the front arrived (say) at Breslau two hours and a half earlier than expected. An error of $2^1/_2$ hours in 24 is insignificant.

The geostrophic wind over Denmark in the rear of the cyclone amounted to 80 m sec^{-1}. The cyclone was accompanied by widespread hurricane, and caused devastations which, according to newspaper reports, amounted to more than £ 100 000 in Denmark only.

It does not appear from the weather bulletins of the meteorological institutes in NW-Europe that the hurricane force had been appropriately forecasted already on the noon chart of the 22nd. The above calculations, however, show that it could have been forecasted with an accurary hitherto unknown.

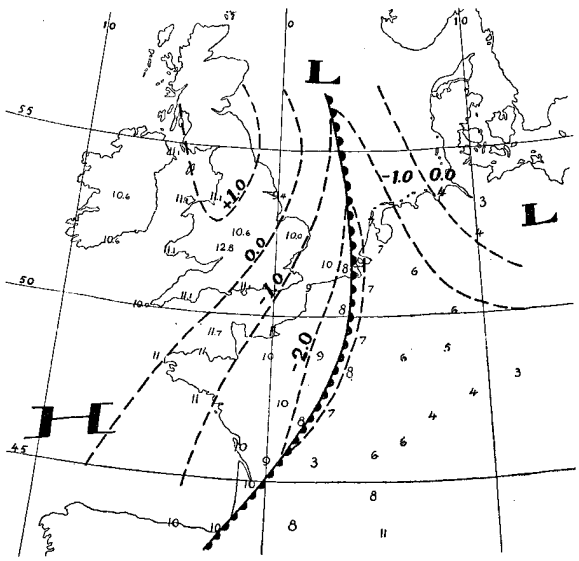

Fig. 33.

40. Examples of Frontogenesis. *Example 9.* Fig. 33 shows a quasi-stationary front which on the 10th of December 1931 14h extended from Bordeaux to the middle of the North Sea. The chart gives the position of the front, the field of isallobars, and the temperatures at a large number of stations. The isallobars (the broken lines) are drawn for each millibar.

According to the considerations in paragraph 26, it is to be expected that the distribution of isallobaric gradient would tend to make the front increase in intensity. In order to test the theory, we have computed the mean temperature for a zone of 100 km at either side of the front. The following table shows how the mean temperature varied in each of the said zones.

Table 14.

Dates	Warm	Cold	Difference
10. XII 1931. 14h . .	9.0 ° C	7.1 ° C	1.9
19h . .	8.8	5.8	3.0
11. XII 1931. 08h . .	9.0	5.4	3.6
14h . .	9.2	5.0	4.2
19h . .	9.2	3.1	6.1
12. XII 1931. 08h . .	8.9	0.4	8.5

Throughout the period the isallobaric gradients were directed towards the front from both sides, and the temperature difference increased from 1.9 to 8.5 degrees centigrade.

It is interesting to see that the temperature of the warm air remained almost constant, whereas the temperature on the cold side decreased steadily. This is what we should expect, because, owing to the homogeneous conditions of the warm (tropical) air, the flux of warm air towards the front (see paragraph 29) would not cause concentration of isothermal surfaces. On the cold side, however, the flux of air towards the front, (caused by the isallobaric gradient, see paragraph 29) would bring the temperature surfaces towards the front.

Example 10. Fig. 34 shows a front which on the 5th of December 1931 at 19h extended from the Bay of Bothnia towards Poland. The chart shows the distribution of pressure (full lines) and isallobars (broken lines). The observed temperatures are plotted

in small figures. The mean temperatures within zones of 200 km. at either side of the front, were computed. The difference was 8,5° C. As the isallobaric gradients were directed away from the front, it was to be expected that the front would decrease in intensity. Fig. 35 shows the situation the next morning. The pressure trough is then indistinct, and the difference in temperature has decreased from 8.5 to 5.4. The decrease continued on the following charts.[1])

The examples stated above are typical, and the rules referred to, have proved to be of great value for estimating the increase or decrease in front intensity.

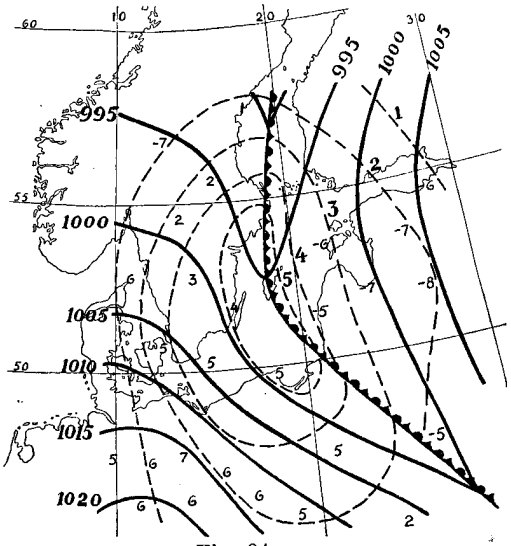

Fig. 34.

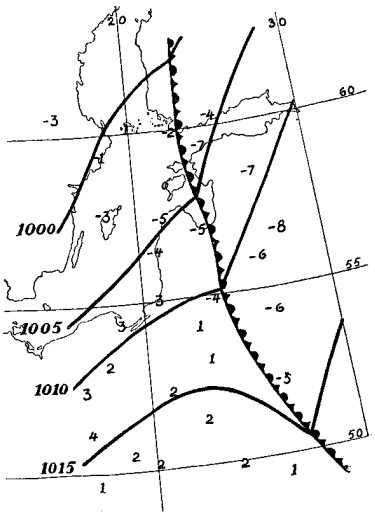

Fig. 35.

41. Isallobaric Gradient and Precipitation. *Example 11.* In paragraph 29 we have made some comments on the distribution of vertical velocity in the vicinity of fronts, and shown that the vertical velocity is caused by the flux of air along the isallobaric gradient, which, as a rule, are directed towards the front. We shall here give one example which illustrates the theory.

Fig. 36 shows a young warm sector cyclone which occured over Great Britain on January 23rd 1926 8h. This cyclone has been examined by J. Bjerknes,[2]) where a closer description is to be found. The arrows in fig. 36 show the directions of the isallobaric gradients, and the alotted numbers give the 'isallobaric wind' component in m sec^{-1}, computed from equation 28 (5).

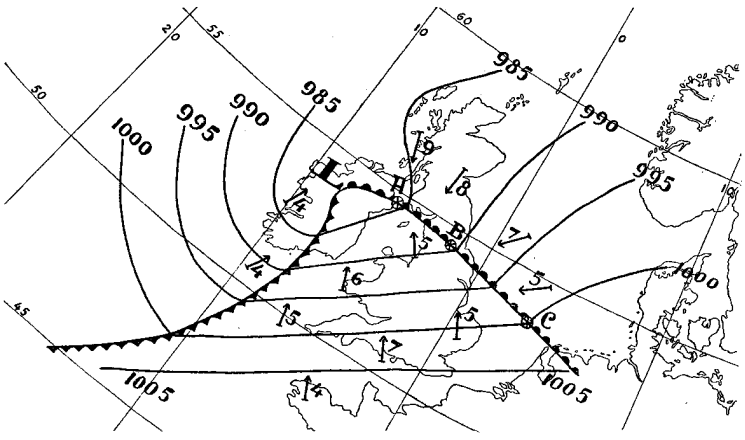

Fig. 36.

It is seen that there is a strong flux towards the warm front on both sides, the flux increasing towards the center of the cyclone.

[1]) The rapid decreace in temperature difference may partly be caused by radiation. The rapid destruction of the pressure trough, however, indicates intense frontolysis.

[2]) Practical Examples, loc. cit.

Along the cold front (which is of type B, described in paragraph 25), the flux is very small, the isallobaric gradients being almost parallel to the front. The theoretical considerations in paragraph 26 show that this front is exposed to frontolysis, which is corroborated by the empirical investigations of Bjerknes.

The properties of these two fronts have been examined and the results are contained in the tables 15, 16 and 17. ΔI then stands for the difference in isallobaric wind perpendicular to the front, ΔI being expressed in m sec^{-1}. ΔI is computed for the three points A, B and C as shown in fig. 36. These points correspond to the parts of the front that passed the three stations: Eskdalemuir, Holyhead and Andover, from where complete autographic records have been published by J. Bjerknes (loc. cit.). The figures in the following tables are taken from these records.

Table 15. The Warm Front.

Items	Andover	Holyhead	Eskdalemuir
ΔI	5.3	7.8	10.2
Amount of rain during the front passage	7 mm	5.2 mm	10.6 mm
Duration of rainfall (hours)	8	4.5	3.5
Rain intensity (mm per hour)	0.9	1.1	3.0
Temperature difference at the front	2.0 ° C	1.8 ° C	2.5 ° C
Duration of the passage	1 hour	1 hour	20 minutes
Front intensity, ° C per hour	2	1.8	7.5

It is seen from the table that the rain intensity is directly proportional to the flux of air towards the front.

The warm front which at Eskdalemuir is of type B (see paragraph 25), is retarded and exposed to frontogenesis. This explains the large front intensity at Eskdalemuir. The front at Eskdalemuir became almost stationary, and the strong flux of air towards the front would cause increased front intensity (see paragraph 40).

At the cold front there is but slight flux towards the front. It is then to be expected that the rain intensity should be smaller at the cold front than at the warm front. Table 16 shows this:

Table 16. The Cold Front.

Items	Andover	Holyhead	Eskdalemuir
Amount of rain	4 mm	1 mm	1 mm
Duration	$2^3/_4$ h.	1 h.	$4^1/_2$ h.
Intensity	1.5	1.0	0.2

It is seen that the rain intensity decreases along the cold front from South to North. This is usually the case with cold fronts of type B. In the vicinity of the center such fronts are ill-defined. In the present case, the front is hardly distinguishable at Eskdalemuir.

It is seen from fig. 36 that there can be but slight convergence or divergence of isallobaric gradients in the southern part of the warm sector. The flux is fairly uniform and directed towards the top of the warm sector. As there can be no piling-up of air at the top of the warm sector, the air must ascend. In general, the isallobaric gradient

is small in the vinicity of the center. There would then be a strong convergence in the warm air near the center. According to considerations in paragraph 28, this convergence would result in a strong ascending motion in the warm air at the top of the sector. From the distribution of isallobaric gradients in fig. 36, we would conclude that there ought to be intense precipitation in the warm air at the top of the warm sector. Table 17 shows the amount and intensity of the warm sector precipitation at the three stations.

Table 17. Warm Sector.

Items	Andover	Holyhead	Eskdalemuir
Amount of rain	2 mm	1 mm	27 mm
Duration . . .	20h.	$9^1/_2$ h.	5 h.
Intensity . . .	0.1	0.1	5.4

It is seen from the table that the rain intensities at Andover and Holyhead, where the convergence is slight, are insignificant, whereas at Eskdalemuir the rain intensity is excessively large. The autographic records published by J. Bjerknes, clearly show that the rain fell in the warm air.

It is well to note that the isallobaric gradients in this warm sector were exceptionally strong, and that part of the rain at Eskdalemuir might be of orographical origin. In most cases the isallobaric gradients are much smaller, and the amount of rain recorded at the top of the warm sector, rarely amounts to more that 1 mm per hour.

This one example presumably suffices to show the importance of studying the details of the distribution of the isallobars. The pressure tendencies and the isallobaric gradients, being the cause of all changes, are deeply rooted in all forecasting problems.

BIBLIOGRAPHY

It would be difficult and probably but of little value to obtain a complete list of the literature which more less directly deals with fronts, cyclones, airmass analysis and forecasting. A fine list of bibliography is contained in Bergeron's: Die dreidimensional verknüpfende Wetteranalyse. Geof. Pub. Vol. V No. 6.

Of papers dealing with numerical methods, the following deserve special mention:

(1) A. Giao: La Mécanique differentielle des Fronts et du Champ issallobaric. Memorial de l'Office Nat. Met. No. 20. Paris 1929.

(2) I. M. Angervo: Über die Vorausberechnung der Wetterlage für mehrere Tage. Gerlands Beiträge zur Geophysik. Bd. 27. 1930.

(3) I. M. Angervo: Zur Theorie der Zyklonen- und Antizyklonenbahn. Gerl. Beitr. Bd. 33. 1931.

(4) I. M. Angervo: Wann entsteht aus einer V-Depression ein Teilminimum oder aus einem Keil hohon Druckes ein selbständiges Hochdruckzentrum. Gerl. Beitr. Bd. 35. 1932.

(5) H. Wagemann: Über die Anwendung der Angervoschen Formeln etc. Met. Zeitschr. 1930.

(6) H. Wagemann: Eine Faustformel zur Berechnung der Verlagerungsgeschwindigkeit von Hoch- und Tiefdruckausläufer. Ann. d. Hydr. u. mar. Met. 1931.

(7) L. F. Richardsen: Weather Prediction by Numerical Process. Cambridge 1922.

ACKNOWLEDGEMENTS

During the preparation of the present memoir, I have received valuable assistance from various members of the staff of Værvarslingen på Vestlandet, without which it would have been impossible to finish the investigations during the limited time which was at my disposal. Messrs. Spinnangr and Holmboe have kindly carried out most of my duties during the time which I needed for undisturbed work. Mr. Winther Hansen has checked all the formulae, and Mr. Johansen has worked out the practical examples and assisted in preparing the tables. Miss E. Getz has spent much of her time in the unremunerative work of type-writing and correcting the text.

Værvarslingen på Vestlandet. Bergen. December 1932.

Sverre Petterssen.

Printed June 1st, 1933.

ERRATA

Page	Line	Instead of	Read
20	2nd f. above	$(1+p^2_{100})^{\frac{5}{2}}$	$(1+p^2_{100})^{\frac{5}{2}}$
22	in equation (11)	p^2_{100}	p^2_{101}
23	in equation (13)	C^2_L	$C'_L{}^2$
26	12th f. below	Chapter	chapter
27	4th f. above	characterised	characterized
28	5th f. above	p_{021}	p_{011}
28	2nd f. below	p_{102}	p_{012}
29	6th f. below	to used	to be used
30	in equation (1)	p_{120}	p_{012}
30	15th f. below	prohlem	problem
30	14th f. below	succeeding	succeeding
33	8th f. above	$a$and	a and
36	5th f. below	Formnla	Formula
38	in equation (2)	$C'_f \frac{\partial^3 p}{\partial x^2 \partial t}$	$2\,C'_f \frac{\partial^3 p}{\partial x^2 \partial t}$
38	in equation (3)	$C'_f p_{201}$	$2\,C'_f p_{201}$
39	17th f. above	forpressure	for pressure
44	7th f. above	Cyklonĕ	Cyclone
45	3rd f. above	sinee	since
45	1st f. below	p_2	p_1
56	1st f. above	possibilitis	possibilities
56	4th f. above	wawe	wave
63	20th f. below	disolve	dissolve
66	4th f. above	exed	exceed
73	10th f. above	18	18)
75	16th f. above	seetor	sector
76	6rh f. above	deepning	deepening
81	16th f. below	denote	denotes
82	4th f. above	forthe	for the
82	24th f. above	inaccnuracy	inaccuracy
83	1st f. below	M 8 mb	8 mb
89	3rd f. below	decreace	decrease